Sphingolipid topology and membrane protein nanoclusters

Sandra Hötzl

Paranimfen:
Sonja Hötzl
Philipp Dietachmair

ISBN: 978-90-393-5154-3
Printed by: Gildeprint Drukkerijen, Enschede

The research described in this thesis was performed at the department of Membrane Enzymology, Bijvoet Center and Institute of Biomembranes, Utrecht University, The Netherlands, with financial support from the Dutch Organization of Sciences (NWO-MtC).

Printing of this thesis was financially supported by:
J.E. Jurriaanse stichting, Rotterdam, The Netherlands
Greiner Bio-One, Frickenhausen, Germany

Sphingolipid topology and membrane protein nanoclusters

Topologie van sfingolipiden en membraaneiwit nanoclusters

(met een samenvatting in het Nederlands)

Proefschrift

ter verkrijging van de graad van doctor aan de Universiteit Utrecht
op gezag van de rector magnificus, prof.dr. J.C. Stoof,
ingevolge het besluit van het college voor promoties
in het openbaar te verdedigen op
maandag 19 oktober 2009 des middags te 2.30 uur

door

Sandra Hötzl

geboren op 19 April 1978 te Feldbach, Oostenrijk

Promotor: Prof. dr. G.F.B.P. van Meer

Table of Contents

Abbreviations

C_6-NBD-Cer	N-6-(7-nitro-2,1,3-benzoxadiazol-4-yl)-aminohexanoyl-Ceramide
CPE	Ceramide PhosphoEthanolamine
CPES	Ceramide PhosphoEthanolamine Synthase
CPI	Ceramide PhosphoInositol
CPOs	CholinePhosphoryl-substituted Oligosaccharides
CSR	Complete Spatial Randomness
DAG	DiAcylGlycerol
EGFR	Epidermal Growth Factor Receptor
ER	Endoplasmic Reticulum
EV	Empty Vector
GalCer	GalactosylCeramide
gDNA	genomic DNA
GFP	Green Fluorescent Protein
GlcCer	GlucosylCeramide
GPI	GlycoPhosphatidylInositol
GSLs	GlycoSphingoLipids
LPP	Lipid Phosphate Phosphatase
mCFP	monomeric Cyan Fluorescent Protein
MDCK	Madin-Darby Canine Kidney epithelial cell line
mGFP	monomeric Green Fluorescent Protein
mYFP	monomeric Yellow Fluorescent Protein
PC	PhosphatidylCholine
PM	Plasma Membrane
SM	SphingoMyelin
SMS	SM synthase
TGN	trans-Golgi Network
tH	Truncated H-ras, the minimal membrane-targeting motif of H-ras
tK	Truncated K-ras, the minimal membrane-targeting motif of K-ras
TLC	Thin Layer Chromatography

Chapter 1

Sphingolipid topology and the dynamic organization and function of membrane proteins

Sandra Hoetzl, Seléne van der Poel and Gerrit van Meer

Based on:
Invited review for special issue FEBS Letters
"Frontiers in Membrane Biochemistry", submitted

Membrane Enzymology, Bijvoet Center and Institute of Biomembranes, Utrecht University, Utrecht, The Netherlands

Abstract
When acquiring internal membranes and vesicular transport, eukaryotic cells started to synthesize sphingolipids and sterols. The physical differences between these and the glycerophospholipids must have enabled the cells to segregate lipids in the membrane plane. Localizing this event to the Golgi then allowed them to create membranes of different lipid composition, notably a thin, flexible ER membrane, consisting of glycerolipids, and a sturdy plasma membrane containing at least 50% sphingolipids and sterols. Besides sorting membrane proteins, in the course of evolution the simple sphingolipids obtained key positions in cellular physiology by developing specific interactions with (membrane) proteins involved in the execution and control of signaling. The few signaling sphingolipids in mammals must provide basic transmission principles, which evolution has applied in specific and convoluted ways in the different cell types in the body.

Sphingolipid synthesis in mammalian cells
The first step in sphingolipid synthesis is the condensation of palmitoyl-SCoA and serine to 3-ketodihydrosphingosine. This lipid is reduced to dihydrosphingosine, also named sphinganine, essentially all of which is converted to dihydroceramide by the attachment of a fatty acid to the aminogroup at C2 of the sphinganine backbone. This reaction is catalyzed by one of the ceramide synthases, a family of enzymes that have different fatty acid specificities (Pewzner-Jung et al., 2006). Most dihydroceramides are desaturated at C4-C5, to yield ceramide with sphingosine (sphingenine) as a sphingoid base, while dependent on cell type a fraction of the dihydroceramides is hydroxylated at C4 to yield phytoceramide, which carries phytosphingosine (4-hydroxysphinganine). Ceramide synthases also yield ceramides directly from sphingosine that originates from sphingolipid hydrolysis in the lysosomes (Kitatani et al., 2009). Until this point all events occur on the cytosolic surface of the ER membrane. Ceramide may also be produced from sphingosine and fatty acid via the reverse action of ceramidases, or by the action of sphingomyelinases. Sphingosine can also be phosphorylated by sphingosine kinase to sphingosine-1-phosphate (Kim et al., 2009). This latter lipid is degraded by either a phosphatase to yield sphingosine, or by the lyase into hexadecenal (to be reduced to palmitate) and ethanolamine-phosphate.

In most cells, the bulk of the ceramide is converted to sphingomyelin (SM) by sphingomyelin synthase 1 (SMS1), on the lumenal surface of the trans-Golgi, or by SMS2 on the noncytosolic surface of the plasma membrane (Huitema et al., 2004; Yamaoka et al., 2004). Both SMS1 and 2 contribute to cellular SM synthesis (Tafesse et al., 2007). Alternatively, ceramide is galactosylated by the galactosyltransferase Gal-T1 on the lumenal surface of the ER membrane, or glucosylated on the cytosolic surface of a Golgi membrane (or the ER in flies; Kohyama-Koganeya et al., 2004). Galactosylceramide (GalCer) can be sulfated to

sulfatide (SGalCer) in the trans-Golgi. In contrast, glucosylceramide (GlcCer) can be converted to lactosylceramide (LacCer), which can be further glycosylated to an array of different glycosphingolipids (GSLs) by the stepwise addition of monosaccharides via a number of pathways. Essentially every cell contains GM3 (sialic acid-galactose-glucose-ceramide). Most cells express at least one additional glycolipid synthesis pathway. These glycosylation reactions occur in the lumen of the Golgi (Figure 1).

GSLs and SM are broken down to sphingosine by a series of dedicated enzymes in the lysosomal lumen. The GSLs are first degraded to ceramide by the removal of the sugars by a set of acid hydrolases, most of which require a helper protein for their activity (Schulze et al., 2009). The phosphocholine headgroup of SM is removed by acid sphingomyelinase (Jenkins et al., 2009), after which ceramide is degraded by acid ceramidase. Alternatively, SM is degraded by the neutral sphingomyelinase (nSMase2) on the cytosolic surface of the plasma membrane (Tani and Hannun, 2007). Also ceramide can be degraded outside the lysosome by the neutral ceramidase on the outside of the plasma membrane (Hwang et al., 2005) or one of the three alkaline ceramidases (Mao and Obeid, 2008).

Sphingolipid topology and transport

Sphingoid bases and signaling receptors

The sphingoid bases possess the physical property that they rapidly exchange between membrane surfaces across the aqueous phase because of the fact that their single lipid tail is only a weak membrane anchor and because they have a polar head group due to the partially charged amino group. When present on a cytosolic surface, they can therefore be expected to rapidly equilibrate between the cytosolic surfaces of the organelles. In addition, sphingoid bases readily move across membranes at neutral pH. At acidic pH the amino moiety no longer partially occurs as an uncharged amine but becomes positively charged which antagonizes spontaneous transport. It is therefore very likely that the sphingosine that is generated in the lysosomes and must reach the ER membrane for reutilization can only move across the lysosomal membrane by means of an active transporter. An involvement has been proposed for the Niemann-Pick C protein NPC1 (Lloyd-Evans et al., 2008). Likewise, sphingosine-1-phosphate is synthesized by a kinase in the cytosol but has extracellular functions and must cross the plasma membrane. It has been reported that the transmembrane translocation is mediated by the multidrug ABC transporters ABCC1 and ABCA1 (see Kim et al., 2009). Extracellular sphingosine-1-phosphate can bind to members of the sphingosine-1-phosphate receptors of the EDG family of G-protein coupled receptors on the surface of cells.

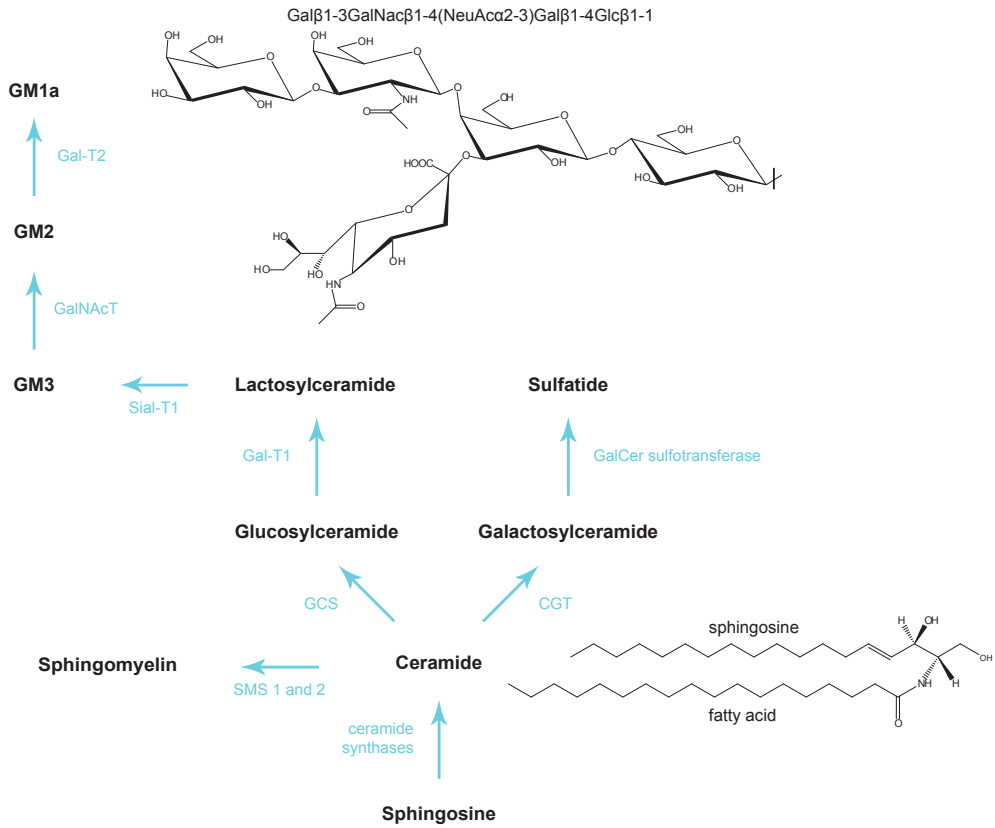

Figure 1. Biosynthetic pathway of some common sphingolipids. CGT, ceramide galactosyltransferase; GCS, GlcCer synthase. The pentasaccharide headgroup of GM1 is shown.

Ceramide and signaling

In contrast to sphingosine, ceramide is deeply embedded in the membrane. Like any other lipid it laterally diffuses in the fluid cellular membranes, but in contrast to lipids that have a large or charged headgroup, ceramide rapidly moves across membranes spontaneously (López-Montero et al., 2005). It does not move between membranes as a monomer at a significant rate. For example, ceramide produced in the lysosomes must be degraded to sphingosine to be able to leave the lysosomes: inactivating mutations in acid ceramidase cause the ceramide storage disorder Farber disease, probably because ceramide is produced in the intralumenal vesicles of lysosomes and is unable to reach the limiting membrane (as is the case for cholesterol in the cholesterol storage disease Niemann-Pick C). After synthesis in the ER, ceramide reaches the site of SM synthesis in the Golgi not by vesicular traffic: this transport requires the ceramide transfer protein CERT, which binds to a protein on the ER and to the phosphoinositide PI-4-P on the Golgi possibly at ER-

Golgi contact sites. CERT binding is regulated via phosphorylation (Hanada et al., 2009). Under certain conditions new ceramide in the ER and ceramide generated in the plasma membrane by sphingomyelinases activate cytosolic protein kinases and phosphatases (Hannun and Obeid, 2008), which suggests that ceramides in a membrane can be recognized by proteins outside that membrane. Indeed, antibodies have been generated that recognize ceramide in the membrane. However, interpretation of the results is not always straightforward due to technical complications (Cowart et al., 2002; Hoetzl et al., 2007). A high ceramide level in the ER has been correlated with apoptosis. Possibly this raises ceramide levels in the mitochondria and activates apoptotic pathways (see Morales et al., 2007). ER ceramide levels should thus be controlled, and recently an ER member of the family of SM synthases with low enzymatic activity towards ceramide, SMSr, has been proposed to be a ceramide sensor (Vacaru et al., 2009). How it couples to possible effectors is not yet known. It is also not clear whether plasma membrane SMS2, having a side activity similar to the activity of SMSr (Ternes et al., 2009), has a sensor function as well. Although mitochondria contain very low levels of SM (Hovius et al., 1990), the existence of a specific mitochondrial SM pool as a precursor for mitochondrial "apoptotic" ceramide has been suggested (Birbes et al., 2001).

Sphingomyelin and lipid segregation

After delivery by CERT to the trans-Golgi, ceramide is converted to SM in its lumen. In COP-I vesicles budded from the Golgi and heading for the ER the concentration of SM and cholesterol was found to be reduced as compared to the major phospholipid phosphatidylcholine (Brügger et al., 2000), whereas sphingolipids and sterols were enriched in secretory vesicles (Klemm et al., 2009). These findings illustrate the general principle of lipid segregation in the Golgi, whereby SM, glycosphingolipids and cholesterol are sorted towards the plasma membrane while unsaturated PC is enriched in the retrograde pathway. The location of SM and the complex GSLs in the lumenal leaflet of the Golgi has thus led to the proposal that a lateral sorting event occurs in this lumenal leaflet whereby sphingolipids and cholesterol are enriched in areas of the membrane that are destined for the plasma membrane, and PC in areas where the vesicles bud that are bound for the ER (van Meer, 1989). The physical basis of this lipid segregation into two domains that differ in the degree of order, or fluidity, has been worked out in great detail (see van Meer et al., 2008). Although the lateral segregation of lipids in Golgi membranes has not been shown in a direct experiment, such evidence has been provided for endosomes. In the latter case, however, the authors have made use of fluorescent analogs of membrane lipids, and it is not really clear how the native lipids distribute over the various transport pathways out of the endosomes, to the late endosomes, to the Golgi and back to the plasma membrane (Koval and Pagano, 1990; Willem et al., 1990; Martin

and Pagano, 1994; Chen et al., 1997; Mukherjee et al., 1999; Sharma et al., 2003). Because the directional delivery of membrane vesicles depends on the presence of specific targeting proteins like SNAREs and Rabs, the two (or more) lipid environments in the donor membrane must be able to recruit the unique sets of proteins needed to ensure the delivery of the different membrane vesicles at the correct target membranes. That certain proteins partition into more ordered membrane patches has been operationally determined by their preferential partitioning into detergent resistant membranes. Direct evidence at the level of vesicle budding is still lacking.

Monohexosylsphingolipids and their multiple transport mechanisms

GalCer synthesized on the lumenal surface of the ER can reach the lumen of the trans-Golgi (network), where it can be sulfated, and the outside of the plasma membrane by vesicular traffic (Figure 2). In contrast, GlcCer is synthesized on the cytosolic surface of the Golgi (Coste et al., 1986; Futerman and Pagano, 1991; Jeckel et al., 1992). In order for it to be converted to LacCer and further complex GSLs on the lumenal surface, it must cross the membrane (Figure 2). Surprisingly, it was found that conversion to the complex glycolipid GM3 was dependent on FAPP2, a cytosolic protein bound to the trans-Golgi via PI-4-P and possessing a glycolipid binding domain. This was taken to imply that FAPP2 transported GlcCer from the early Golgi to the trans-Golgi where it was translocated to the lumen (D'Angelo et al., 2007). However, Halter et al. (2007) provided evidence for transport of GlcCer back to the ER membrane and across to the lumenal side, which would then be followed by vesicular traffic of GlcCer from the ER into the lumen of the Golgi (just like GalCer). Such retrograde transport of GlcCer might occur at the same contact site where CERT putatively transfers ceramide in the anterograde direction (Neumann and van Meer, 2008). Translocation of GlcCer across the ER membrane would be expected from the fact that GlcCer rapidly translocated towards the lumen of the merged ER-Golgi compartment in the presence of brefeldin A (Halter et al., 2007), and that spin-labeled GlcCer and GalCer easily translocated across isolated ER membranes without ATP consumption (Buton et al., 2002). Rapid translocation was also reported for isolated total Golgi membranes, which leaves open the possibility that spontaneous translocation can also occur across late (D'Angelo et al., 2007) or early (Halter et al., 2007) Golgi membranes.

Unexpectedly, it was found that both newly synthesized GlcCer and GalCer still reached the surface of the plasma membrane in the presence of brefeldin A. Under those conditions new GM3 no longer reached the surface confirming that vesicular traffic from the merged ER-Golgi compartment to the plasma membrane is fully blocked (Halter et al., 2007). Therefore, GlcCer and GalCer must have moved across the cytosol to the cytosolic side of the plasma membrane, and subsequently they must have translocated across the plasma membrane. Transport of

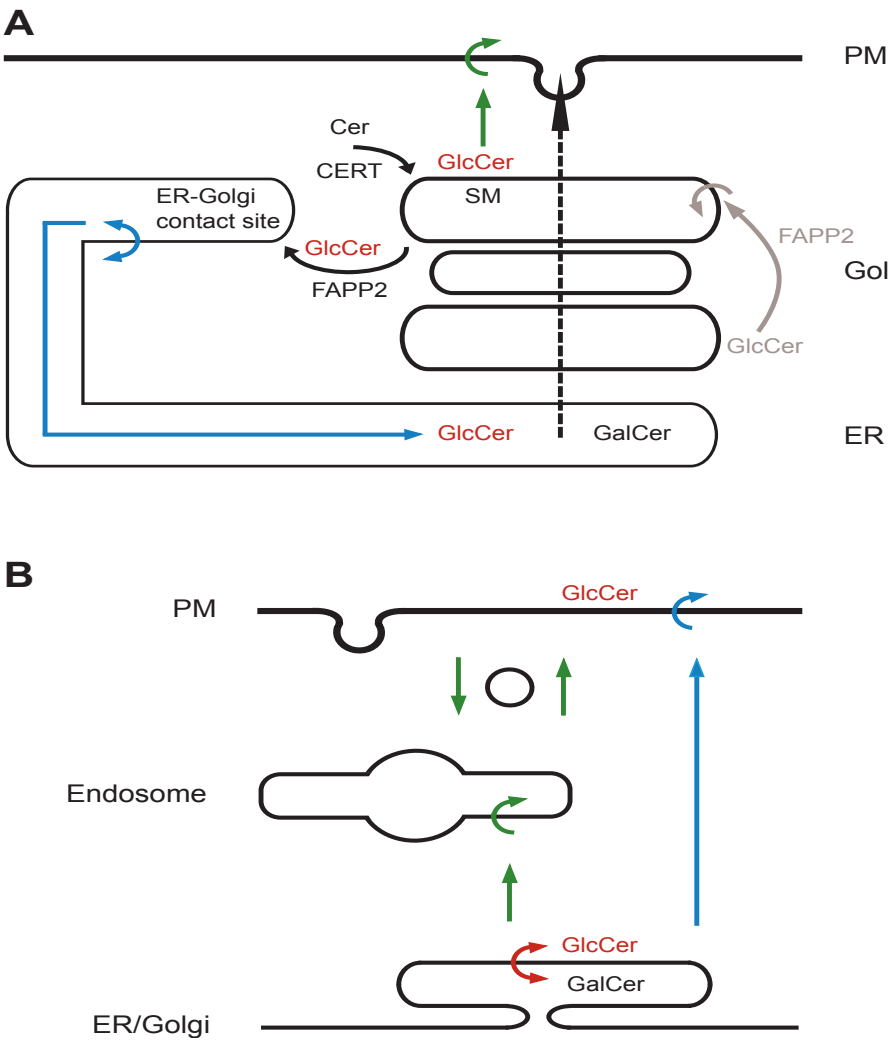

Figure 2. Pathways of intracellular GlcCer transport. (A) Under normal conditions, ceramide (Cer) is transported to the trans-Golgi by the ceramide transport protein CERT. GlcCer is synthesized on the cytosolic surface of the Golgi and is transported back to the ER by FAPP2. If flips across the ER membrane and is transported to the lumen of the Golgi, possibly involving GlcCer and GalCer clustering at ER exit sites (Halter et al., 2007). In an alternative model GlcCer synthesized in cis-Golgi is transported to the trans-Golgi via FAPP2 where it flips by an unknown mechanism (D'Angelo et al., 2007). SM and all complex GSLs are synthesized on the lumenal surface. Cholesterol has been shown to have a high affinity for sphingolipids, which are thought to reside mainly in the non-cytosolic leaflets. Unexpectedly, cholesterol was found enriched in the opposed leaflet of the bilayer (Mondal et al., 2009). GlcCer also reaches the inside of the plasma membrane and flips across (Halter et al., 2007). (B) In the presence of brefeldin A the Golgi and ER merge. In the absence of vesicular traffic from the ER, GlcCer and GalCer are able to reach other cytosolic surfaces and translocate to the outside of the plasma membrane, or the lumenal surface of endosomes (Halter et al., 2007).

GlcCer across the cytosol had been reported (Warnock et al., 1994). The mechanism remains unclear, as no role for FAPP2 or for the glycolipid transfer protein GLTP was observed (Halter et al., 2007). Translocation across the plasma membrane has been observed for GlcCer analogs carrying one or two shortened fatty tails, and it was found that this was mediated by the multidrug ABC transporters ABCB1 (van Helvoort et al., 1996) and ABCC1 (Raggers et al., 1999). In contrast, inhibition or knock-out of these transporters did not affect transport of natural GlcCer and GalCer (Halter et al., 2007). Interestingly, studies on the skin disorder harlequin ichthyosis have indicated that ABCA12 transports GlcCer across the membrane of skin lamellar bodies, making it a candidate for the translocation across plasma membranes (or endosomal membranes) in non-skin cells (see Hovnanian, 2005). The convoluted pathways of GlcCer may indicate that GlcCer concentrations are controlled. Also the non-lysosomal glucosylceramidases may exert control on local GlcCer concentrations (Yildiz et al., 2006; Boot et al., 2007; Hayashi et al., 2007). GlcCer on the cytosolic surface of cell organelles appears to exert functions in the sorting of membrane proteins to lysosomes and lysosome-related organelles (Sprong et al., 2001; Groux-Degroote et al., 2008). GlcCer and the complex GSLs derived from it are required for mammalian embryonic development (Yamashita et al., 1999).

Glycosphingolipids and clustering

Non-random distributions of GSLs were first observed in model membranes by spin-label studies (Maggio et al., 1978; Sharom and Grant, 1978) and on erythrocyte membranes (Tillack et al., 1983). The conclusion that GSLs may occur on biomembranes in clusters was complicated by potential pitfalls in those studies: it was not verified whether maybe the GSLs in the liposomes were in solid gel domains, which do not occur in mammalian membranes, or whether clustering was due to redistribution caused by the labeling with multivalent ligands. It was then proposed that the self-aggregation of GSLs was functionally relevant in the lumenal leaflet of the TGN membrane, where it is part of the mechanism for enriching GSLs on the apical surface of kidney and intestinal epithelia (Simons and van Meer, 1988). These surfaces are virtually covered by GSLs. Clustering of GSLs has been directly observed on the plasma membrane of non-epithelial cells. While in most studies it could not be excluded that clustering was induced by the use of multivalent ligands (Hoetzl et al., 2007), in a reliable study using immuno-electron microscopy after freeze-substitution Parton (1994) demonstrated that the ganglioside GM1 (negatively charged sialic acid containing GSL) was enriched in caveolae. Also the presence of GM1 in detergent-resistant membranes has been taken as evidence that it resided in microdomains or “rafts”, but it was clearly demonstrated by microscopy (Mayor and Maxfield, 1995) that detergent extraction resulted in large detergent-resistant domains that had not been observed before the detergent was added.

Nowadays, the general perception of rafts is that under resting conditions in plasma membranes rafts are transient nanoscale cholesterol-dependent assemblies of specific lipids and proteins, where interactions with specific proteins, scaffolds and membrane lipids influence the formation, stability and size of the cluster (Hancock, 2006; Henis et al., 2009). These nanoclusters (20 nm diameter, <10 proteins and <1,000 lipids) may occur on both sides of the plasma membrane. In homogeneous model membranes a large scale phase segregation can be driven by the induction of curvature with a radius of 20 nm (Sorre et al., 2009). Plasma membranes may generally be close to a point where the nanoclusters coalesce into large domains (Lingwood et al., 2008). This behavior has been observed after incubating T-cells in the cold (Magee et al., 2005), and after release of the plasma membrane from the underlying cytoskeleton and temperature reduction (Baumgart et al., 2007). Nanocluster coalescence has been observed in physiological processes: signaling by EGF (Hofman et al., 2008), cross-linking of lipids by e.g. toxin and subsequent membrane invagination (Römer et al., 2007; Lingwood et al., 2008), and, obviously, membrane budding from caveolae (Parton, 1994). GPI-proteins, anchored to the outside of the membrane by a glycosylphosphatidylinositol lipid tail, in steady state reside in cholesterol-dependent nanoclusters (Varma and Mayor, 1998), but not in caveolae. Indeed, different GPI-proteins on the same plasma membrane have been observed to occur in spatially different rafts (Madore et al., 1999; Wang et al., 2002) having different lipid compositions (Brügger et al., 2004). Interestingly, also different GSLs, like the gangliosides GM1 and GM3 (Gómez-Mouton et al., 2001; Fujita et al., 2007; 2009; Janich and Corbeil, 2007; Chen et al., 2008), were found to reside in unique rafts. In line with this, the various GSLs displayed unique distributions over the different cellular membranes (Matyas and Morré, 1987). The coexistence of different types of lipid rafts in the same membrane provides another layer of complexity to the physiological functions of these structures.

Glycosphingolipids and their trans- and cis-interactions

GSLs are used as cell surface receptors by a number of toxins, viruses, bacteria and parasites, and it is now realized that in many cases the partitioning behavior of the gangliosides is crucial for correct delivery of the infectious agent to its target organelle. In addition, GSLs have been proposed to fulfill a role in cell-cell recognition, whereby a GSL on one cell would bind in trans to a lectin, or even to a different GSL on a neighboring cell (Kojima and Hakomori, 1989) similar to carbohydrate-based glycoprotein-glycoprotein interactions found before. This concept was later extended by the idea that the glycosylated molecules might aggregate into a “glycosynapse” that would strongly enhance the binding by multivalency (reviewed in Regina Todeschini and Hakomori, 2008). The glycosynapse could be formed by two opposed lipid rafts where binding selectively depends on GSL-GSL interactions in trans. Alternatively, a GSL raft on one cell

could be recognized by lectins on the neighboring cell. Interestingly, in specific cases the recognition of GSL by antibodies was found to depend on the presence of other GSLs (Lloyd et al., 1992). More recently, disease cases have been reported where autoimmune antibodies turned out to be directed against a combination of different GSLs, while not binding to the GSLs when presented individually (Kaida et al., 2004). In other cases, GSLs on the cell surface were shielded against anti-GSL antibodies by other GSLs (Greenshields et al., 2009). These observations are of utmost importance for disease pathology, but, in addition, similar phenomena may be involved in the regulation of glycoconjugate-mediated (and GSL-mediated in particular) cell-cell and cell-matrix interactions. The aggregation and segregation of GSLs on the cell surface described above may be part of such regulatory processes. In the ER membrane GlcCer was found needed for organizing the Shiga toxin receptor, the GSL Gb3, in lipid rafts as defined by detergent-resistance (Smith et al., 2006).

The lateral interactions of GSLs are not limited to their aggregation into lipid nanoclusters or rafts. Early observations demonstrated an inhibitory action of specific gangliosides on cell growth, and suggested that gangliosides modulate receptors (Bremer et al., 1984). Later work suggested that the ganglioside GM3 directly interacted with N-linked sugars on the extracellular domain of the activated EGF receptor to inhibit its receptor tyrosine kinase activity (Miljan et al., 2002; Yoon et al., 2006; Milani et al., 2007), and that GM3 induced the receptor's presence in DRMs, suggesting a change in the organization of the receptor and its coreceptor ErbB2 on the cell surface (Sottocornola et al., 2006). Similar interactions have been described for other receptors, like the insulin receptor (Kabayama et al., 2007) and for integrins, in which case GM3 and GM2 mediated their interaction with other proteins (Regina Todeschini and Hakomori, 2008). Possibly, gangliosides form an indispensable part of the machinery allowing other regulatory factors to modulate the process. Even more likely, changes in the concentration and lipid tail composition of the ganglioside are directly relevant for the signaling processes in which the ganglioside-binding proteins are involved. It is therefore important to learn about the glycosyltransferases in the Golgi, the transport of the ganglioside to and from the cell surface, its lateral organization in relation to the relevant receptors, and its degradation. Of utmost importance in the regulation appears to be the desialylation and inactivation by sialidases on the plasma membrane (Miyagi et al., 2008). First of all, the presence of sialidases on the surface appears to be regulated, second, they display properties of lipid raft proteins, third, they may work in cis on gangliosides in the same membrane, but may also work in trans on gangliosides present in the opposed membrane upon the establishment of cell-cell contact. Sialidases preferentially cleave the sialic acid on GM3 and the terminal sialic acids on the complex GSLs. GM1 is a good substrate only in the presence of a lysosomal activator protein (see Miyagi et al., 2008).

Perspectives

The contribution of sphingolipids to the barrier function of the plasma membrane is vital. Beyond that, their involvement in signaling pathways regulating survival and apoptosis is well known. Over the last years, their function in more specific signaling events at the plasma membrane, modulating interactions with receptors and integrins, has been studied extensively. However, it remains still unclear how cells and organisms use these essential mechanisms for their vital functions. Besides the basic physical principles underlying the sphingolipid-mediated interactions, the localization of sphingolipids and the identification of all the enzymes involved in sphingolipid synthesis, transport and degradation also deserve our full attention. How do cells sense and regulate the local concentration of sphingolipids and how are sphingolipid metabolism and transport regulated in whole organisms? It will be a tremendous challenge to reveal the secrets of sphingolipid metabolism in cells and organisms. Let's start with it!

Scope of this thesis

Sphingolipids are an essential class of membrane lipids in eukaryotic cells. Besides their ability to promote bilayer rigidity and impermeability and their function in sorting of proteins, they also have been invoked in domain formation at the cell surface and they play important roles in signaling events. Complex glycosphingolipids (GSLs) have been found to modulate the activity of cell surface receptors, either by direct interactions with the (membrane) proteins, or by organizing them laterally, concentrating or excluding specific (membrane) proteins into domains. To get a better insight into how (glyco)sphingolipids influence and regulate/modulate different membrane proteins at the molecular level, a thorough knowledge of the localization of these lipids in the cell, of their transbilayer distribution and lateral organization is essential. The spatial organization of sphingolipids is determined by their synthesis, transport and degradation. In **chapter 2** of this thesis we focus on the synthesis of sphingomyelin (SM) and its analog ceramide phosphoethanolamine (CPE). SM is a ubiquitous component of the animal plasma membrane, and major source of ceramide, which is an antiproliferation factor involved in signal transduction. By balancing the levels of ceramide and diacylglycerol (DAG) in opposite directions, SM synthesis and degradation may play an essential role in cell growth and survival. In this study, we carried out a first systematic analysis of the 5 SM synthase family members in *C. elegans*. By using heterologous expression systems and gene KO approaches, we were able to uncover two SM synthases (SMS) and one CPE synthase in *C. elegans*. In the past decades, unexpected findings in sphingolipid-mediated events have drawn the organization and localization of these lipids into focus. Studying morphology by microscopy may be one of the technical approaches to

uncover the underlying molecular interactions of these events. In **chapter 3** we discuss the technical issues restraining progress in the elucidation of nanoscale localization of GSLs. Given the various pitfalls of the traditional methods, resolving these methodological problems provides a tremendous challenge. Various complex GSLs are of high medical interest, because they are used as receptors by viruses, bacteria and parasites. The accumulation of the monosialoganglioside GM1, due to enzyme defects in the degradation of this lipid, leads to a clinical phenotype called GM1 gangliosidosis or Landing disease. As for many other storage diseases, also for GM1 gangliosidosis it is unclear how the underlying molecular defect causes the pathology. **Chapter 4** of this thesis is set out to unravel the subcellular localization of GM1 in cells that lack β-galactosidase activity and therefore accumulate the ganglioside GM1. Electron microscopic immunolocalization after freeze substitution was chosen to detect GM1 in the storage cells, avoiding the potential methodological pitfalls which are discussed in chapter 3. GM1 appears to be mainly localized to the endosomal system of storage cells. GSLs, together with SM and cholesterol are able to self-organize into lipid domains, that laterally organize membrane function by regulating the participation of specific (membrane) proteins into these domains. These domains have been proposed to act as platforms for numerous cellular events, including signal transduction at the plasma membrane. In **chapter 5** we combine, for the first time, EM and homo-FRET analysis, to investigate the influence of GSLs on the nanoscale organization of small lipid-anchored proteins at the inner leaflet of the plasma membrane. Depletion of GSLs has no significant effect on the size of nanodomains. Strikingly, the number of proteins per nanodomain and the level of interaction between molecules in one cluster are clearly affected by the absence of GSLs. Finally, in **chapter 6**, the major findings of this thesis are presented and further implications are discussed.

References

Baumgart, T., Hammond, A.T., Sengupta, P., Hess, S.T., Holowka, D.A., Baird, B.A., and Webb, W.W. (2007). Large-scale fluid/fluid phase separation of proteins and lipids in giant plasma membrane vesicles. *Proc. Natl. Acad. Sci. USA* 104:3165-3170.

Birbes, H., El Bawab, S., Hannun, Y.A., and Obeid, L.M. (2001). Selective hydrolysis of a mitochondrial pool of sphingomyelin induces apoptosis. *Faseb J.* 15:2669-2679.

Boot, R.G., Verhoek, M., Donker-Koopman, W., Strijland, A., van Marle, J., Overkleeft, H.S., Wennekes, T., and Aerts, J.M. (2007). Identification of the non-lysosomal glucosylceramidase as beta-glucosidase 2. *J. Biol. Chem.* 282:1305-1312.

Bremer, E.G., Hakomori, S., Bowen-Pope, D.F., Raines, E., and Ross, R. (1984). Ganglioside-mediated modulation of cell growth, growth factor binding, and receptor phosphorylation. *J. Biol. Chem.* 259:6818-6825.

Brügger, B., Graham, C., Leibrecht, I., Mombelli, E., Jen, A., Wieland, F., and Morris, R. (2004). The membrane domains occupied by glycosylphosphatidylinositol-anchored prion protein and Thy-1 differ in lipid composition. *J. Biol. Chem.* 279:7530-7536.

Brügger, B., Sandhoff, R., Wegehingel, S., Gorgas, K., Malsam, J., Helms, J.B., Lehmann, W.D., Nickel, W., and Wieland, F.T. (2000). Evidence for segregation of sphingomyelin and cholesterol during formation of COPI-coated vesicles. *J. Cell Biol.* 151:507-517.

Buton, X., Herve, P., Kubelt, J., Tannert, A., Burger, K.N., Fellmann, P., Muller, P., Herrmann, A., Seigneuret, M., and Devaux, P.F. (2002). Transbilayer movement of monohexosylsphingolipids in endoplasmic reticulum and Golgi membranes. *Biochemistry* 41:13106-13115.

Chen, C.S., Martin, O.C., and Pagano, R.E. (1997). Changes in the spectral properties of a plasma membrane lipid analog during the first seconds of endocytosis in living cells. *Biophys. J.* 72:37-50.

Chen, Y., Qin, J., and Chen, Z.W. (2008). Fluorescence-topographic NSOM directly visualizes peak-valley polarities of GM1/GM3 rafts in cell membrane fluctuations. *J. Lipid Res.* 49:2268-2275.

Coste, H., Martel, M.B., and Got, R. (1986). Topology of glucosylceramide synthesis in Golgi membranes from porcine submaxillary glands. *Biochim. Biophys. Acta* 858:6-12.

Cowart, L.A., Szulc, Z., Bielawska, A., and Hannun, Y.A. (2002). Structural determinants of sphingolipid recognition by commercially available anti-ceramide antibodies. *J. Lipid Res.* 43:2042-2048.

D'Angelo, G., Polishchuk, E., Di Tullio, G., Santoro, M., Di Campli, A., Godi, A., West, G., Bielawski, J., Chuang, C.C., van der Spoel, A.C., Platt, F.M., Hannun, Y.A., Polishchuk, R., Mattjus, P., and De Matteis, M.A. (2007). Glycosphingolipid synthesis requires FAPP2 transfer of glucosylceramide. *Nature* 449:62-67.

Fujita, A., Cheng, J., Hirakawa, M., Furukawa, K., Kusunoki, S., and Fujimoto, T. (2007). Gangliosides GM1 and GM3 in the living cell membrane form clusters susceptible to cholesterol depletion and chilling. *Mol. Biol. Cell* 18:2112-2122.

Fujita, A., Cheng, J., and Fujimoto, T. (2009). Segretation of GM1 and GM3 clusters in the cell membrane depends on the intact actin cytoskeleton. *Biochim Biophys Acta* 1791:388–396.

Futerman, A.H., and Pagano, R.E. (1991). Determination of the intracellular sites and topology of glucosylceramide synthesis in rat liver. *Biochem. J.* 280:295-302.

Gómez-Moutón, C., Abad, J.L., Mira, E., Lacalle, R.A., Gallardo, E., Jiménez-Baranda, S., Illa, I., Bernad, A., Mañes, S., and Martínez-A., C. (2001). Segregation of leading-edge and uropod components into specific lipid rafts during T cell polarization. *Proc. Natl. Acad. Sci. USA* 98:9642-9647.

Greenshields, K.N., Halstead, S.K., Zitman, F.M., Rinaldi, S., Brennan, K.M., O'Leary, C., Chamberlain, L.H., Easton, A., Roxburgh, J., Pediani, J., Furukawa, K., Goodyear, C.S., Plomp, J.J. and Willison, H.J. (2009). The neuropathic potential of anti-GM1 autoantibodies is regulated by the local glycolipid environment in mice. *J. Clin. Invest.* 119:595-610.

Groux-Degroote, S., van Dijk, S.M., Wolthoorn, J., Neumann, S., Theos, A.C., De Maziere, A.M., Klumperman, J., van Meer, G., and Sprong, H. (2008). Glycolipid-dependent sorting of melanosomal from lysosomal membrane proteins by lumenal determinants. *Traffic* 9:951-963.

Halter, D., Neumann, S., van Dijk, S.M., Wolthoorn, J., de Maziere, A.M., Vieira, O.V., Mattjus, P., Klumperman, J., van Meer, G., and Sprong, H. (2007). Pre- and post-Golgi translocation of glucosylceramide in glycosphingolipid synthesis. *J. Cell Biol.* 179:101-115.

Hanada, K., Kumagai, K., Tomishige, N., and Yamaji, T. (2009). CERT-mediated trafficking of ceramide. *Biochim. Biophys. Acta* 1791:684-691.

Hancock, J.F. (2006). Lipid rafts, contentious only from simplistic standpoints. Nat. Rev. Mol. Cell Biol. 7:456-462.

Hannun, Y.A., and Obeid, L.M. (2008). Principles of bioactive lipid signalling: lessons from sphingolipids. *Nat. Rev. Mol. Cell Biol.* 9:139-150.

Hayashi, Y., Okino, N., Kakuta, Y., Shikanai, T., Tani, M., Narimatsu, H., and Ito, M. (2007). Klotho-related protein is a novel cytosolic neutral beta-glycosylceramidase. *J. Biol. Chem.* 282:30889-30900.

Henis, Y.I., Hancock, J.F., and Prior, I.A. (2009). Ras acylation, compartmentalization and signaling nanoclusters. *Mol. Membr. Biol.* 26:80-92.

Hoetzl, S., Sprong, H., and van Meer, G. (2007). The way we view cellular (glyco)sphingolipids. *J. Neurochem.* 103 Suppl 1:3-13.

Hofman, E.G., Ruonala, M.O., Bader, A.N., van den Heuvel, D., Voortman, J., Roovers, R.C., Verkleij, A.J., Gerritsen, H.C., and van Bergen en Henegouwen, P.M. (2008). EGF induces coalescence of different lipid rafts. *J. Cell Sci.* 121:2519-2528.

Hovnanian, A. (2005). Harlequin ichthyosis unmasked: a defect of lipid transport. *J. Clin. Invest.* 115:1708-1710.

Hovius, R., Lambrechts, H., Nicolay, K., and de Kruijff, B. (1990). Improved methods to isolate and subfractionate rat liver mitochondria. Lipid composition of the inner and outer membrane. *Biochim. Biophys. Acta* 1021:217-226.

Huitema, K., van den Dikkenberg, J., Brouwers, J.F., and Holthuis, J.C. (2004). Identification of a family of animal sphingomyelin synthases. *Embo J.* 23:33-44.

Hwang, Y.H., Tani, M., Nakagawa, T., Okino, N., and Ito, M. (2005). Subcellular localization of human neutral ceramidase expressed in HEK293 cells. *Biochem. Biophys. Res. Commun.* 331:37-42.

Janich, P., and Corbeil, D. (2007). GM1 and GM3 gangliosides highlight distinct lipid microdomains within the apical domain of epithelial cells. *FEBS Lett* 581:1783-1787.

Jeckel, D., Karrenbauer, A., Burger, K.N., van Meer, G., and Wieland, F. (1992). Glucosylceramide is synthesized at the cytosolic surface of various Golgi subfractions. *J. Cell Biol.* 117:259-267.

Jenkins, R.W., Canals, D., and Hannun, Y.A. (2009). Roles and regulation of secretory and lysosomal acid sphingomyelinase. *Cell Signal.* 21:836-846.

Kabayama, K., Sato, T., Saito, K., Loberto, N., Prinetti, A., Sonnino, S., Kinjo, M., Igarashi, Y., and Inokuchi, J. (2007). Dissociation of the insulin receptor and caveolin-1 complex by ganglioside GM3 in the state of insulin resistance. *Proc. Natl. Acad. Sci. USA* 104:13678-13683.

Kaida, K., Morita, D., Kanzaki, M., Kamakura, K., Motoyoshi, K., Hirakawa, M., and Kusunoki, S. (2004). Ganglioside complexes as new target antigens in Guillain-Barre syndrome. *Ann. Neurol.* 56:567-571.

Kim, R.H., Takabe, K., Milstien, S., and Spiegel, S. (2009). Export and functions of sphingosine-1-phosphate. *Biochim. Biophys. Acta* 1791:692-696.

Kitatani, K., Sheldon, K., Rajagopalan, V., Anelli, V., Jenkins, R.W., Sun, Y., Grabowski, G.A., Obeid, L.M., and Hannun, Y.A. (2009). Involvement of acid beta-glucosidase 1 in the salvage pathway of ceramide formation. *J. Biol. Chem.* 284:12972-12978.

Klemm, R.W., Ejsing, C.S., Surma, M.A., Kaiser, H.J., Gerl, M.J., Sampaio, J.L., de Robillard, Q., Ferguson, C., Proszynski, T.J., Shevchenko, A., and Simons, K. (2009). Segregation of sphingolipids and sterols during formation of secretory vesicles at the trans-Golgi network. *J. Cell Biol.* 185:601-612.

Kohyama-Koganeya, A., Sasamura, T., Oshima, E., Suzuki, E., Nishihara, S., Ueda, R., and Hirabayashi, Y. (2004). Drosophila glucosylceramide synthase, a negative regulator of cell death mediated by proapoptotic factors. *J. Biol. Chem.* 279:35995-36002.

Kojima, N., and Hakomori, S. (1989). Specific interaction between gangliotriaosylceramide (Gg3) and sialosyllactosylceramide (GM3) as a basis for specific cellular recognition between lymphoma and melanoma cells. *J. Biol. Chem.* 264:20159-20162.

Koval, M., and Pagano, R.E. (1990). Sorting of an internalized plasma membrane lipid between recycling and degradative pathways in normal and Niemann-Pick, Type A fibroblasts. *J. Cell Biol.* 111:429-442.

Lingwood, D., Ries, J., Schwille, P., and Simons, K. (2008). Plasma membranes are poised for activation of raft phase coalescence at physiological temperature. *Proc. Natl. Acad. Sci. USA* 105:10005-10010.

Lloyd, K.O., Gordon, C.M., Thampoe, I.J., DiBenedetto, C. (1992) Cell surface accessibility of individual gangliosides in malignant melanoma cells to antibodies is influenced by the total ganglioside composition of the cells. *Cancer Res.* 52:4948-4953.

Lloyd-Evans, E., Morgan, A.J., He, X., Smith, D.A., Elliot-Smith, E., Sillence, D.J., Churchill, G.C., Schuchman, E.H., Galione, A., and Platt, F.M. (2008). Niemann-Pick disease type C1 is a sphingosine storage disease that causes deregulation of lysosomal calcium. *Nat. Med.* 14:1247-1255.

López-Montero, I., Rodriguez, N., Cribier, S., Pohl, A., Velez, M., and Devaux, P.F. (2005). Rapid transbilayer movement of ceramides in phospholipid vesicles and in human erythrocytes. *J. Biol. Chem.* 280:25811-25819.

Madore, N., Smith, K.L., Graham, C.H., Jen, A., Brady, K., Hall, S., and Morris, R. (1999). Functionally different GPI proteins are organized in different domains on the neuronal surface. *EMBO J.* 18:6917-6926.

Magee, A.I., Adler, J., and Parmryd, I. (2005). Cold-induced coalescence of T-cell plasma membrane microdomains activates signalling pathways. *J. Cell Sci.* 118:3141-3151.

Maggio, B., Cumar, F.A., and Caputto, R. (1978). Interactions of gangliosides with phospholipids and glycosphingolipids in mixed monolayers. *Biochem. J.* 175:1113-1118.

Mao, C., and Obeid, L.M. (2008). Ceramidases, regulators of cellular responses mediated by ceramide, sphingosine, and sphingosine-1-phosphate. *Biochim. Biophys. Acta* 1781:424-434.

Martin, O.C., and Pagano, R.E. (1994). Internalization and sorting of a fluorescent analogue of glucosylceramide to the Golgi apparatus of human skin fibroblasts: utilization of endocytic and nonendocytic transport mechanisms. *J. Cell Biol.* 125:769-781.

Matyas, G.R., and Morre, D.J. (1987). Subcellular distribution and biosynthesis of rat liver gangliosides. *Biochim. Biophys. Acta* 921:599-614.

Mayor, S., and Maxfield, F.R. (1995). Insolubility and redistribution of GPI-anchored proteins at the cell surface after detergent treatment. *Mol. Biol. Cell* 6:929-944.

Milani, S., Sottocornola, E., Zava, S., Berselli, P., Berra, B., and Colombo, I. (2007). Ganglioside GM3 is stably associated to tyrosine-phosphorylated ErbB2/EGFR receptor complexes and EGFR monomers, but not to ErbB2. *Biochim. Biophys. Acta* 1771:873-878.

Miljan, E.A., Meuillet, E.J., Mania-Farnell, B., George, D., Yamamoto, H., Simon, H.G., and Bremer, E.G. (2002). Interaction of the extracellular domain of the epidermal growth factor receptor with gangliosides. *J. Biol. Chem.* 277:10108-10113.

Miyagi, T., Wada, T., Yamaguchi, K., Hata, K., and Shiozaki, K. (2008). Plasma membrane-associated sialidase as a crucial regulator of transmembrane signalling. *J. Biochem.* 144:279-285.

Mondal, M., Mesmin, B., Mukherjee, S., and Maxfield, F.R. (2009). Sterols are mainly in the cytoplasmic leaflet of the plasma membrane and the endocytic recycling compartment in CHO cells. *Mol. Biol. Cell* 20:581-588.

Morales, A., Lee, H., Goni, F.M., Kolesnick, R., and Fernandez-Checa, J.C. (2007). Sphingolipids and cell death. *Apoptosis* 12:923-939.

Mukherjee, S., Soe, T.T., and Maxfield, F.R. (1999). Endocytic sorting of lipid analogues differing solely in the chemistry of their hydrophobic tails. *J. Cell Biol.* 144:1271-1284.

Neumann, S., and van Meer, G. (2008). Sphingolipid management by an orchestra of lipid transfer proteins. *Biol. Chem.* 389:1349-1360.

Parton, R.G. (1994). Ultrastructural localization of gangliosides; GM1 is concentrated in caveolae. J. *Histochem. Cytochem.* 42:155-166.

Pewzner-Jung, Y., Ben-Dor, S., and Futerman, A.H. (2006). When do LASSes (longevity assurance genes) become CerS (ceramide synthases)?, Insights into the regulation of ceramide synthesis. *J. Biol. Chem.* 281:25001-25005.

Raggers, R.J., van Helvoort, A., Evers, R., and van Meer, G. (1999). The human multidrug resistance protein MRP1 translocates sphingolipid analogs across the plasma membrane. *J. Cell Sci.* 112:415-422.

Regina Todeschini, A., and Hakomori, S.I. (2008). Functional role of glycosphingolipids and gangliosides in control of cell adhesion, motility, and growth, through glycosynaptic microdomains. *Biochim. Biophys. Acta* 1780:421-433.

Römer, W., Berland, L., Chambon, V., Gaus, K., Windschiegl, B., Tenza, D., Aly, M.R., Fraisier, V., Florent, J.C., Perrais, D., Lamaze, C., Raposo, G., Steinem, C., Sens, P., Bassereau, P., and Johannes, L. (2007). Shiga toxin induces tubular membrane invaginations for its uptake into cells. *Nature* 450:670-675.

Schulze, H., Kolter, T., and Sandhoff, K. (2009). Principles of lysosomal membrane degradation: Cellular topology and biochemistry of lysosomal lipid degradation. *Biochim. Biophys. Acta* 1793:674-683.

Sharma, D.K., Choudhury, A., Singh, R.D., Wheatley, C.L., Marks, D.L., and Pagano, R.E. (2003). Glycosphingolipids internalized via caveolar-related endocytosis rapidly merge with the clathrin pathway in early endosomes and form microdomains for recycling. *J. Biol. Chem.* 278:7564-7572.

Sharom, F.J., and Grant, C.W. (1978). A model for ganglioside behaviour in cell membranes. *Biochim. Biophys. Acta* 507:280-293.

Simons, K., and van Meer, G. (1988). Lipid sorting in epithelial cells. *Biochemistry* 27:6197-6202.

Smith, D.C., Sillence, D.J., Falguieres, T., Jarvis, R.M., Johannes, L., Lord, J.M., Platt, F.M., and Roberts, L.M. (2006). The association of Shiga-like toxin with detergent-resistant membranes is modulated by glucosylceramide and is an essential requirement in the endoplasmic reticulum for a cytotoxic effect. *Mol. Biol. Cell* 17:1375-1387.

Sorre, B., Callan-Jones, A., Manneville, J.B., Nassoy, P., Joanny, J.F., Prost, J., Goud, B., and Bassereau, P. (2009). Curvature-driven lipid sorting needs proximity to a demixing point and is aided by proteins. *Proc. Natl. Acad. Sci. USA* 106:5622-5626.

Sottocornola, E., Misasi, R., Mattei, V., Ciarlo, L., Gradini, R., Garofalo, T., Berra, B., Colombo, I., and Sorice, M. (2006). Role of gangliosides in the association of ErbB2 with lipid rafts in mammary epithelial HC11 cells. *FEBS J.* 273:1821-1830.

Sprong, H., Degroote, S., Claessens, T., van Drunen, J., Oorschot, V., Westerink, B.H., Hirabayashi, Y., Klumperman, J., van der Sluijs, P., and van Meer, G. (2001). Glycosphingolipids are required for sorting melanosomal proteins in the Golgi complex. *J. Cell Biol.* 155:369-380.

Tafesse, F.G., Huitema, K., Hermansson, M., van der Poel, S., van den Dikkenberg, J., Uphoff, A., Somerharju, P., and Holthuis, J.C. 2007. Both sphingomyelin synthases SMS1 and SMS2 are required for sphingomyelin homeostasis and growth in human HeLa cells. *J Biol Chem* 282:17537-17547.

Tani, M., and Hannun, Y.A. (2007). Neutral sphingomyelinase 2 is palmitoylated on multiple cysteine residues. Role of palmitoylation in subcellular localization. *J. Biol. Chem.* 282:10047-10056.

Ternes, P., Brouwers, J.F., van den Dikkenberg, J., and Holthuis, J.C. (2009). Sphingomyelin synthase SMS2 displays dual activity as ceramide phosphoethanolamine synthase. *J. Lipid Res.*, in press.

Tillack, T.W., Allietta, M., Moran, R.E., and Young, W.W., Jr. (1983). Localization of globoside and Forssman glycolipids on erythrocyte membranes. *Biochim. Biophys. Acta* 733:15-24.

Vacaru, A.M., Tafesse, F.G., Ternes, P., Kondylis, V., Hermansson, M., Brouwers, J.F., Somerharju, P., Rabouille, C., and Holthuis, J.C. (2009). Sphingomyelin synthase-related protein SMSr controls ceramide homeostasis in the ER. *J. Cell Biol.* 185:1013-1027.

van Helvoort, A., Smith, A.J., Sprong, H., Fritzsche, I., Schinkel, A.H., Borst, P., and van Meer, G. (1996). MDR1 P-glycoprotein is a lipid translocase of broad specificity, while MDR3 P-glycoprotein specifically translocates phosphatidylcholine. *Cell* 87:507-517.

van Meer, G. (1989). Lipid traffic in animal cells. *Annu. Rev. Cell Biol.* 5:247-275.

van Meer, G., Voelker, D.R., and Feigenson, G.W. (2008). Membrane lipids: where they are and how they behave. *Nat. Rev. Mol. Cell Biol.* 9:112-124.

Varma, R., and Mayor, S. (1998). GPI-anchored proteins are organized in submicron domains at the cell surface. *Nature* 394:798-801.

Wang, J., Gunning, W., Kelley, K.M., and Ratnam, M. (2002). Evidence for segregation of heterologous GPI-anchored proteins into separate lipid rafts within the plasma membrane. *J. Membr. Biol.* 189:35-43.

Warnock, D.E., Lutz, M.S., Blackburn, W.A., Young, W.W., Jr., and Baenziger, J.U. (1994). Transport of newly synthesized glucosylceramide to the plasma membrane by a non-Golgi pathway. *Proc. Natl. Acad. Sci. USA* 91:2708-2712.

Willem, J., ter Beest, M., Scherphof, G., and Hoekstra, D. (1990). A non-exchangeable fluorescent phospholipid analog as a membrane traffic marker of the endocytic pathway. *Eur. J. Cell Biol.* 53:173-184.

Yamaoka, S., Miyaji, M., Kitano, T., Umehara, H., and Okazaki, T. (2004). Expression cloning of a human cDNA restoring sphingomyelin synthesis and cell growth in sphingomyelin synthase-defective lymphoid cells. *J. Biol. Chem.* 279:18688-18693.

Yamashita, T., Wada, R., Sasaki, T., Deng, C., Bierfreund, U., Sandhoff, K., and Proia, R.L. (1999). A vital role for glycosphingolipid synthesis during development and differentiation. *Proc. Natl. Acad. Sci. USA* 96:9142-9147.

Yildiz, Y., Matern, H., Thompson, B., Allegood, J.C., Warren, R.L., Ramirez, D.M., Hammer, R.E., Hamra, F.K., Matern, S., and Russell, D.W. (2006). Mutation of beta-glucosidase 2 causes glycolipid storage disease and impaired male fertility. *J. Clin. Invest.* 116:2985-2994.

Yoon, S.J., Nakayama, K., Hikita, T., Handa, K., and Hakomori, S.I. (2006). Epidermal growth factor receptor tyrosine kinase is modulated by GM3 interaction with N-linked GlcNAc termini of the receptor. *Proc. Natl. Acad. Sci. USA* 103:18987-18991.

Chapter 2

Systematic analysis of the sphingomyelin synthase family in *C. elegans*

Sandra Hoetzl, Fikadu Geta Tafesse, Joep van den Dikkenberg and Joost C. M. Holthuis

Manuscript in preparation

Membrane Enzymology, Bijvoet Center and Institute of Biomembranes, Utrecht University, Utrecht, The Netherlands

Abstract
Besides sustaining the integrity and organization of cellular membranes, the enzymes responsible for the production of sphingomyelin (SM) and its analog ceramide phosphoethanolamine (CPE) have considerable biological potential as regulators of the anti-proliferation factor ceramide and the pro-survival factor diacylglycerol. The identification of a multigenic SM synthase (SMS) family has created new opportunities to address the biological roles of these enzymes and their metabolites. The nematode *C. elegans* is an attractive model system for animal growth and development. This organism contains five SMS homologues, but none of these have been characterized in any detail. Here, we carried out the first systematic analysis of SMS family members in *C. elegans.* Using heterologous expression systems and gene KO approaches, we show that *C. elegans* contains multiple SM and CPE synthases in various compartments of the secretory pathway. Surprisingly, a combinatorial loss of these enzymes had no obvious impact on *C. elegans* growth or lifespan, unlike the situation in mammalian cells.

Introduction
Sphingolipids are an essential class of membrane lipids in eukaryotic cells. Their high packing density and affinity for sterols make a vital contribution to the barrier function of cellular membranes. In recent years, considerable attention has been drawn to the concept that sphingolipids and sterols can self-organize into lipid assemblies, called membrane microdomains or rafts, that laterally organize membrane functions by specifically concentrating or excluding specific membrane proteins (Hancock, 2006; van Meer et al. 2008). These microdomains have been postulated to serve as platforms for various cellular events, including protein sorting and signal transduction at the plasma membrane (Simons and Toomre, 2000). Besides their roles in membrane integrity and organization, sphingolipids have emerged as a novel class of signaling molecules that regulate a wide spectrum of cellular processes. Ceramide, a central intermediate of sphingolipid metabolism, induces anti-proliferative responses such as cell cycle arrest, apoptosis and senescence by activating an array of protein kinases and phosphatases (Verheij et al., 1996; Hannun, 1996; Kolesnick and Krönke, 1998; Hannun and Obeid, 2008). Attenuation of ceramide levels and/or increased levels of the phosphorylated ceramide derivative sphingosine-1-phosphate have been implicated in various stages of cancer pathogenesis, including anti-apoptotic phenotype, metastasis and escape from senescence (Kolesnick and Krönke, 1998; Spiegel and Milstien, 2003; Ogretmen and Hannun, 2004).

Sphingomyelin (SM) is a ubiquitous component of animal plasma membranes and a major source of ceramide involved in signal transduction. Both acid and neutral SMases can catalyze the hydrolysis of SM, resulting in the liberation of

ceramide and phosphocholine. Signals that activate SMases range from ultraviolet light, irradiation and hypoxia to biological factors such as tumor necrosis factor-α, interferon-γ and Fas antibody (Wiegmann et al., 1994; Adam-Klages et al., 1996; Marchesini and Hannun, 2004). SM production involves the transfer of phosphocholine from phosphatidylcholine onto ceramide. This reaction is catalyzed by SM synthase and yields diacylglycerol (DAG) as a side product. DAG is a well-established signaling molecule for cell proliferation through activation of protein kinase C and acts competitively against ceramide-induced apoptosis (Hampton and Morand, 1989; Hannun and Bell, 1989; Yang and Kazanietz, 2003). Thus, by simultaneously regulating ceramide and DAG in opposite directions, SM synthase may play a fundamental role in cell growth and survival.

Even though the organizing and regulatory capacity of sphingolipids is widely acclaimed, direct evidence for this has been limited in part due to incomplete knowledge of the enzymes involved in their synthesis and breakdown. We previously reported the identification of a conserved family of polytopic membrane proteins that display all the characteristics attributed to SM synthase (Huitema et al. 2004). Strikingly, we uncovered a multitude of SM synthase (SMS) genes in each organism capable of SM production. Human cells contain two isoforms of SM synthase, namely SMS1 in the Golgi complex, responsible for producing the bulk of cellular SM, and SMS2 at the plasma membrane, likely serving a principle role in signal transduction (Huitema et al., 2004; Tafesse et al., 2007). In addition, the human genome contains a third, SM synthase-related (SMSr) gene that catalyses the production of the SM analog ceramide phosphoethanolamine (CPE) in the ER (Ternes et al., 2009; Vacaru et al., 2009). All three enzymes contribute significantly to the local regulation of ceramide levels and serve critical roles in cell growth and survival (Yamaoka et al., 2004; Tafesse et al., 2007; Tafesse et al., MS in prep).

The identification of a multigenic SMS family opened up important new avenues for studying sphingolipid function in animals. In this respect, *C. elegans* offers an attractive model system. The availability of a detailed description of the animal's morphology, development and physiology combined with the ease to manipulate gene function through mutation and RNAi makes this model ideal for dissecting the biological roles of SM synthases and related enzymes at the molecular level. In many cases where mammalian systems are too complicated to obtain clear information on the molecular ordering of signaling pathways, *C. elegans* has been instructive. This is particularly true for the mechanisms controlling apoptosis and cell division, two integral and invariant components of *C. elegans* development (Metzstein et al., 1998; Koreth and van den Heuvel, 2005). The *C. elegans* genome encodes five SMS family members, but none of these have been characterized in any detail.

In here, we carried out the first systematic analysis of SMS family members in *C. elegans* with the long-term goal to uncover the full regulatory potential of SM synthases and related enzymes in animal growth and development.

Results

Phylogenetic analysis and expression of SMS family members in C. elegans

The *C. elegans* genome encodes five SMS family members, which we have named SMSα, SMSβ, SMSγ, SMSδ and SMSr. These proteins contain six membrane spans, share a common LPP-like active site motif and display at least 24% sequence identity with the human SM synthase SMS1. Phylogenetically, SMSα, SMSβ, SMSγ and SMSδ form clusters with homologues of other nematodes (i.e. *C. briggsae, C. remanei,* and *C. brenneri*) that are separate from those containing vertebrate SMS1 and SMS2 (Figure 1A). SMSr, on the other hand, shows a higher degree of conservation and forms a cluster containing both vertebrate and invertebrate homologues.

To investigate the expression of SMS family members in *C. elegans,* we performed RT-PCR on total RNA isolated from a mixed state population of the wild type strain N2. This allowed the detection of transcripts for SMSα, SMSβ, SMSγ and SMSr (Figure 1B). In contrast, we were unable to detect a transcript for SMSδ. The same was true when RT-PCR was performed with an independent, SMSδ–specific primer set (data not shown). This precluded cloning of the SMSδ cDNA. For the remainder of this study, we therefore focused on the characterization of SMSα, SMSβ, SMSγ and SMSr.

► **Figure 1. Phylogenetic analysis of SM synthases in nematodes and vertebrates.** (A) Phylogenetic Tree of SM synthase proteins from *Homo sapiens* (hs), *Drosophila melanogaster* (dm), *Gallus Gallus* (gg), *Xenopus tropicalis* (xt), *Xenopus laevis* (xl), *Danio rerio* (dr) and the nematodes *Caenorhabditis elegans* (ce), *Caenorhabditis briggsae* (cb), *Caenorhabditis remanei* (cr) and *Caenorhabditis brenneri* (cn). The tree was constructed with Tree Puzzle (Schmidt et al., 2002) from protein sequences that were aligned using T-Coffee (Notredame et al., 2000), and displayed using TreeIllustrator (http://www.genohm.com). SwissProt accession numbers, NCBI reference sequences or wormbase protein IDs are: (1) A8KBN3; (2) Q5U3Z9; (3) Q640R5; (4) NP_001018461.1; (5) Q86VZ5; (6) NP_989721.2; (7) A0JMNO; (8) XP_426501.2; (9) XP_00123149.2 (10) Q8NHU3 (11) Q5M7L7; (12) Q6DEI3; (13) Q9VS60; (14) A4QNV5; (15) B0BLX7; (16) Q28CJ3; (17) XP_426501.2; (18) Q96LT4; (19) RP:RP39824; (20) Q20696; (21) BP:CBP26306; (22) CN:CN16655; (23) CN:CN19482; (24) RP:RP33128; (25) BP:CBP15849; (26) Q9TYV2; (27) BP:CBP32601; (28) Q965Q4; (29) RP:RP06655; (30) CN:CN14615; (31) RP:RP15984; (32) BP:CBP01983; (33) CN:CN23351; (34) Q20735; (35) CN:CN26856; (36) RP:RP41176; (37) BP:CBP31089; (38) CE:CE19930. (B) Expression of SM synthase homologues in *C. elegans* using RT-PCR. Reverse transcription PCR of mRNAs of SMSα, SMSβ, SMSγ, SMSδ and SMSr using total RNA isolated from *C. elegans* N2 worms. To verify that same amounts of RNA were used for each reaction, the *gapdh* gene is shown.

SMS family members display different subcellular distributions

Previous work showed striking differences in subcellular distributions between the three members of the human SMS family, with SMS1 localized to the Golgi, SMS2 at the plasma membrane, and SMSr in the ER (Huitema et al., 2004; Vacaru et al., 2009). Thus, one potential explanation for the expansion of SMS family members in *C. elegans* could be a further diversification of the cellular sites of SM production.

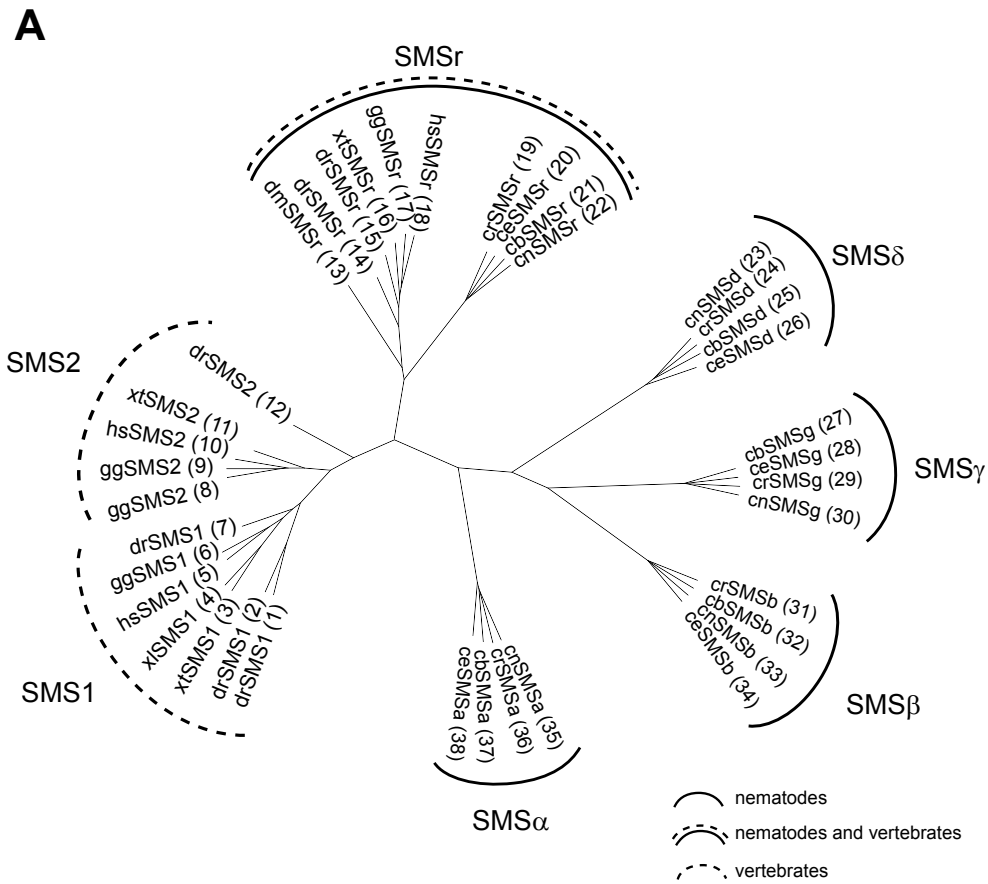

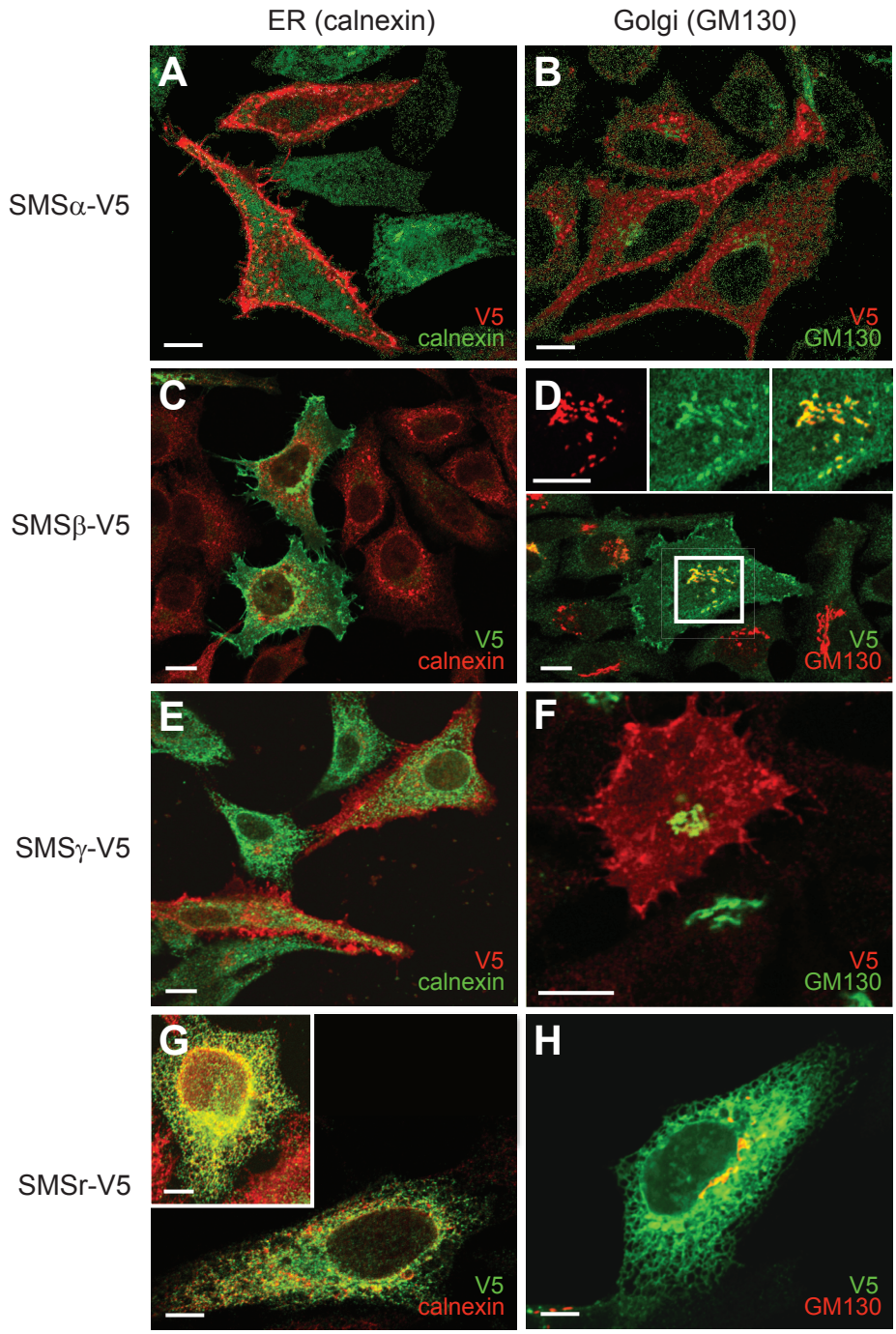
ER (calnexin)
Golgi (GM130)
SMSα-V5
SMSβ-V5
SMSγ-V5
SMSr-V5
A
B
C
D
E
F
G
H
V5
calnexin
V5
GM130

To investigate this possibility, we expressed V5-tagged versions of SMSα, SMSβ, SMSγ gand SMSr in human HeLa cells and analyzed their subcellular distributions by immunofluorescence microscopy. SMSα, SMSβ, and SMSγ primarily localized at the plasma membrane (Figures 2A,C,E). In addition, SMSα was found in internal vesicles that were spread throughout the cytoplasm, did not contain the Golgi marker GM130, and likely correspond to compartments of the endosomal/lysosomal system (Figures 2A,B). Besides its association with the PM, a significant portion of SMSβ co-localized with GM130, indicating that at least part of the protein is retained in the Golgi (Figure 2D). SMSγ, on the other hand, localized almost exclusively at the plasma membrane (Figures 2E,F). SMSr, like its human counterpart, resided in the ER, as evidenced by an extensive co-localization with the ER marker calnexin (Figure 2G). Immunofluorescence microscopy of *Drosophila* S2 cells expressing the four *C. elegans* SMS proteins revealed the same localization patterns (data not shown). From this we conclude that members of the *C. elegans* SMS family have partially overlapping but also unique subcellular distributions, and together occupy all principal compartments of the secretory pathway (ER, Golgi, plasma membrane and endosomes).

The SMS family harbors both SM and CPE synthases

While human SMS1 and SMSr act as monofunctional SM and CPE synthase activities, respectively, human SMS2 possesses dual activity as SM and CPE synthase (Huitema et al. 2004; Ternes et al., 2009; Vacaru et al. 2009). To analyze the enzymatic properties of the four SMS homologues of *C. elegans*, V5-tagged versions of SMSα, SMSβ, SMSγ and SMSr were expressed in budding yeast, an organism lacking endogenous SM and CPE synthase activity. Expression was verified by immunoblotting using an antibody against the V5 epitope (Figure 3A). SMS-expressing yeast cells were lysed and then incubated with fluorescent C_6-NBD-ceramide (NBD-Cer). TLC analysis of the reaction mixture of SMSr-expressing cells showed the presence of an NBD-labeled product with a retention value distinct from that of NBD-SM or C_6-NBD-ceramide phosphoinositol (NBD-CPI), but similar to that of NBD-CPE (Figure 3B). This product was missing in reactions performed with control (empty vector, EV) cells, but present in reactions carried out with cells expressing human or *Drosophila* SMSr. Moreover, LC-MS/MS analysis of a lipid extract of yeast cells expressing *C. elegans* SMSr revealed the presence of several molecular species of CPE (data not shown). The extract was devoid of SM. No CPE was detectable in control cells. These results show that *C. elegans* SMSr, like its human and *Drosophila*

◄ **Figure 2. Subcellular localization analysis of SMS proteins in Hela cells.** Immunofluorescence microscopy of HeLa cells transfected with V5-tagged versions of SMS proteins. Cells were grown on coverslips, fixed and then co-stained with rabbit anti-V5 and mouse anti-GM130 antibodies or anti-calnexin, respectively. Counterstaining was done with Alexa-conjugated goat anti-rabbit and goat anti-mouse antibodies. Bar, 10 μm.

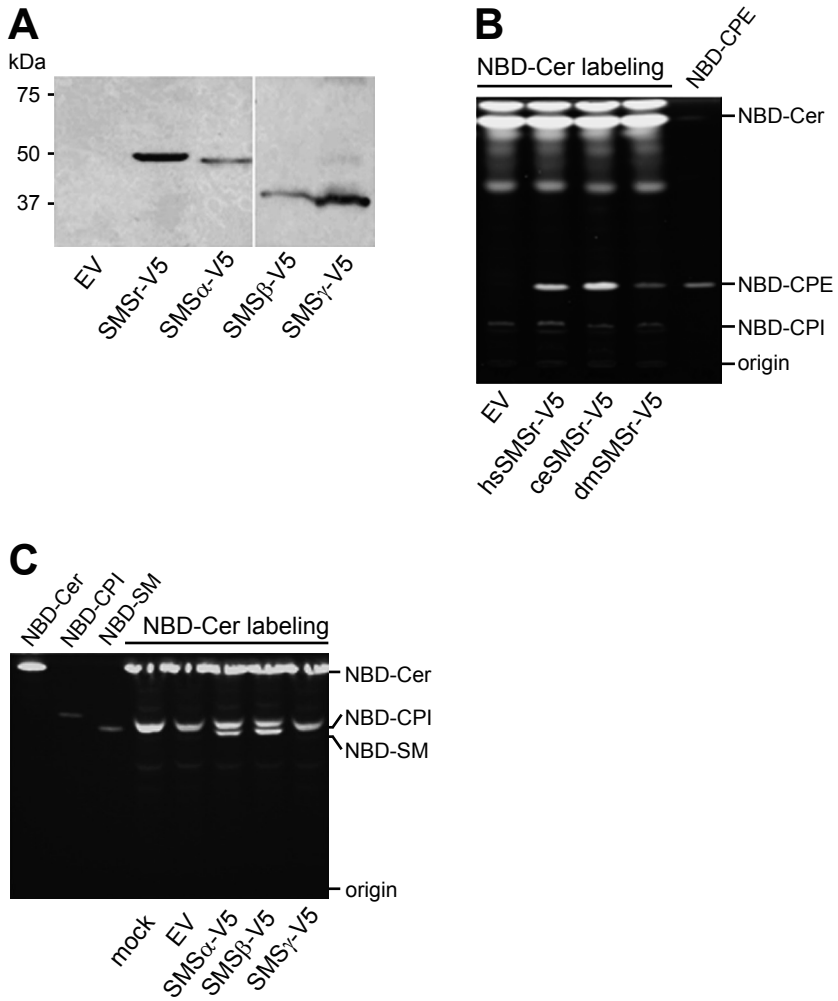

Figure 3. Heterologous expression of SMS proteins in yeast reveals SM and CPE synthase activity. (A) Expression of ceSMS-V5 proteins in yeast cells. Immunoblot of membrane protein extracts derived from yeast cells, transfected with empty vector (EV) or V5-tagged versions of *C. elegans* SMS proteins. Constructs were probed with mouse anti-V5 monoclonal antibody. (B) CPE synthase and (C) SM synthase activity in yeast cells (NBD-Cer labeling). Post-nuclear supernatants of yeast strains expressing human, drosophila and *C. elegans* SMS, or transformed with empty vector (EV) were incubated with NBD-Cer. NBD-labeled lipids were separated by TLC and detected by fluorescence scanning.

counterparts, functions as a CPE synthase. TLC analysis of the reaction mixtures from cells expressing SMSα or SMSβ showed the presence of NBD-SM (Figure 3C). These mixtures lacked NBD-CPE, but contained NBD-CPI, which is due to an endogenous

CPI synthase. Together, these results indicate that SMSα and SMSβ act as SM synthases. Reaction mixtures of cells expressing SMSγ, on the other hand, lacked any detectable level of NBD-SM or NBD-CPE.

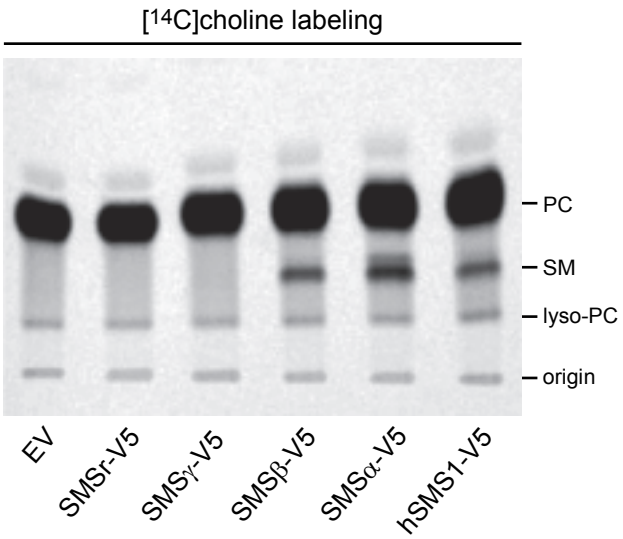

Figure 4. SM synthase activity in S2 insect cells ([^{14}C]choline metabolic labeling). *Drosophila* S2 cells, expressing hSMS1-V5 and SMSα-V5, SMSβ-V5, SMSγ-V5 and ceSMSr-V5 were labeled with [^{14}C]choline for 2 h and subjected to lipid extraction. Lipid extracts were analyzed by TLC and autoradiography.

To verify the substrate specificities of *C. elegans* SMS proteins and to exclude the possibility that the lack of a detectable SM and/or CPE synthase activity of SMSγ is due to the use of yeast as heterologous expression system, we next analyzed the ability of the SMS proteins to support SM production in *Drosophila* S2 cells. In comparison to budding yeast, *Drosophila* is evolutionary closer related to *C. elegans,* but also offers the advantage that the organism lacks an endogenous SM synthase activity. We therefore expressed V5-tagged SMSα, SMSβ, SMSγ and SMSr in S2 cells and then performed metabolic labeling with [^{14}C]choline to monitor the production of [^{14}C]-labeled SM (Figure 4). TLC analysis of labeled cell extracts showed that SMSα and SMSβ each supported production of SM, hence consistent with the outcome of the experiments in yeast. However, expression of SMSγ did not result in any detectable production of SM in S2 cells.

In sum, these results show that *C. elegans* contains at least one CPE synthase, namely SMSr, and two SM synthases, namely SMSα and SMSβ. The reaction catalyzed by SMSγ, on the other hand, remains unclear. As acomplementary approach to define the functional characteristics of these proteins, we next analyzed the consequences of their genetic ablation in *C. elegans*.

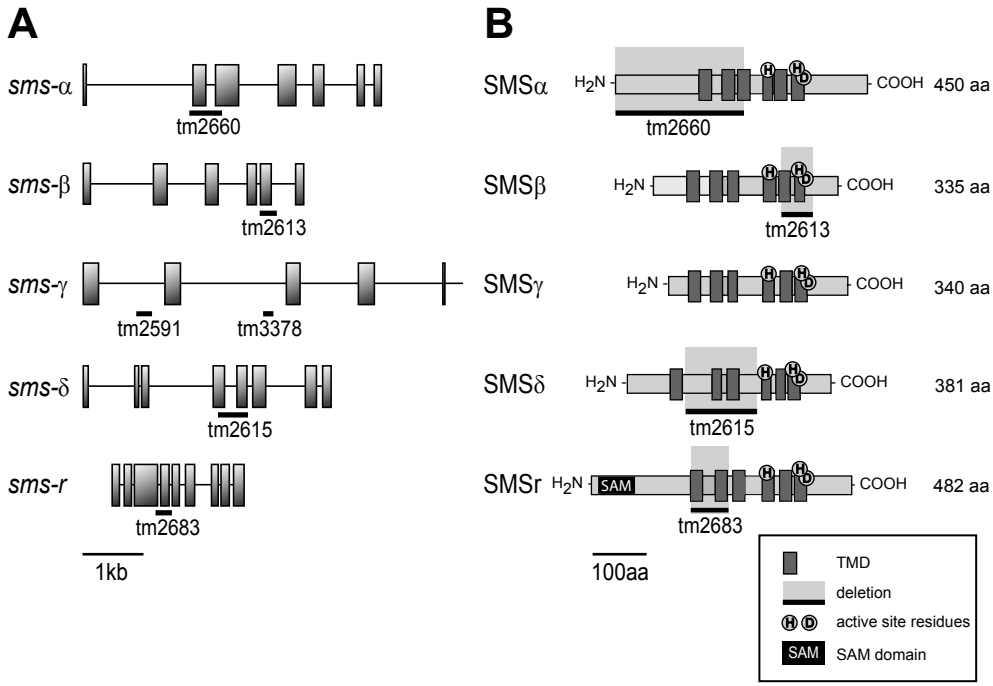
A
sms-α
tm2660
sms-β
tm2613
sms-γ
tm2591
tm3378
sms-δ
tm2615
sms-r
tm2683
1kb
B
SMSα
SMSβ
SMSγ
SMSδ
SMSr
H2N
COOH
SAM
450 aa
335 aa
340 aa
381 aa
482 aa
100aa
TMD
deletion
active site residues
SAM domain

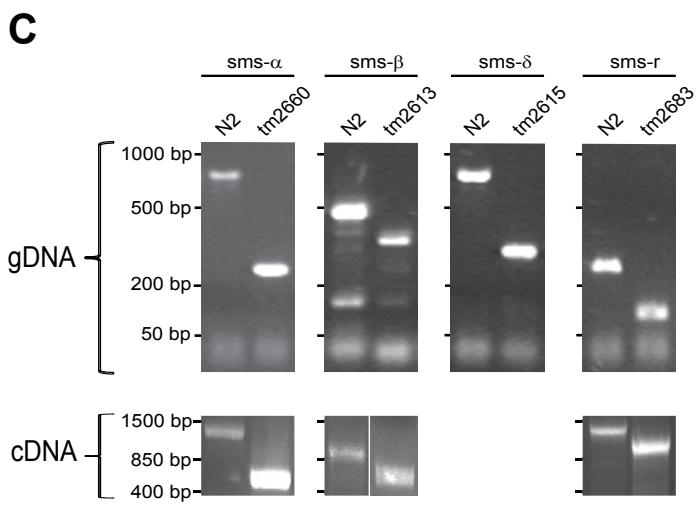
C
sms-α
sms-β
sms-δ
sms-r
N2
tm2660
tm2613
tm2615
tm2683
gDNA
1000 bp
500 bp
200 bp
50 bp
cDNA
1500 bp
850 bp
400 bp

Characterization of C. elegans sms mutants

To analyze the impact of eliminating individual SMS family members in *C. elegans*, deletion mutants in the different *sms* loci were obtained from the National Biosource Project in Japan (NBP). Mutant strains with deletions in the open reading frames of *sms*-α (tm2660), *sms*-β (tm2613), *sms*-δ (tm2615), and *sms*-r (tm2683) genes were obtained. The precise extent and location of the deletions in the *sms* mutants are depicted in Figures 5A,B. Mutations were mapped by single worm PCR on genomic DNA using primers flanking the deletion areas (Figure 5C, upper panel). The primer sets used for PCR are displayed in Supplementary Table 1. To check whether the respective deletions in *sms* genes would lead to a complete loss-of-function, the cDNAs corresponding to the mutated *sms* genes were cloned by RT-PCR on total RNA isolated from the *sms* mutant strains (Figure 5C, lower panel).

The tm2660 allele has a deletion of 588 bp that affects two exons in *sms*-α (Figure 5A). At the mRNA level, this results in a frameshift at the codon for Gly17 and introduces a premature stop after residue 37. The first available start methionine corresponds to Met232 in wild type sms-α. When used, this would give rise to a N-terminally truncated protein that lacks the first three membrane spans (Figure 5B). SMS family members normally have six membrane spans, a feature that is conserved throughout the LPP superfamily (Huitema et al., 2004). Consequently, it is very unlikely that tm2660 codes for an enzymatically active version of SMSα. A 176-bp deletion in the tm2613 allele leads to a gap in the protein-coding region of *sms*-β from residue 234 to 292 (Figures 5A,B). This deletion covers membrane spans 5 and 6 as well as the conserved active site residues His339 and Asp343. From this we conclude that tm2613 corresponds to a total loss-of-function allele of *sms*-β. A 507-bp deletion in tm2615 leads to removal of membrane spans 4 and 5 as well as active site residue His255 in SMSδ. This indicates that tm2615 corresponds to a loss-of-function allele of *sms*-δ.

◄ **Figure 5. Characterization of SM synthases in *C. elegans*.** (A) Genetic map of *C. elegans sms* genes. The genomic structures of the *sms-α, sms-β, sms-γ, sms-δ and sms-r* genes are shown. Gray boxes correspond to coding exons, introns are depicted as lines. The positions of mutations with respect to the gene are indicated below, namely tm2660, tm2613, tm2615 and tm2683. Mutation strains carrying deletions in the *sms-γ* gene, tm2591 and tm3378 have only recently become available, and are not included in this study. (B) Schematic structure of the *C. elegans* SMS proteins. The schemes show common domains as the transmembrane domains (solid boxes), the SAM domain (black box) and indicate the position of histidine (H) and aspartate (D) residues, forming the active site of the proteins. The positions of mutations are indicated, and the effect of the deletions on the proteins, are marked by the light gray box. In contrast to the other proteins, the position of the deletion in SMSδ could not be confirmed by PCR on cDNA. (C) Mutant alleles and their mRNA transcripts were characterized by PCR. Locus-specific PCR tests on genomic DNA (gDNA) were used to track deletion alleles. On agarose gels, products from deletion alleles are visibly smaller than the wild type alleles. PCR tests on cDNA reveal a deletion of 588 bp for SMSα, a deletion of 176 bp for SMSβ and a deletion of 210 bp for SMSr. Primers used in this studies are described in Material and Methods.

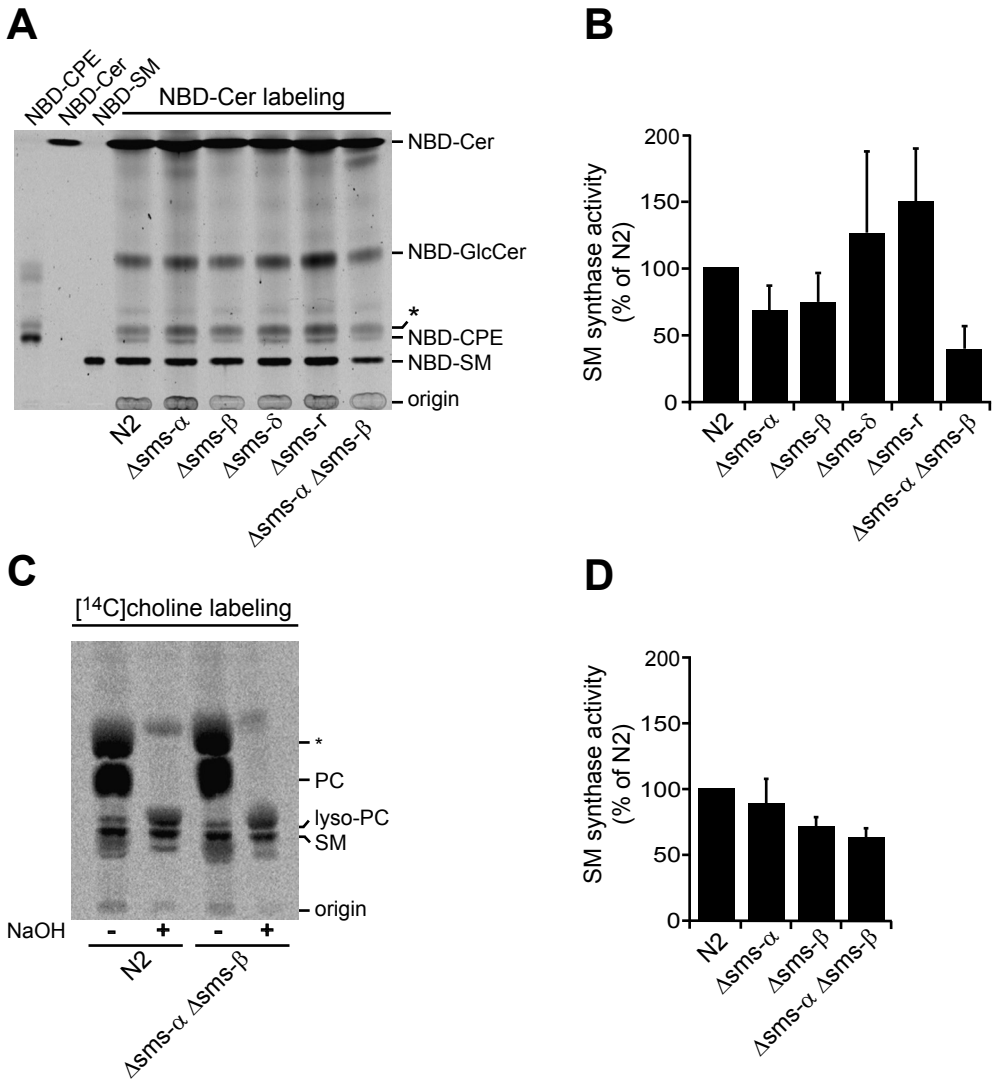

Figure 6. At least 3 different SM synthases contribute to SM synthesis in *C. elegans* worms. (A) TLC analysis of reaction products formed, when lysates of worms were incubated with NBD-Cer for 1 h at 20°C. (B) SM synthase activity levels were determined in lysates of *C. elegans* worms, labeled with NBD-Cer and expressed relative to activity levels in wild type N2 worms. (C) N2 worms and mutant strains were labeled with [^{14}C]choline for 5 h and subjected to lipid extraction, TLC analysis and autoradiography. Glycerolipids were deacylated by mild alkaline hydrolysis (NaOH;+). (D) SM synthase levels of worms metabolically labeled with [^{14}C]choline for 5 h, activity levels are expressed relative to N2 worm levels. Unknown by-products are marked with an asterisk (*). Error bars: (B) SD, n=5; (C) range, n=2.

Finally, a 210-bp deletion in tm2683 causes a gap in the protein-coding region of *sms-r* that covers the first two membrane spans. In view of the conserved membrane topology of SMS and LPP proteins, this most likely results in a complete loss of enzymatic activity. Unfortunately, no loss-of-function alleles could be obtained for *sms*-γ.

All four *sms* mutants were homozygous viable, and their overall growth and morphology were indistinguishable from that of wild type. To eliminate background mutations, each mutant was crossed four times to the wild-type N2 strain. Next, we analyzed the impact of each mutation on SM synthase activity using both *in vitro* and *in vivo* assays.

C. elegans contains at least three distinct SM synthases

The foregoing heterologous expression studies in yeast and insect cells showed that SMSα and SMSβ both possess SM synthase activity. To address the contribution of each enzyme to SM biosynthesis in *C. elegans*, we incubated total worm lysates of the corresponding deletion mutants tm2660 (Δ*sms*-α) and tm2613 (Δ*sms*-β) with NBD-Cer and monitored the formation of NBD-SM by TLC. Lysates of the wild type N2 strain served as control. This showed that disruption of SMSα or SMSβ in each case produced a modest (20 to 30%) but reproducible reduction in SM synthase activity (Figures 6A,B). In contrast, no reduction in SM synthase activity was found in the deletion mutants tm2615 (Δ*sms*-δ) or tm2683 (Δ*sms*-r). Together, these results indicate that both SMSα and SMSβ contribute to SM synthase activity in *C. elegans*. To investigate whether SMSα and SMSβ represent the only SM synthases in *C. elegans*, we created a *Δsms*-α *Δsms*-β double mutant by crossing tm2660 to tm2613. The double mutant was viable, grew well, and did not display any obvious morphological or behavioural phenotype. Interestingly, the double mutant displayed a strongly reduced but still clearly detectable SM synthase activity (30% of N2; Figures 6A,B).

Table 1. Characteristics of *C. elegans* SMS family members

	Predicted MW	Enzymatic activity		Subcellular localization			
	kDa	SM synthase	CPE synthase	ER	Golgi	Endosomes	PM
SMSα	50.9	+	-	-	-	+	+
SMSβ	38.7	+	-	-	+	-	+
SMSγ	38.1	-	-	-	-	-	+
SMSδ	44.0	n. d.	n. d.	n. d.	n. d.	n. d.	n. d.
SMSr	54.9	-	+	+	-	-	-

n. d. not determined

To investigate the contribution of SMSα and SMSβ to SM biosynthesis *in vivo,* the corresponding single and double mutants were metabolically labeled with [^{14}C]choline for 4 h at 20°C and the amount of [^{14}C]–labeled SM formed was quantified by TLC and autoradiography. Loss of SMSα or SMSβ in each case caused only a minor drop (10-30%) in newly synthesized SM levels. Worms lacking SMSα and SMSβ simultaneously showed a further drop in *de novo* SM synthesis, yet still retained 60% of the wild type level (Figure 6D).

Together, these results provide complementary evidence that SMSα and SMSβ operate as SM synthases in *C. elegans*. They also indicate that besides SMSα and SMSβ *C. elegans* must contain at least one additional enzyme that contributes to SM biosynthesis.

Discussion

In this study, we performed a first and systematic analysis of the SMS protein family in the nematode *C. elegans*. The use of heterologous expression systems and gene KO approaches allowed us to assign primary functions to three of the five SMS family members and to map their sites of action. We found that *C. elegans* SMSr catalyses the production of CPE in the ER, hence analogous to the SMSr homologue in mammals (Ternes et al., 2009; Vacaru et al., 2009). SMSα and SMSβ, on the other hand, function as SM synthases at the plasma membrane. These proteins also reside in intracellular compartments. While a substantial amount of SMSα was found in endosomes, SMSβ partially localized to the Golgi complex. Thus, SMSβ may well represent the *C. elegans* counterpart of SMS1 in mammals. SMSγ was found almost exclusively at the plasma membrane, but we were unable to assign any enzymatic activity to this protein. The same was true for SMSδ, whose expression during the various stages of *C. elegans* development was below the detection limit of our assay. Genetic ablation of both SMSα and SMSβ caused a substantial reduction in, but did not wipe out SM biosynthesis in *C. elegans.* Likewise, a mutant strain lacking SMSr retained detectable levels of CPE. This indicates that *C. elegans* contains at least one additional SM synthase and one additional CPE synthase whose identities remain to be established.

Previous work has shown that SMS proteins in mammals serve critical roles in cell growth and survival. For example, SMS1 is required for sustaining growth in mouse WR19L/Fas lymphoid cells when cultured under serum-free conditions (Yamaoka et al., 2004), and depletion of either SMS1 or SMS2 causes reduces growth in human HeLa cervical carcinoma cells (Tafesse et al., 2007). Moreover, we recently observed that depletion of SMSr triggers mitochondria-induced apoptosis in a variety of human cell lines (Tafesse et al., man in prep). In this respect, it is striking that disruption of SMSr or removal of both SMSα and SMSβ in *C. elegans* did not produce any recognizable aberration in organismal growth, morphogen-

esis or lifespan. It is possible that the corresponding mutants have minor aberrations that escaped our attention, or that they become defective in growth when exposed to stressful conditions. As none of the mutants described in this study displayed a complete block in SM or CPE biosynthesis, it is feasible that residual levels of SM and CPE synthase activities are sufficient to sustain growth and survival. Alternatively, the survival of *sms* mutants may depend on the activation of pro-mitogenic/anti-apoptotic pathways. Finally, we cannot exclude the possibility that nematodes simply do not rely on SMS proteins for their vital functions. The creation of novel mutants lacking multiple SMS family members combined with RNAi approaches should allow us to address these different scenarios.

Remarkably, nematodes consistently contain more SMS homologues than all other SM and/or CPE-producing organisms (e.g. mammals, insects, etc). While SMSα, SMSβ and SMSr synthesize SM or CPE, this may not necessarily be the case for SMSγ and/or SMSδ. A particular feature of *C. elegans* is the animal's ability to esterify its secreted *N*-glycoproteins and glycosphingolipids with phosphorylcholine (Cipollo et al., 2004). This property is shared with filarial nematodes in which production of cholinephosphoryl-substituted oligosaccharides (CPOs) serves to avoid the host immune response and contributes to the chronic nature of diseases caused by these parasites (Houston and Harnett, 2004). Whether cholinephosphoryl-substituted glycoproteins and glycolipids also have intrinsic activities that contribute to nematode development or physiology is unclear. CPO synthesis is catalyzed by a PC:oligosaccharide cholinephosphoryl transferase (Cipollo et al., 2004). Because this enzyme is absent in humans, it offers an ideal therapeutic modality for the treatment of filarial infections (Houston and Harnett, 2004). The identity of the CPO synthase is not known. Since CPO synthesis is mechanistically similar to SM and EPC synthesis, an attractive possibility is that SMSγ and/or SMSδ functions as a CPO synthase. This possibility is currently under investigation.

Acknowledgements
We thank Philippe Devaux and Andreas Conzelmann for gifts of reagents and cell lines and the National Biosource Project in Japan (NBP) for *C. elegans* strains. J.C.M. Holthuis was supported by grants from the Dutch Organization of Sciences (NWO-CW) and the Utrecht University High Potential Program.

Material and Methods

Chemicals and antibodies

NBD-Cer was obtained from Invitrogen (Leek, The Netherlands). NBD-SM, NBD-GlcCer, NBD-PC, POPE (1-palmitoyl-2-oleoyl-sn-glycerol-3-phosphoethanolamine), and POPC (1-palmitoyl-2-oleoyl-sn-glycerol-3-phosphocholine) were obtained from Avanti Polar Lipids, Inc (Alabaster, AL). NBD-CPE was generously provided by P. Devaux (Institut de Biologie Physico-chimique, Paris, France). Methyl-[^{14}C]choline chloride was obtained from MP Biomedicals (Santa Ana, CA). All other lipids and chemicals were obtained from Sigma-Aldrich (St Louis, MO).

The following antibodies were used in this study: rabbit polyclonal anti-human calnexin (Santa Cruz, Santa Cruz, CA), rabbit anti-drosophila calnexin (Abcam Ltd., Cambridge, MA), mouse monoclonal anti-Golgi130 (BD Biomedicals, Alphen aan den Rijn, The Netherlands), mouse/rabbit polyclonal anti-V5 antibodies (Sigma), rabbit polyclonal anti-biotin (Rockland, Gilbertsville, PA) and mouse monoclonal anti-d120kd (EMD). As secondary antibodies we used: Alexa Fluor 488 conjugated goat anti-rabbit (Invitrogen), Alexa Fluor 568 conjugated goat anti-mouse (Invitrogen), HRP-conjugated goat anti-rabbit (Biorad, Veenendaal, The Netherlands) and HRP-conjugated goat anti-mouse (Perbio, Breda, The Netherlands).

DNA constructs

hSMS1, ceSMSα, ceSMSβ, ceSMSγ and ceSMSr cDNAs were cloned into yeast expression vector pYES2.1/V5-His-TOPO and mammalian expression vector pcDNA3.1/V5-His-TOPO (Invitrogen) as described previously (Huitema et al., 2004). For expression studies in *Drosophila* S2 cells, hSMS1, ceSMSα, ceSMSβ, ceSMSγ and ceSMSr cDNAs were PCR amplified and ligated into the copper-inducible pMT/V5-His B vector (Invitrogen).

Yeast culture

Yeast strain 4Δ.Lass5 (*MAT*a *ade2-101^{ochre} his3-Δ200 leu2-Δ1 lys2-801^{amber} trp1-Δ63 ura3-52 lag1::TRP1 lac1::LEU2 ydc1::natMX ypc1::kanMX4* p413MET25:*Lass5*; Cerantola et al., 2007) was transfected with human and *C. elegans* SMS cDNAs in pYES2.1/V5-His-TOPO and grown in selective synthetic medium containing 2% (wt/vol) galactose and 50 mg/l myo-inositol.

Cell culture and transfection

HeLa cells were grown in DMEM with 10% FCS (PAA laboratories GmbH, Pasching, Austria). 10 cm cell culture dishes were obtained from Greiner Bio-One (Frickenhausen, Germany). Using Lipofectamine2000 (Invitrogen), cells were transiently transfected with SMS-V5/pcDNA3.1 constructs. *Drosophila* S2 cells were

grown in Schneider's insect medium with 10% FBS (Cambrex, Rockland, ME) at 27°C in a humidified atmosphere. Insect cells were transfected with SMS/pMT/V5-HisB constructsusing Effectene (Qiagen, Hilden, Germany) following the manufacturer's protocol. Expression of recombinant SMS protein was induced by addition of 1 mM $CuSO_4$ for 3 h followed by a 2 h-chase.

Nematode culture
Worms were maintained on 10 cm nematode growth medium (NGM) agar plates carrying a lawn of *E. coli* OP50 or in liquid culture (S-medium, described by Sulston and Hodgkin, 1988) supplemented with *E. coli* OP50. Culture plates and liquid cultures were maintained at 20°C. Worm strains used in these experiments were: N2 (wild type), Δ*sms-α* (tm2660), Δ*sms*-β (tm2613), Δ*sms-r* (tm2683) and Δ*sms*-δ (tm2615). All strains were provided by the National Biosource Project in Japan (NBP). All mutant strains have been backcrossed 4 times to N2. Mutant alleles were followed by PCR on single worm lysates, detecting the presence of genomic deletions (588 bp in the case of *tm2660*, 176 bp in the case of *tm2613*, 507 bp in the case of *tm261*5 and 210 bp in the case of *tm2683*). Primers, flanking the deletions alleles are listed in Supplementary Table 1.

Supplementary Table 1. Primers used for the characterization of *sms* deletion mutants

Gene / mutant	Primer pairs 5'-3'
sms-α / tm2660	ttggctattcactccaccct / tcgaagtccccatggaatct
sms-β / tm2613	tctgcttacattgggcacat / tcattaacttggccagtgcag
sms-δ / tm2615	tctagggcgtcggttggct / tgtaatcgttgtggagcatac
sms-r / tm2683	cgacaagtcgagagacccg / cgggtctctcgacttgtcg

Creation of double mutant (Δsms-α Δsms-β)
Backcrossed Δ*sms-α* (tm2660) worms were heat shocked (30°C for 4 h) at L4 larval stage and 6 young resulting male offspring were transferred to a plate containing one single L4 Δ*sms*-β (tm2613) hermaphrodite. The progeny were singled out onto plates and maintained until maturity (identified by the presence of eggs). Following single worm lysis, a genomic polymerase chain reaction (PCR) was performed to screen and identify double knockout mutants. Homozygous double mutant strains were selected and assessed and confirmed over at least 2 generations.

RT-PCR
RNA of worms was isolated using NucleoSpin RNA II kit (Macherey-Nagel, Düren, Germany) according to manufacturer's protocol. The amount and quality was verified by gel electrophoresis and spectrophotometry. Single strand

complementary DNA (cDNA) was generated from 1 µg RNA using dT-oligo primers and Superscript II reverse transcriptase (Invitrogen). PCR was performed using Phusion DNA polymerase (Finnzymes, Espoo, Finland) on 5 µl of cDNA using the cloning primers previously described in Huitema et al. (2004) except for sms-*α* where the following primer pair was used 5'-*gcggccgc*cttcgaaagcaggtcgtgcagctcc-3'/5'-*ggtacc*aagccatgaaaatgtcttggaatcatcaa-3'.

*Immunofluorescence microscop***y**
Cells were fixed in 4% paraformaldehyde/PBS, processed for immunofluorescence as described previously for S2 (Kondylis and Rabouille, 2003) and HeLa cells (Vacaru et al., 2009), and mounted in Vectashield medium containing DAPI (Vector Laboratories, Burlingame, CA). Images were captured at room temperature using a confocal microscope (LSM 510 Meta; Carl Zeiss, Inc., Sliedrecht, The Netherlands) with a 63x 1.40 NA Plan Apo oil objective. The fluorochromes used were DAPI, λ_{ex} = 360 nm and λ_{em}= 460 nm; Alexa Fluor 488, λ_{ex} = 488 nm and λ_{em}= 515 nm; Alexa Fluor 568, λ_{ex} = 568 nm and λ_{em} = 585 nm. Images were captured using EZ-C1 software (Nikon Instruments Europe, Badhoevedorp, The Netherlands) and further processed using Photoshop software (version 7.0.1; Adobe).

Western blotting
S2 *a*nd yeast cells were lysed in RIPA buffer (50mM Tris/HCl, 0.1% (wt/vol) SDS, 0.5% (vol/vol) NP40, 150 mM NaCl, 2 mM EDTA, pH 7.4), supplemented with Complete Protease Inhibitor Cocktail (PIC, Roche, Basle, Switzerland). Nuclear DNA was sheared by passing lysates through a 23G needle. Protein content of lysates was determined by the bicinchoninic acid method (Pierce, Breda, The Netherlands). Equal amounts of protein in 1x SDS sample buffer were separated by SDS-PAGE and subsequently transferred to a nitrocellulose membrane (Schleicher & Schuell, Dassel, Germany). Membranes were blocked in TBS (25 mM Tris/HCl, 137 mM NaCl, 2.7 mM KCl, pH 7.4) containing 0.05% (vol/vol) Tween20 and 4% (wt/vol) dried skim milk (Fluka, Zwijndrecht, The Netherlands) and incubated overnight with primary antibody of interest. Membranes were washed three times in TBS containing 0.05% (vol/vol) Tween20 and incubated for 1 h with secondary antibody. Proteins were detected using HRP-conjugated secondary antibodies and enhanced chemiluminescence (Amersham, Roosendaal, The Netherlands).

In vitro enzyme assays
100 ODs of yeast cells was lysed by bead bashing in 10 ml ice-cold reaction buffer (0.3 M sucrose, 15 mM KCl, 5 mM NaCl, 1 mM EDTA, 20 mM Hepes-KOH, pH 7.0) containing freshly added protease inhibitors. 200 µl postnuclear supernatant (PNS; 700 *g* for 10 min at 4°C) were combined with 200 µl reaction buffer containing 0.002% Triton X-100, 40 nmol POPE and/or POPC, and 50 µM NBD-

Cer (Avanti Polar Lipids, Inc.), and incubated at 37°C for 2 h. $2x10^5$ worms were homogenized in an eppendorf tube with 40 strokes of a teflon pestle in 300 µl ice-cold reaction buffer. 200 µl of worm lysate were combined with 200 µl reaction buffer containing 25 µM NBD-Cer (Avanti Polar Lipids, Inc.), and incubated at 20°C for 2 h. Reactions were stopped by adding 1 ml MeOH and 0.5 ml $CHCl_3$, and lipids were extracted according to Bligh and Dyer (1959). The lower phase was evaporated under N_2 and the reaction products analyzed by TLC, which was developed in $CHCl_3$/acetone/MeOH/acetic acid/H_2O (50/20/10/10/5 [vol/vol/vol/vol/vol]). Fluorescent lipids were visualized on an image analysis system (STORM 860; GE Healthcare) and quantified with Quantity One software (Bio-Rad Laboratories).

Metabolic labeling

S2 cells (2–5 x 10^6) grown in 0.5 ml complete Schneider's insect medium and *C. elegans* worms ($2x10^5$) grown in liquid culture (S-medium) were labeled with 1 µCi [^{14}C]choline for different time points as indicated. Lipids were extracted in $CHCl_3$/MeOH/10 mM acetic acid (1/4.4/0.2 [vol/vol/vol]) and processed according to Bligh and Dyer (1959). Half of the extract was subjected to mild alkaline hydrolysis. Radiolabeled lipids were analyzed by TLC in $CHCl_3$/MeOH/25% NH_4OH (50/25/6 [vol/vol/vol]) detected by exposure to imaging screens (BAS-MS; FujiFilm), scanned on a Personal Molecular Imager (Bio-Rad Laboratories), and quantified using Quantity One software.

References

Adam-Klages, S., Adam, D., Wiegmann, K., Struve, S., Kolanus, W., Schneider-Mergener, J., and Krönke, M. 1996. FAN, a novel WD-repeat protein, couples the p55 TNF-receptor to neutral sphingomyelinase. *Cell* 86:937-947.

Bligh, E.G., and Dyer, W.J. 1959. A rapid method of total lipid extraction and purification. *Can J Biochem Physiol*. 37:911-7.

Cerantola, V., Vionnet, C., Aebischer, O.F., Jenny, T., Knudsen, J., and Conzelmann, A. 2007. Yeast sphingolipids do not need to contain very long chain fatty acids. *Biochem J*. 401:205-16.

Cipollo, J.F., Awad, A., Costello, C.E., P.W. Robbins, and C.B. Hirschberg. 2004. Biosynthesis *in vitro* of *Caenorhabditis elegans* phosphorylcholine oligosaccharides. *Proc Natl Acad Sci USA*. 101:3404-8.

Hampton, R.Y., and Morand, O.H. 1989. Sphingomyelin synthase and PKC activation. *Science* 246:1050.

Hancock, J.F. 2006. Lipid rafts: contentious only from simplistic standpoints. *Nat Rev Mol Cell Biol* 7:456-462.

Hannun, Y.A. 1996. Functions of ceramide in coordinating cellular responses to stress. *Science* 274:1855-1859.

Hannun, Y.A., and Bell, R.M. 1989. Functions of sphingolipids and sphingolipid breakdown products in cellular regulation. *Science* 243:500-507.

Hannun, Y.A., and Obeid, L.M. 2008. Principles of bioactive lipid signalling: lessons from sphingolipids. *Nat Rev Mol Cell Biol* 9:139-150.

Houston, K.M., and Harnett, W. 2004. Structure and synthesis of nematode phosphorylcholine-containing glycoconjugates. *Parasitology*. 129:655-61.

Huitema, K., van den Dikkenberg, J., Brouwers, J.F., and Holthuis, J.C. 2004. Identification of a family of animal sphingomyelin synthases. *Embo J*. 23:33-44.

Kolesnick, R.N., and Krönke, M. 1998. Regulation of ceramide production and apoptosis. *Annu Rev Physiol* 60:643-665.

Kondylis, V., and Rabouille, C. 2003. A novel role for dp115 in the organization of tER sites in Drosophila. *J Cell Biol* 162:185-198.

Koreth, J., and van den Heuvel, S. 2005. Cell-cycle control in *Caenorhabditis elegans*: how the worm moves from G1 to S. *Oncogene* 24:2756-2764.

Marchesini, N., and Hannun, Y.A. 2004. Acid and neutral sphingomyelinases: roles and mechanisms of regulation. *Biochem Cell Biol* 82:27-44.

Metzstein, M.M., Stanfield, G.M., and Horvitz, H.R. 1998. Genetics of programmed cell death in *C. elegans*: past, present and future. *Trends Genet* 14:410-416.

Notredame, C., Higgins, D.G., and Heringa, J. 2000. T-Coffee: A novel method for fast and accurate multiple sequence alignment. *J. Mol. Biol.* 302:205–217.

Ogretmen, B., and Hannun, Y.A. 2004. Biologically active sphingolipids in cancer pathogenesis and treatment. *Nat Rev Cancer* 4:604-616.

Schmidt, H.A., Strimmer, K., Vingron, M., and von Haeseler, A. 2002. TREE-PUZZLE: maximum likelihood phylogenetic analysis using quartets and parallel computing. *Bioinformatics* 18:502-504.

Simons, K., and Toomre, D. 2000. Lipid rafts and signal transduction. *Nat Rev Mol Cell Biol* 1:31-39.

Spiegel, S., and Milstien, S. 2003. Exogenous and intracellularly generated sphingosine 1-phosphate can regulate cellular processes by divergent pathways. *Biochem Soc Trans* 31:1216-1219.

Sulston, J., and Hodgkin, J. 1988. *Methods. WB. Wood, Editor, The nematode Caenorhabditis elegans, Cold Spring Harbor Laboratory Press, Cold Spring Harbor, NY, p*587-606.

Tafesse, F.G., Huitema, K., Hermansson, M., van der Poel, S., van den Dikkenberg, J., Uphoff, A., Somerharju, P., and Holthuis, J.C. 2007. Both sphingomyelin synthases SMS1 and SMS2 are required for sphingomyelin homeostasis and growth in human HeLa cells. *J Biol Chem*. 282:17537-47.

Ternes, P., Brouwers, J.F., van den Dikkenberg, J., and Holthuis J.C. 2009. Sphingomyelin synthase SMS2 displays dual activity as ceramide phosphoethanolamine synthase. *J Lipid Res*., accepted manuscript.

Vacaru, A.M., Tafesse, F.G., Ternes, P., Kondylis, F., Hermansson, M., Brouwers, J.F., Somerharju, P., Rabouille, C., and Holthuis, J.C. 2009. Sphingomyelin synthase-related protein SMSr controls ceramide homeostasis in the ER. *J Cell Biol*. 185:1013-27.

van Meer, G., Voelker, D.R., and Feigenson, G.W. 2008. Membrane lipids: where they are and how they behave. *Nat Rev Mol Cell Biol* 9:112-124.

Verheij, M., Bose, R., Lin, X.H., Yao, B., Jarvis, W.D., Grant, S., Birrer, M.J., Szabo, E., Zon, L.I., Kyriakis, J.M., et al. 1996. Requirement for ceramide-initiated SAPK/JNK signalling in stress-induced apoptosis. *Nature* 380:75-79.

Wiegmann, K., Schutze, S., Machleidt, T., Witte, D., and Krönke, M. 1994. Functional dichotomy of neutral and acidic sphingomyelinases in tumor necrosis factor signaling. *Cell* 78:1005-1015.

Yamaoka, S., Miyaji, M., Kitano, T., Umehara, H., and Okazaki, T. 2004. Expression cloning of a human cDNA restoring sphingomyelin synthesis and cell growth in sphingomyelin synthase-defective lymphoid cells. *J Biol Chem*. 279:18688-93.

Yang, C., and Kazanietz, M.G. 2003. Divergence and complexities in DAG signaling: looking beyond PKC. *Trends Pharmacol Sci* 24:602-608.

Chapter 3

The way we view cellular (glyco)sphingolipids

Sandra Hoetzl[1], Hein Sprong[2] and Gerrit van Meer[1]

Based on:
J. Neurochem. (2007) 103 (Suppl. 1), 3-13

[1]Membrane Enzymology, Bijvoet Center and Institute of Biomembranes, Utrecht University, Utrecht, The Netherlands

[2]Present address: National Institute of Public Health and Environment (RIVM), Bilthoven, The Netherlands

Abstract
Mammalian cells synthesize ceramide in the endoplasmic reticulum (ER) and convert this to sphingomyelin and complex glycosphingolipids on the inner, non-cytosolic surface of Golgi cisternae. From there, these lipids travel towards the outer, non-cytosolic surface of the plasma membrane and all membranes of the endocytic system, where they are eventually degraded. At the basis of the selective, anterograde traffic out of the Golgi lies the propensity of the sphingolipids to self-aggregate with cholesterol into microdomains termed 'lipid rafts'. At the plasma membrane surface these rafts are thought to function as the scaffold for various types of (glyco)signaling domains of different protein and lipid composition that can co-exist on one and the same cell. In the past decade, various unexpected findings on the sites where sphingolipid-mediated events occur have thrown a new light on the localization and transport mechanisms of sphingolipids. These findings are largely based on biochemical experiments. Further progress in the field is hampered by a lack of morphological techniques to localize lipids with nanometer resolution. In the present paper, we critically evaluate the published data and discuss techniques and potential improvements.

Sphingolipid sorting and function
Sphingolipids form a highly diverse class of lipids, characterized by a lipid backbone that consists of a long-chain sphingoid base that is mostly amide-linked to a fatty acid: ceramide. The polar headgroup of the most abundant sphingolipid in mammalian cells, sphingomyelin (SM), is phosphocholine. It is transferred from the cell's most abundant glycerophospholipid phosphatidylcholine (PC) onto ceramide by sphingomyelin synthase on the lumenal side of the Golgi membrane, giving rise to SM plus diacylglycerol. Both ceramide and diacylglycerol fulfill dual functions as metabolic precursors and as secondary messengers. The glycosphingolipids contain polar headgroups that contain one or more carbohydrates. The basic glycosphingolipid in every cell is glucosylceramide (GlcCer; Table 1), to which carbohydrates are added in a stepwise fashion on the lumenal surface of the Golgi. This yields glycosphingolipids containing one up to ten or more carbohydrates, which are often organized as branched chains. Glycosphingolipids containing sialic acids are termed gangliosides. Independently, a number of cell types synthesize galactosylceramide (GalCer), part of which is modified in the trans-Golgi lumen to GalCer sulfate (sulfatide). These latter lipids are relevant for the proper function and stability of the myelin sheath, as evidenced by tremor, late-onset paralysis and premature death of knockout mice for the ceramide GalCer synthase. The GlcCer-based glycosphingolipids are crucial for mammalian development. Once again, this has become clear from studies on knockout mice. Mice with null-alleles for the GlcCer synthase, causing a lack of all complex glycosphingolipids (Yamashita et al., 1999), die as embryos. Mice lacking more distal

transferases display milder defects, which however, when translated to humans, would still be recognized as major inherited diseases (Proia, 2003). For example, whereas mice lacking the GM3 synthase displayed enhanced insulin sensitivity (Yamashita et al., 2003), humans with this defect display infantile-onset symptomatic epilepsy syndrome (Simpson et al., 2004). While SM generally makes up some 15-20% of the lipids in plasma membranes, the levels of glycosphingolipids are generally much lower. However, particularly high levels of glycosphingolipids have been reported for apical membranes of epithelial cells (Simons and van Meer, 1988), for myelin (Bosio et al., 1996; Coetzee et al., 1996) and neurons (Vanier, 1999).

Table 1. Glycosphingolipid designation according to the recommendations of the IUPAC-IUB Joint Commission on Biochemical Nomenclature[a], using the Svennerholm abbreviations for gangliosides[b]

Abbreviation	Name	Structure	Synonyms
GlcSph	Glucosylsphingosine	Glcβ1-Sph	Glucopsychosine
GalSph	Galactosylsphingosine	Galβ1-Sph	(galacto)Psychosine
GlcCer	Glucosylceramide	Glcβ1-Cer	Glucocerebroside
GalCer	Galactosylceramide	Galβ1-Cer	(galacto)Cerebroside
LacCer	Lactosylceramide	Galβ4Glcβ1-Cer	
SGalCer	Sulfogalactosylceramide	HSO_3-3Galβ1-Cer	Sulfatide, SM4
SLacCer	Sulfolactosylceramide	HSO_3-3Galβ4Glcβ1-Cer	SM3
Gb3	Globotriaosylceramide	Galα4Galβ4Glcβ1-Cer	Gb_3Cer
Gangliosides			
GM1a	II^3NeuAc-Gg_4Cer	Galβ3GalNAcβ4(Neu5Acα3)--Galβ4Glcβ1Cer	GM1
GM1b	IV^3NeuAc-Gg_4Cer	Neu5Acα3Galβ3GalNAcβ4--Galβ4Glcβ1Cer	G_{M1b}
GM3	II^3NeuAc-LacCer	Neu5Acα3Galβ4Glcβ1Cer	G_{M3}
GD3	$II^3$$NeuAc_2$-LacCer	Neu5Acα8Neu5Acα3--Galβ4Glcβ1Cer	
GM4	I^3NeuAc-GalCer	Neu5Acα3Galβ1Cer	G_{M4}

[a]Chester (1998), [b]Svennerholm (1963).

The molecular basis for the need for glycosphingolipids was originally supposed to reside in the tremendous variability in three-dimensional structure, that can be generated by combining various carbohydrates in different combinations and orders and with different glycosidic bonds. Already early on, this variability suggested that the oligosaccharides on glycoproteins and glycosphingolipids might serve to mediate highly specific interactions between cells, cells and

matrix and between cells and soluble signaling molecules (see Hakomori, 2002). The high structural specificity is illustrated by the fact that many natural high-affinity antibodies have turned out to be directed against specific glycosphingolipids instead of proteins. An alternative role for sphingolipids was suggested by the lipid raft hypothesis in the late 1980s. The original hypothesis stated that glycosphingolipids in the lumenal leaflet of the membrane of the trans Golgi network self-aggregate and that epithelial cells selectively include these aggregates into budding transport vesicles destined for the apical plasma membrane domain of epithelial cells, sorting glycolipids with the apical proteins (van Meer et al., 1987). With the inclusion of SM and cholesterol, the hypothesis also nicely explains how cells enrich sphingolipids and cholesterol in the anterograde secretory pathway and thereby keep the endoplasmic reticulum (ER) concentrations of these lipids low (Figure 1). The apical sorting of glycosphingolipids would then be superimposed on the general sorting of all sphingolipids and cholesterol towards the plasma membrane (van Meer, 1989). Because the complex sphingolipids reside on

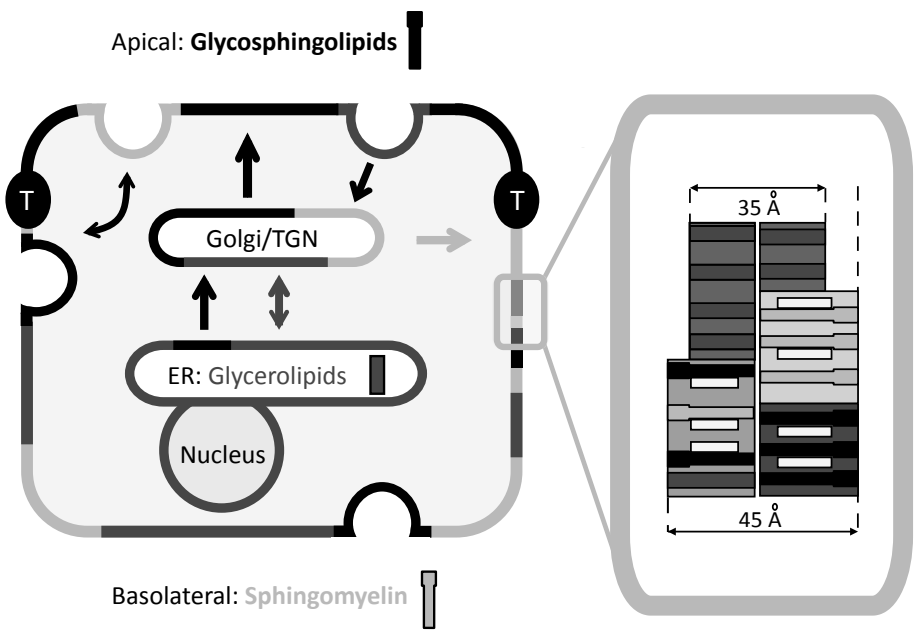

Figure 1. Lipid sorting in intestinal epithelial cells (Simons and van Meer, 1988; van Meer, 1989). Glycosphingolipids (black) and cholesterol are enriched on the apical surface, whereas SM (light gray) with cholesterol is preferentially transported to the basolateral surface. All three lipids are sorted in the anterograde direction, while unsaturated glycerophospholipids (dark gray) are enriched in the retrograde pathway to the ER. The sorting occurs in the non-cytosolic leaflet of the various membranes, because the tight junctions (T) act as a barrier to lipid diffusion in the outer bilayer leaflet only. However, some sphingolipids are presumably present in the cytosolic leaflet. For the differences in membrane thickness (see Sprong et al., 2001).

the non-cytosolic surface they can reach other organelles by vesicular transfer only. The absence of a vesicular transport connection to mitochondria and peroxisomes then explains the general lack of SM and glycosphingolipids from these membranes as assessed biochemically (van Meer, 1989). Because cholesterol readily flips across membranes and has a relatively high rate of monomeric transfer between membranes, its cellular distribution is determined essentially by its high affinity for sphingolipids (Wattenberg and Silbert, 1983). (Glyco)sphingolipid-based rafts have received most attention for their roles in the signaling by immune receptors (Barbat et al., 2007; Gomez-Mouton et al., 2001; Holowka et al., 2005; Pierce, 2002), in glycosignaling platforms on the cell surface (Hakomori, 2002), and in other signal transduction events (see Mayor et al., 2006).

In the past decade, various unexpected genetic and biochemical findings have opened new vistas on the organization of sphingolipids in the mammalian cell bringing up as many new sets of questions on the topology of the respective sphingolipids. (i) The simple glycosphingolipid GlcCer is not synthesized in the luminal leaflet of the Golgi membrane, but on the cytosolic surface (Ichikawa et al., 1996). Across which membrane does GlcCer translocate on its way into the Golgi lumen where it is required for the synthesis of higher glycosphingolipids? (ii) In contrast, the ceramide galactosyltransferase synthesizes (GalCer) on the lumenal surface of the ER (Schulte and Stoffel, 1993), where like all other lipids tested it has free access to the cytosolic surface by an energyindependent flip-flop process (Figure 2). Do both GlcCer and GalCer redistribute to all other cytosolic surfaces via, for example, the cytosolic glycolipid transfer protein GLTP? (iii) Biochemically, complex glycosphingolipids and SM are found to some extent in the ER and even in the nuclear matrix (Albi and Viola Magni, 2004; Hunt and Postle, 2006). Are they really there and do they, as a consequence, have access to the cytosolic surface of the ER and that of other organelles as well? Recently, a non-lysosomal GlcCer degrading enzyme has been found in the ER (Boot et al., 2007). (iv) While mitochondria contain exceedingly low concentrations of (glyco)sphingolipids, in apoptotic cells SM and the ganglioside GD3 do seem to reach the mitochondria and to cause mitochondrial rupture and dysfunction (Birbes et al., 2001; Garcia-Ruiz et al., 2002; Rippo et al., 2000).

Where exactly are these lipids located and how do these processes work? (v) The biosynthesis of SM and part of the GlcCer depends on transport of newly synthesized ceramide from the ER to the trans Golgi by the ceramide transfer protein CERT (Hanada et al., 2003). Does CERT act as a soluble carrier or as a contact-site protein, and where exactly does it deliver the ceramide? (vi) Finally, evidence has been presented that different types of microdomains can co-exist on the cell surface and that these domains have different (sphingo)lipid compositions (Brügger et al., 2004; Gomez-Mouton et al., 2001).

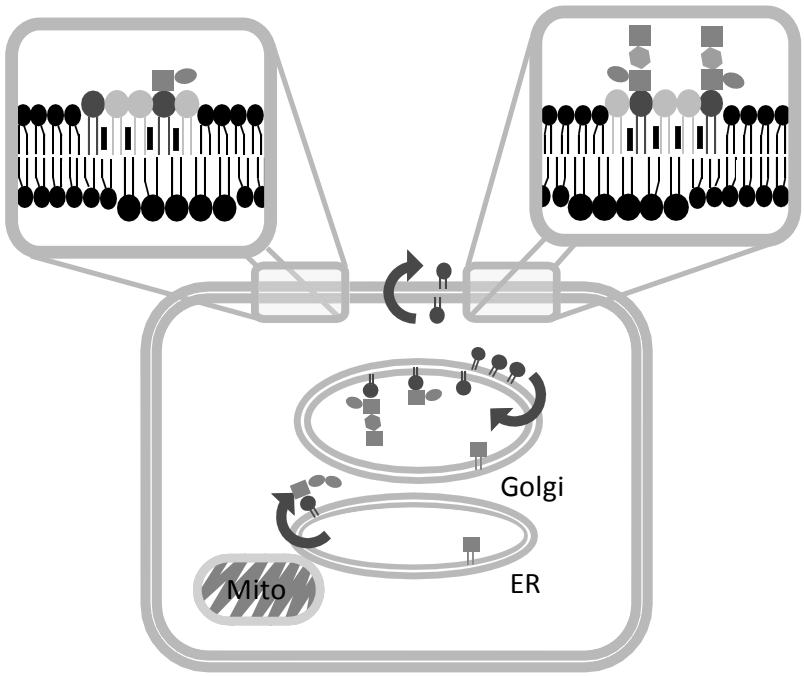

Figure 2. Synthesis and transport of glycosphingolipids. Glucosylceramide (Glccer; dark gray circles) is synthesized on the cytosolic surface of the Golgi but is flipped to the lumenal surface of the Golgi, where it is converted to complex glycosphingolipids by the sequential addition of galactose (light gray squares) and sialic acid (dark gray ellipses), to yield GM3. GM1 is synthesized by the further addition of N-acetylgalactosamine (gray hexagons) and another galactose (Table 1). GM3 and GM1 occupy different domains on the surface of polarizing T-cells, probably with SM (light gray circles). Some GD3 makes it back to the ER, where it can presumably flip freely across the membrane and now has access to, for example, mitochondria via contact sites.

How are these domains structured and do such domains exist along the vesicular transport pathways as well? These examples clearly illustrate the need for data on the location of (glyco)sphingolipids, if possible with nm resolution.

Localization of (glyco)sphingolipids; the methods

So, what do we want to know about where the sphingolipid is located in the *in vivo* situation? In increasing order of resolution: (i) In which tissue or part of the tissue? (ii) In which cells? (iii) In which membranes in the cells? (iv) On which side of the membrane? (v) And, finally, at which lateral location within that membrane leaflet? At that point, we have reached the realm of chemistry and physics, where we can ask with which other membrane components our lipid interacts. Because natural lipids are not visible in the microscope (except for the very few that are auto-fluorescent), two general approaches and the combination of them have been

followed to visualize them. (i) Lipids have been labeled by reagents that can be discriminated microscopically, mostly proteins that bind to a certain lipid, like antibodies, followed by fluorescent or gold-labeled secondary antibodies; (ii) analogs of lipids have been inserted into cells that are visible by themselves, because they are fluorescent, or can be visualized by the previous approach.

Labeling of endogenous lipids

Because of the remarkable antigenicity of glycosphingolipids, many anti-glycosphingolipid antibodies have been described. After binding to their target, they can be visualized by the traditional methods of immunofluorescence and immuno-electron microscopy. In comparison to the well-established immunolocalization of proteins, the localization of lipids is hampered by a number of special technical problems connected with their small size and hydrophobic nature. As a general principle, the burden is on the investigator to make sure that the interpretation adequately recognizes these problems. Only meaningful data can lay the solid foundation for the field that is needed before we can start to discuss the effects of lipids on the cellular organization, trafficking and signaling of proteins at the molecular level.

Access without loss or redistribution

The first and overriding condition that should be fulfilled by any method is that the method should not affect the feature that is to be studied, which in this case is the localization of the sphingolipid in the living cell. So the method should not change the level of the lipid or redistribute the lipid. The concentration of the lipid may change due to metabolism during the labeling procedure. This is especially realistic for signaling lipids which have a very high turnover. In addition, some enzymes are particularly resistant to fixatives. In these cases there are still various possibilities to record the *in vivo* situation: (i) to label *in vivo*, and study the label *in vivo* under a fluorescence microscope, (ii) to label *in vivo*, and fix the label instead of the lipid, and (iii) to freeze the situation by rapid freezing after which the lipids must be fixed in the frozen state.

A second problem is accessibility. Only glycosphingolipids on the cell surface can be labeled directly by exogenous antibodies. When one tries to approach intracellular lipids, problems arise that do generally not exist for protein targets. For protein localization, proteins are first fixed by aldehydes after which they are made accessible to the antibodies by opening the membranes. Because lipids are generally not fixed by aldehydes (and if they are, they mostly lose their antigenicity) special care must be taken to ensure that the opening method does not displace (or remove) the lipids. First of all, membranes have been opened by detergents or organic solvents like cold methanol or acetone. Such methods generally

result in dissolution and release (Maneta-Peyret et al., 1999) and redistribution of lipids. This point has been convincingly made even at the level of tissues. The incubation with low concentrations of Triton X-100 resulted in the redistribution of glycosphingolipids between brain tissue samples that were co-processed in the same solution (Heffer-Lauc et al., 2005). Subcellular labeling patterns of lipids observed after such treatments must be verified by independent techniques. It should be realized that even a fixation procedure using aldehydes by itself can make membranes leaky to the labeling agent (Sugii et al., 2003). Such a change in the physical state of the membrane may well induce redistribution of lipids across, or in the plane of, the membrane or even between organelles.

A detergent-independent, general method to make proteins accessible for localization is the preparation of sections from frozen samples, frozen sections, which is followed by antibody labeling on the thawed sections. It is clear from lipid physics that cross-sectioned, and thereby opened, membranes have an inherent strong tendency to close. The lipids on the edge of the cross-sectioned lipid bilayer are inevitably unstable (Figure 3), resulting in lipid redistribution across membranes and high background labeling over the section (van Genderen et al., 1991). A dramatic improvement in organelle-specific labeling on sections was observed after freeze-substitution: freezing the cells, followed by embedding in a polymer that is subsequently cross-linked by UV, all below 0°C. The complex glycosphingolipid Forssman antigen was found to reside in specific cellular membranes and to be absent from mitochondria and peroxisomes (van Genderen et al. 1991). First of all, this confirms that freeze-substitution does not redistribute the lipid over organelles, second, the results suggest that it is technically possible to address the question whether glycosphingolipids are present in mitochondria under specific conditions. The labeling density was high in the plasma membrane and in endosomes, threefold lower in the Golgi and 10-fold lower in the nuclear membrane. This fits the expectations from biochemical analyses, which suggested that this immunolocalization technique can be used to quantitate the surface density of the lipid in the various membranes. A later study using freeze-substitution (Parton, 1994) even supplied sufficient resolution to conclude that the glycosphingolipid GM1 was not distributed uniformly over the plasma membrane but was concentrated approximately fourfold in non-coated invaginations, identified as caveolae. This was the first morphological evidence for the occurrence of glycosphingolipid-enriched domains in a mammalian plasma membrane. Vielhaber et al. (2001b) successfully demonstrated a concentration of GlcCer in lamellar bodies of the skin. Excellent preservation of the galacto-sphingolipids GalCer and S-GalCer to myelin sheets in rat brain was reported as well (Kirschning et al., 1998). Still, there are many variables in the fixation and embedding steps of the method that must be optimized to minimize lipid loss (Maneta-Peyret et al., 1999), and redistribution.

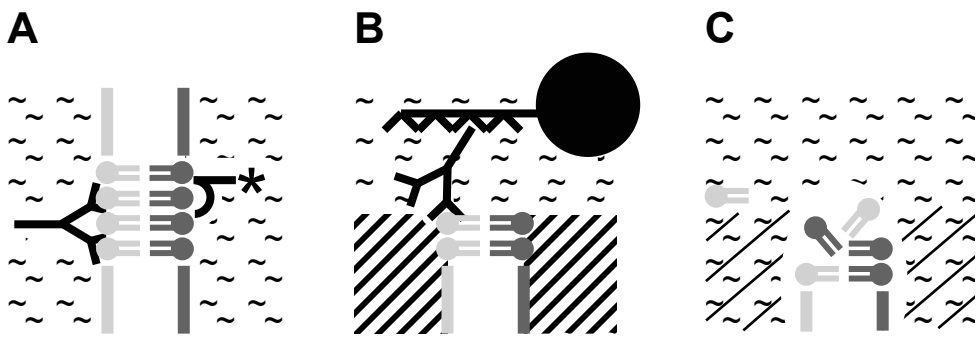

Figure 3. The sidedness of lipid labeling. (A) Membrane impermeable probes can be added selectively from one side of the lipid bilayer. Examples are the exogenous addition of antibodies or toxins to the outer surface of intact cells (light gray; e.g., Parton, 1994), or the expression of cytosolic fluorescent PH domains to label phosphoinositides on cytosolic surfaces (dark gray; Downes et al., 2005). Besides studying them by fluorescence, these labels can be fixed and processed for electron microscopy by a variety of techniques (thin frozen sections, plasma membrane sheets, fracture-label), whereby the label is visualized by pre- or post-embedding with, e.g., protein A-gold. (B) In freeze-substitution the samples are frozen, and the ice replaced by a polymer below 0°C. Thin sections are cut, and a primary reagent (antibody) followed by a secondary reagent (protein A-5 nm gold) labels lipids at the surface of the section. The gold does not reflect the sidedness of the lipid antigen. (C) In conventional thin frozen sections, the sample is thawed and labeled. As illustrated lipids at the interface will redistribute and some will spread. Labeling as in (B). While antibodies can penetrate the section, the gold label will not.

One other method to gain access to the cytosolic surface of the plasma membrane is the preparation of plasma membrane sheets. Labeling such sheets with gold-labeled antibodies, followed by imaging and pattern analysis allowed an assessment of the clustered appearance of lipid-anchored kinases on the cytosolic surface (Plowman et al., 2005), and an assessment of the lateral distribution of phosphoinositides and phosphatidylserine, lipids restricted to the cytosolic surface, should not be problematic: An analysis of the distribution of prelabeled GM1 (in the outer leaflet) showed a difference between the random distribution in the control and the clustering occurring after cross-linking (Wilson et al., 2004).

A final problem of accessibility is shielding of the lipid by either proteins or by other lipids. This particularly applies to lipids that are deeply embedded in the lipid bilayer and expose only a small headgroup. A clear example is the observation that the cholesterol–binding agent filipin does not bind to cholesterol in coated vesicles until after removal of the clathrin coat (McGookey et al., 1983; Steer et al., 1984). This predicts that agents proposed to label lipids like ceramide (Vielhaber et al., 2001a) may not label their target with similar efficiencies in different membranes or different membrane domains. The labeling of SM by the SM-binding toxin lysenin, or probes derived thereof, depended on the lipid environment.

The presence of glycolipids inhibited binding (Ishitsuka et al., 2004). Such probes can therefore not be used for the quantitative assessment of the distribution of a lipid over various locations, because the absence of labeling does necessarily mean that the lipid target is not present.

Labeling without redistribution

A subsequent set of problems with the microscopic localization of glycosphingolipids is connected to the nature of the labeling reagents. First of all, the agent should be specific. A standard test for the specificity of the label for a certain glycosphingolipid is a binding assay on TLC plates, but it is impossible to test all lipids for cross reactivity. Moreover, a lipid is presented differently on a TLC plate and in a biomembrane: the possibility exists that a protein specific in a TLC assay cross-recognizes other epitopes in the cellular context. The ideal test to exclude such cross-reactivity is to study the same cells but lacking this specific glycosphingolipid (van Genderen et al., 1991). This is now facilitated by the availability of a cell line without glycosphingolipids (Ichikawa et al., 1996). Second, the agent should have a high affinity for the lipid in order to increase the labeling density. The avidity increases when the labeling reagent is multivalent, which takes us to the next problem: because lipids are not fixed by routine fixation protocols, they can be redistributed by multivalent ligands abolishing their original distribution pattern. This is especially true when these primary ligands are subsequently labeled by secondary ligands that are multivalent by themselves. Labeling of the complex glycosphingolipids globoside and Forssman antigen by an antibody, or labeling of GM1 by cholera toxin, followed by tetra- or pentavalent protein A or by a second antibody resulted in clustering (Butor et al., 1991; Fujimoto, 1996; Spiegel et al., 1984; Tillack et al., 1983)[1]. The artificial clustering by the second protein label could be prevented by fixation of the first label before addition of the second (Butor et al., 1991; Fujimoto et al., 1996)[2]. A disturbance of the lipid distribution may also occur as a consequence of the fact that the reagent changes an essential physical property of the lipid. The label is generally big as compared to the target lipid and may change its diffusion co-efficient. Especially, labels that insert into the membrane like (agents based on) membrane penetrating toxins, e.g., lysenin for SM and perfringolysin for cholesterol, are likely to interfere with those lipid–lipid interactions that determine their phase behavior, and thereby affect their lateral distribution. Whereas the cellular dynamics of phosphoinositides have

[1] Clustering of asialo-GM1 was also observed by near-field scanning optical microscopy (NSOM). Unfortunately, little attention was paid to potential redistribution (Abulrob et al., 2008; Chen et al., 2008).

[2] In a number of more recent studies cholera toxin B subunit was directly tagged with a fluorescent marker, which avoids clustering by anti-cholera toxin antibody (see e.g. Hofman et al., 2008; Sorice et al., 2008). Still, this does not exclude the possibility that the pentavalent binding of the toxin may change the distribution of GM1.

been studied extensively using the (green fluorescent protein-coupled) truncated binding domains (PH-, PX-, ENTH-, and FYVE domains) of proteins that bind specifically to distinct phosphoinositides (Downes et al., 2005), remarkably few probes (antibodies/toxins) are available that bind one (glyco)sphingolipid molecule with sufficient affinity to study singular (glyco)sphingolipids.

Finally, the resolution of the labeling is limited by the dimensions of the labeling reagent: whereas the crosssectional area of a typical lipid is 0.6 nm^2, the diameter of the gold particles is 5-10 nm or more, and the linker between the antigenic lipid and the gold particle again has a length of >10 nm (Figure 3). It is therefore of paramount importance to devise monovalent high-affinity reagents of a limited size. Still, it is clear that the size of the electron microscopic reagents by themselves makes it impossible to define the sidedness of an epitope on membranes by the post-embedding of thin sections (Figure 3). Protocols must be used where the accessibility to the labeling reagent is limited to one side of the membrane only. This can be achieved by labeling intact membranes (or cells) prior to freezing, embedding or cutting. Alternative approaches that have been applied to lipids are the immunolabeling of membrane sheets (Wilson et al., 2004), and the fracture-label technique, which is immunolabeling of membrane halves produce produced by freeze-fracture (Barbosa and Pinto da Silva, 1983).

Fluorescent lipid analogs

Thirty years ago Simoni and colleagues demonstrated how parinaric acid, a family of unnatural fluorescent C_{18} fatty acids with 4 conjugated cis- and trans-double bonds can be used to study physical properties of fatty acids and phospholipids *in vitro* and *in vivo* (Rintoul and Simoni, 1977; Sklar et al., 1975). Since then, a variety of fluorescent lipophilic dyes have been applied that unlike parinaric acid are visible by fluorescence microscopy. They have been used in numerous cases to study physical properties of cellular membranes and to unravel transport pathways of cellular lipids, for example the barrier properties of epithelial tight junctions (Dragsten et al., 1981; van Meer and Simons, 1986). However, an important break-through in this field was the broad application by Pagano et al. (1981) of visible fluorescent lipids that sufficiently resembled the natural mammalian lipids in structure to be recognized by the cellular metabolic pathways. Because these analogs carried a short fluorescent and relatively polar fatty acid (C_6-NBD), they were rather well soluble in water, which property enabled the investigators to efficiently deliver them to, or deplete them from, the cell surface. Over the years, these probes provided a wealth of topological data (Pagano and Sleight, 1985) and laid the basis for the lipid raft hypothesis (van Meer et al., 1987).

By the time that it became clear that the C_6-NBD lipids did not faithfully reflect the phase properties of especially the raft forming sphingolipids (Wang and Silvius, 2000), a new fluorescent fatty acid analog was introduced, C_5-Bodipy,

that is more hydrophobic and has the attractive possibility that its fluorescence is concentration-dependent (Pagano et al., 1991). Its use has provided information on glycolipid concentration in microdomains in the endocytic pathway (Sharma et al., 2003), to which picture also other fluorescent probes had contributed (reviewed in Barbat et al., 2007; Mukherjee and Maxfield, 2000). Still, the phase properties of even the Bodipy-sphingolipids are different from those of their natural analogs (Wang and Silvius, 2000), and the question remains how their localization in cells relates to that of the natural sphingolipids.

A more recent breakthrough in the application of fluorescent analogs of the cellular lipids takes us back full circle to the use of parinaric acids. In the intervening 30 years new delivery technologies and improved microscopy have potentiated the use for cell biology of pyrene fatty acids, as being more stable analogs than the parinaric acids while maintaining close-to-natural properties (Somerharju, 2002). However, the parinaric acids have now been rendered suitable for light microscopy by the chemical addition of yet another conjugated double bond, which brings their excitation and emission wavelengths in the visible part of the spectrum. These fluorescent fatty acids are the first ones to be efficiently incorporated into cellular sphingolipids, illustrating their closest possible resemblance to the natural fatty acids and offering optimal possibilities to study the location and behavior of natural sphingolipids (Kuerschner et al., 2005). Still, there are numerous practical limitations to their broad application. The cunning combinations of biochemical, biophysical, and microscopic experiments devised over the years by numerous investigators for the application of other fluorescent lipid analogs should help to surmount these limitations and develop their utmost potential for the characterization of the topology of glycosphingolipids.

Glycosphingolipid topology in mammalian cells

Glycosphingolipids and SM have been found to be exposed on the surface of the cell by a number of biochemical approaches including enzymatic degradation, enzymatic and non-enzymatic oxidation, and the binding of antibodies and toxins. These data have led to the general impression that 60–70% of the cellular SM and a large fraction of all glycosphingolipids are exposed on the cell surface, i.e., in the outer, non-cytosolic leaflet of the plasma membrane (see Sillence et al., 2000; van Meer and Holthuis, 2000). This fits the overall idea that glycosphingolipids and SM are synthesized in the lumenal leaflet of the Golgi membrane and are transported via the inner leaflet of membrane vesicles (Figure 2). As predicted from this idea these lipids follow the endocytotic recycling pathways and are also present on the lumenal side of membranes of endosomes and lysosomes (van Genderen et al., 1991), where they are finally degraded (Kolter and Sandhoff, 2005).

Diffusion barrier-based lipid macrodomains

It has been realized for a long time that lipids on the surface of some cells display a polarized distribution. This is particularly true for epithelial cells from the intestine and the kidney where glycolipids or SM were found to be at least fourfold enriched in the apical domain of the continuous plasma membrane that surrounds those cells (see Holthuis et al., 2001; Simons and van Meer, 1988). This situation is maintained by the proteinaceous tight junctions, which form a barrier to lipid diffusion in the outer leaflet of the plasma membrane. Thus, the differences in lipid composition reside in the outer leaflet and the glycosphingolipids and SM are enriched in the outer leaflet of the apical membrane (discussed in Simons and van Meer, 1988). The other striking example of stable lipid macrodomains is found on the surface of sperm cells. In this case, the evidence points at a proteinaceous diffusion barrier between the acrosomal and post-acrosomal domain (James et al., 2004; Selvaraj et al., 2006).

Microdomains based on lipid–lipid interactions

Based on the enrichment of glycosphingolipids on the outside of the apical membrane and the preferential apical transport of various fluorescent glycosphingolipids as compared to sphingomyelin analogs in kidney and intestinal epithelial cells, it was proposed that these epithelial cells sort their lipids by the segregation of glycosphingolipids (and cholesterol) away from SM and phosphatidylcholine (plus cholesterol) in the lumenal leaflet of the trans Golgi network (van't Hof et al., 1992; van Meer et al., 1987). It was then suggested that such lipid-based domains might exist at the cell surface where they could be involved in signal transduction (Lisanti et al., 1994). This original suggestion concerned stable structures, the caveolae, for which it was shown at that time that they were enriched in the glycosphingolipid GM1 (Parton, 1994) by the application of cholera toxin on freeze-substituted samples, which was confirmed by photocrosslinking (Fra et al., 1995). Stable glycosphingolipid-enriched domains may also exist in various types of glycosynapses (Hakomori, 2002), e.g., non-caveolar glycosphingolipid signaling domains enriched in GM3 (Iwabuchi et al., 1998), and point contacts between neuronal growth cones and extracellular matrix (Negreiros et al., 2003). However, studies using a variety of biophysical techniques have suggested that microdomains of specific lipid compositions exist but that they are generally small and transient (Pike, 2006), unless they are stabilized by an increase in order. Large scale lipid segregation may be induced by a change in curvature (Roux et al., 2005; Sorre et al., 2009), or by changes occurring in membranes during signal transduction, like the generation of ceramide by a sphingomyelinase (Bollinger et al., 2005). Other factors causing lipid raft coalescence into stable platforms are the relatively subtle changes in lipid raft partitioning of multichain immune recognition receptors following signal initiation by ligandmediated

receptor crosslinking (Holowka et al., 2005; Pierce, 2002). In contrast, a different role for lipid rafts, namely as carriers for signaling molecules, has been suggested during the formation of the immunological synapse between antigen-presenting cells and T cells (Saito and Yokosuka, 2006).

Sorice et al. (1997) properly post-fixed anti-GM3 antibodies before addition of the secondary antibodies to prevent redistribution of the primary antibodies upon cross-linking by the secondary IgM, and observed, by fluorescence and electron microscopy, large, 300 nm clusters of GM3 molecules that covered close to 50% of the surface of T cells. When Spiegel et al. (1984) clustered GM1 into a cap on the lymphocyte surface via cholera toxin, anti-toxin antibodies and protein A, exogenously added (fluorescent) GM3 co-capped with GM1 suggesting that the two gangliosides resided in the same plasma membrane domains. However, Gomez-Mouton et al. (2001) reported that during T cell polarization GM1 and GM3 segregated into specific lipid rafts at the uropod and at the leading edge, respectively (Figure 2). In polarizing MCF-7 adenocarcinoma cells GM1 moved to the leading edge (Manes et al., 1999), which probably also represents the uropod in these fibroblast-like cells (Gomez-Mouton et al., 2001). Finally, partial co-localization of GM1- and GM3- enriched domains was reported by Barbat et al. (2007) after the induction of CD4 signaling in the absence of T cell receptor engagement[1]. However, electron microscopy and proper sample preparation protocols will be required to resolve whether there was real co-localization un-

[1] Since this paper appeared, additional evidence for the segregation of GM1 and GM3 into different domains has been reported. Fujita et al. (2007) used immunolabeling of quick-frozen, freeze fractured samples, where the external leaflet of the plasma membrane was stabilized by carbon and carbon-platinum shadowing. To make the outside of the membrane avaiable for labeling the stabilized outer leaflet was treated with SDS after which the labeling reagents were added. Although clusters of GM1 and GM3 were found to occasionally coincide, these aggregates were separated in most cases, suggesting the presence of heterogeneous microdomains. Janich and Corbeil applyied fluorescent cholera toxin B subunit against GM1 and an anti-GM3 antibody plus fluorescent secondary antibody to study the localization of the gangliosides on living cells, and observed that segregated GM1 and GM3 ganglioside-enriched rafts were found in different apical subdomains of MDCK cells. They obtained the same results when applying three different fixation/permeabilization protocols before the labeling. Although the paper provides a consistent picture, in none of the cases redistribution of the gangliosides during the fixation and labeling procedure was excluded. The segregated organization of GM1 and GM3 in the MDCK apical plasma membrane was confirmed by Chen et al. (2008) but the use of multivalent ligands in this study may have affected the distribution.

Evidence for the coexistence of different types of membrane microdomains has also been obtained by the non-invasive method of fluorescence life-time imaging (FLIM). Hofman et al. (2008) labeled the EGF receptor (EGFR) using single domain antibodies from Llama glama that specifically bind the EGFR without stimulating its kinase activity, and used FLIM to measure colocalization with fluorescent cholera toxin B and a GPI-GFP. In the resting state GM1 colocalized with both EGFR and GPI-GFP, but no colocalization at the nanoscale level was observed between EGFR and GPI-GFP, unless the cells were stimulated with EGF. The authors concluded that EGF induced the coalescence of the two types of GM1-containing microdomains that might lead to the formation of signaling platforms.

der these conditions. The same applies to the observation that GM1 and GD3 did not co-localize on cerebellar neurons (Vyas et al., 2001). Kiyokawa et al. (2005) concluded that GM1-rich membrane domains are spatially distinct from SM-rich domains on Jurkat T cells. However, because the SM-specific probe used, lysenin, does not bind to SM in the presence of glycosphingolipids (Ishitsuka et al., 2005), the possibility exists that (a high concentration of) SM was present in the GM1 rafts.

Evidence for the co-existence of different types of lipid rafts has also been reported for surface of neuronal cells. Two typical raft marker proteins, the glycosyl-phosphatidylinositol-anchored prion and Thy-1 proteins, occupied different domains. While prion protein occurred at high density in domains located primarily at the cell body, Thy-1 was clustered in separate domains mainly on neurites covering half of their surface (Madore et al., 1999). Affinity-purification of the two types of rafts from detergent-resistant membranes showed that prion protein rafts contained fivefold higher levels of glucosylceramide than Thy-1 rafts (Brügger et al., 2004).

Intracellular sphingolipids

In line with its synthesis in the lumen of the Golgi, the complex glycosphingolipid Forssman antigen was found in the Golgi, the plasma membrane and endosomal membranes, but not in mitochondria and peroxisomes (van Genderen et al., 1991). Obviously, high concentrations of glycosphingolipids can accumulate in endocytotic organelles in cells from patients suffering from a variety of storage diseases (Futerman and van Meer, 2004). In addition, a low density of Forssman antigen was observed over the ER and nuclear membrane, demonstrating that complex glycosphingolipids can be retrogradely transported to the ER (van Genderen et al., 1991). A number of glycolipid-binding toxins like cholera toxin (GM1) and Shiga toxin (Gb3) need to be transported back to the ER where their active subunit passes the membrane into the cytosol. It is not clear whether such transport reflects the natural retrograde transport of glycolipids or that it is induced by the pentameric toxins (Chinnapen et al., 2007; Falguieres et al., 2006), but GM1 has been found in the nuclear membrane by itself (Ledeen and Wu, 2006).

Although mitochondria generally contain very low levels of SM (van Meer, 1989), a remarkable increase has been reported for cancer cells (see Holthuis et al., 2001) and mitochondrial SM appears to be the precursor for the apoptotic mitochondrial ceramide (Birbes et al., 2001). Likewise, by immuno-electron microscopy mitochondria were negative for Forssman labeling (van Genderen et al., 1991) and for the disialo-ganglioside GD3 (Garcia-Ruiz et al., 2002; Rippo et al., 2000). However, mitochondrial GD3 labeling was found in Fas- and ceramide-induced apoptosis in lymphocytes (Rippo et al., 2000) and in TNF-treated hepatocytes (Garcia-Ruiz et al., 2002). Unfortunately, these papers did not provide data on the GD3 labeling of the other cellular organelles leaving many unanswered

questions concerning methodological controls and possible mechanisms of how GD3 got into the mitochondria. In any case, if the GD3 was originally synthesized in the lumen of the proximal Golgi (Uliana et al., 2006), it must have crossed a cellular membrane. This transmembrane translocation may have occurred as a consequence of the signaling at the plasma membrane (by the elusive scramblase?) or after retrograde traffic to the ER. Like all lipids tested so far GD3 may spontaneously translocate across the ER membrane. Subsequently, from the cytosolic surface of the ER it may reach the mitochondria, either via the ER-mitochondria contact sites or via monomeric transport through the cytosol, possibly stimulated by, e.g., the glycolipid transfer protein.

The fact that complex glycosphingolipids like Forssman glycolipid have been located to the ER and nuclear membrane and the indiscriminate flip-flop of lipids across the ER membrane suggests that SM and glycosphingolipids in general may occur to some extent in the cytosolic bilayer leaflet of the secretory and endocytotic organelles. Glucosylceramide is a special case in that it is synthesized on the cytosolic surface of the Golgi. Although many interactions between glycosphingolipids and cytosolic proteins have been reported over the years, a number of these studies were carried out *in vitro* and have not been validated in intact cells. In addition, when microscopic co-localization between glycosphingolipids and cytoskeletal elements was observed (i) often redistribution of the glycosphingolipid during sample preparation and labeling has not been thoroughly excluded, and (ii) the glycosphingolipids may have resided in the lumen of transport vesicles attached to the cytoskeleton (Gillard et al., 1993). Still, glycosphingolipids could in principle be present in complexes with proteins in the cytosol and nuclear matrix. A growing body of evidence supports the presence of intact phosphoinositides in the nuclear matrix, where they are thought to take part in signaling (Irvine, 2006), and the same may be the case for SM and glycosphingolipids (Ledeen and Wu, 2006).

A special case are the sphingolipids ceramide, ceramide-1-phosphate, sphingosine and sphingosine-1-phosphate which occur both as metabolic intermediates and as signaling lipids. It would be very important to be able to follow their local concentrations in time. However, there are several technical problems: (i) They are very sensitive to metabolic turnover (even during sample preparation), (ii) The single chain sphingosine and sphingosine-1-phosphate rapidly exchange as monomers through the aqueous phase, (iii) ceramide spontaneously flips across membranes, and finally (Rippo et al., 2000) there are only limited tools for their localization, like anti-ceramide antibodies (Vielhaber et al., 2001a) and it has not been established how well they label ceramide when it is present in different lipid and protein environments.

Perspectives

Glycosphingolipids and SM fulfill important functions within specialized domains of cellular membranes and in their interactions with proteins in, on and outside membranes. A combination of biological, physical, and chemical approaches is required to uncover these functions and the underlying molecular interactions. Morphology may be a great help. However, the traditional methodology is full of pitfalls. Notably, the specificity of the tools (Yanagisawa et al., 2006) and the sample preparation protocol (Heffer-Lauc et al., 2005; Schwarz and Futerman, 1997)[1] have been problematic. It is a tremendous challenge to try and overcome these methodological problems, and to be aware of them is a good start. All eukaryotes have sphingolipids and they display a bewildering range of structures. Evolution must have used their chemical and physical potential and endowed them with vital functions. Let's uncover them.

Acknowledgements

This work was supported by grant 805.47.084 of the program From Molecule to Cell of the Netherlands Foundations for Earth and Life Sciences and Chemical Research (NWO-ALW and NWO-CW) with financial aid from the Netherlands Organization for Scientific Research. We are very grateful for a grant from the Mizutani Foundation for Glycoscience (G. van Meer).

References

Albi, E., and Viola Magni, M.P. 2004. The role of intranuclear lipids. *Biol Cell* 96:657-667.

Abulrob, A., Lu, Z., Brunette, E., Pulla, D., Stanimirovic, D., and Johnston, L.J. 2008. Near-field scanning optical microscopy detects nanoscale glycolipid domains in the plasma membrane. *J Microsc.* 232:225-234.

Barbat, C., Trucy, M., Sorice, M., Garofalo, T., Manganelli, V., Fischer, A., and Mazerolles, F. 2007. p56 lck, LFA-1 and PI3K but not SHP-2 interact with GM1- or GM3-enriched microdomains in a CD4/p56 lck association-dependent manner. *Biochem J* in press.

Barbosa, M.L.F., and Pinto da Silva, P. 1983. Restriction of glycolipids to the outer half of a plasma membrane: Concanavalin A labeling of membrane halves in *acanthamoeba castellanii*. *Cell* 33:959-966.

Birbes, H., El Bawab, S., Hannun, Y.A., and Obeid, L.M. 2001. Selective hydrolysis of a mitochondrial pool of sphingomyelin induces apoptosis. *Faseb J* 15:2669-2679.

Bollinger, C.R., Teichgraber, V., and Gulbins, E. 2005. Ceramide-enriched membrane domains. *Biochim Biophys Acta* 1746:284-294.

Boot, R.G., Verhoek, M., Donker-Koopman, W., Strijland, A., van Marle, J., Overkleeft, H.S., Wennekes, T., and Aerts, J.M. 2007. Identification of the Non-lysosomal Glucosylceramidase as beta-Glucosidase 2. *J Biol Chem* 282:1305-1312.

[1] These authors describe the observation that lipids had redistributed during their preparation procedure, showing that they were insufficiently fixed.

Bosio, A., Binczek, E., and Stoffel, W. 1996. Functional breakdown of the lipid bilayer of the myelin membrane in central and peripheral nervous system by disrupted galactocerebroside synthesis. *Proc Natl Acad Sci USA* 93:13280-13285.

Brügger, B., Graham, C., Leibrecht, I., Mombelli, E., Jen, A., Wieland, F., and Morris, R. 2004. The membrane domains occupied by glycosylphosphatidylinositol-anchored prion protein and Thy-1 differ in lipid composition. *J Biol Chem* 279:7530-7536.

Butor, C., Stelzer, E.H., Sonnenberg, A., and Davoust, J. 1991. Apical and basal Forssman antigen in MDCK II cells: a morphological and quantitative study. *Eur J Cell Biol* 56:269-285.

Chen, Y., Qin, J., and Chen, Z.W. 2008. Fluorescence-topographic NSOM directly visualizes peak-valley polarities of GM1/GM3 rafts in cell membrane fluctuations. *J Lipid Res* 49:2268-2275.

Chinnapen, D.J., Chinnapen, H., Saslowsky, D., and Lencer, W.I. 2007. Rafting with cholera toxin: endocytosis and trafficking from plasma membrane to ER. *FEMS Microbiol Lett* 266:129-137.

Coetzee, T., Fujita, N., Dupree, J., Shi, R., Blight, A., Suzuki, K., Suzuki, K., and Popko, B. 1996. Myelination in the absence of galactocerebroside and sulfatide: normal structure with abnormal function and regional instability. *Cell* 86:209-219.

Downes, C.P., Gray, A., and Lucocq, J.M. 2005. Probing phosphoinositide functions in signaling and membrane trafficking. *Trends Cell Biol* 15:259-268.

Dragsten, P.R., Blumenthal, R., and Handler, J.S. 1981. Membrane asymmetry in epithelia: is the tight junction a barrier to diffusion in the plasma membrane? *Nature* 294:718-722.

Falguieres, T., Romer, W., Amessou, M., Afonso, C., Wolf, C., Tabet, J.C., Lamaze, C., and Johannes, L. 2006. Functionally different pools of Shiga toxin receptor, globotriaosyl ceramide, in HeLa cells. *Febs J* 273:5205-5218.

Fra, A.M., Masserini, M., Palestini, P., Sonnino, S., and Simons, K. 1995. A photo-reactive derivative of ganglioside GM1 specifically cross-links VIP21-caveolin on the cell surface. *FEBS Lett* 375:11-14.

Fujimoto, K., Umeda, M., and Fujimoto, T. 1996. Transmembrane phospholipid distribution revealed by freeze-fracture replica labeling. *J Cell Sci* 109:2453-2460.

Fujimoto, T. 1996. GPI-anchored proteins, glycosphingolipids, and sphingomyelin are sequestered to caveolae only after crosslinking. *J Histochem Cytochem* 44:929-941.

Fujita, A., Cheng, J., Hirakawa, M., Furukawa, K., Kusunoki, S., and Fujimoto, T. 2007. Gangliosides GM1 and GM3 in the Living Cell Membrane Form Clusters Susceptible to Cholesterol Depletion and Chilling. *Mol. Biol. Cell* 18:2112-2122.

Fujita, A., Cheng, J., and Fujimoto, T. 2009. Segretation of GM1 and GM3 clusters in the cell membrane depends on the intact actin cytoskeleton. *Biochim Biophys Acta.* 1791:388-396.

Futerman, A.H., and van Meer, G. 2004. The cell biology of lysosomal storage disorders. *Nat Rev Mol Cell Biol* 5:554-565.

Garcia-Ruiz, C., Colell, A., Morales, A., Calvo, M., Enrich, C., and Fernandez-Checa, J.C. 2002. Trafficking of ganglioside GD3 to mitochondria by tumor necrosis factor-alpha. *J Biol Chem* 277:36443-36448.

Gillard, B.K., Thurmon, L.T., and Marcus, D.M. 1993. Variable subcellular localization of glycosphingolipids. *Glycobiology* 3:57-67.

Gomez-Mouton, C., Abad, J.L., Mira, E., Lacalle, R.A., Gallardo, E., Jimenez-Baranda, S., Illa, I., Bernad, A., Manes, S., and Martinez, A.C. 2001. Segregation of leading-edge and uropod components into specific lipid rafts during T cell polarization. *Proc Natl Acad Sci USA* 98:9642-9647.

Hakomori, S.I. 2002. Inaugural Article: The glycosynapse. *Proc Natl Acad Sci USA* 99:225-232.

Hanada, K., Kumagai, K., Yasuda, S., Miura, Y., Kawano, M., Fukasawa, M., and Nishijima, M. 2003. Molecular machinery for non-vesicular trafficking of ceramide. *Nature* 426:803-809.

Heffer-Lauc, M., Lauc, G., Nimrichter, L., Fromholt, S.E., and Schnaar, R.L. 2005. Membrane redistribution of gangliosides and glycosylphosphatidylinositol-anchored proteins in brain tissue sections under conditions of lipid raft isolation. *Biochim Biophys Acta* 1686 3:200-208.

Hofman, E.G., Ruonala, M.O., Bader, A.N., van den Heuvel, D., Voortman, J., Roovers, R.C., Verkleij, A.J., Gerritsen, H.C., and van Bergen En Henegouwen, P.M. 2008. EGF induces coalescence of different lipid rafts. *J Cell Sci* 121:2519-2528.

Holowka, D., Gosse, J.A., Hammond, A.T., Han, X., Sengupta, P., Smith, N.L., Wagenknecht-Wiesner, A., Wu, M., Young, R.M., and Baird, B. 2005. Lipid segregation and IgE receptor signaling: a decade of progress. *Biochim Biophys Acta* 1746:252-259.

Holthuis, J.C., Pomorski, T., Raggers, R.J., Sprong, H., and Van Meer, G. 2001. The organizing potential of sphingolipids in intracellular membrane transport. *Physiol Rev* 81:1689-1723.

Hunt, A.N., and Postle, A.D. 2006. Mass spectrometry determination of endonuclear phospholipid composition and dynamics. *Methods* 39:104-111.

Ichikawa, S., Sakiyama, H., Suzuki, G., Hidari, K.I., and Hirabayashi, Y. 1996. Expression cloning of a cDNA for human ceramide glucosyltransferase that catalyzes the first glycosylation step of glycosphingolipid synthesis. *Proc Natl Acad Sci USA* 93:4638-4643.

Irvine, R.F. 2006. Nuclear inositide signalling -- expansion, structures and clarification. *Biochim Biophys Acta* 1761:505-508.

Ishitsuka, R., Sato, S.B., and Kobayashi, T. 2005. Imaging Lipid Rafts. *J Biochem (Tokyo)* 137:249-254.

Ishitsuka, R., Yamaji-Hasegawa, A., Makino, A., Hirabayashi, Y., and Kobayashi, T. 2004. A lipid-specific toxin reveals heterogeneity of sphingomyelin-containing membranes. *Biophys J* 86:296-307.

Iwabuchi, K., Handa, K., and Hakomori, S. 1998. Separation of "glycosphingolipid signaling domain" from caveolin-containing membrane fraction in mouse melanoma B16 cells and its role in cell adhesion coupled with signaling. *J Biol Chem* 273:33766-33773.

James, P.S., Hennessy, C., Berge, T., and Jones, R. 2004. Compartmentalisation of the sperm plasma membrane: a FRAP, FLIP and SPFI analysis of putative diffusion barriers on the sperm head. *J Cell Sci* 117:6485-6495.

Janich, P., and Corbeil, D. 2007. GM1 and GM3 gangliosides highlight distinct lipid microdomains within the apical domain of epithelial cells. *FEBS Lett* 581:1783-1787.

Kirschning, E., Rutter, G., and Hohenberg, H. 1998. High-pressure freezing and freeze-substitution of native rat brain: suitability for preservation and immunoelectron microscopic localization of myelin glycolipids. *J Neurosci Res* 53:465-474.

Kiyokawa, E., Baba, T., Otsuka, N., Makino, A., Ohno, S., and Kobayashi, T. 2005. Spatial and Functional Heterogeneity of Sphingolipid-rich Membrane Domains. *J Biol Chem* 280:24072-24084.

Kolter, T., and Sandhoff, K. 2005. Principles of lysosomal membrane digestion: stimulation of sphingolipid degradation by sphingolipid activator proteins and anionic lysosomal lipids. *Annu Rev Cell Dev Biol* 21:81-103.

Kuerschner, L., Ejsing, C.S., Ekroos, K., Shevchenko, A., Anderson, K.I., and Thiele, C. 2005. Polyene-lipids: a new tool to image lipids. *Nat Methods* 2:39-45.

Ledeen, R.W., and Wu, G. 2006. Sphingolipids of the nucleus and their role in nuclear signaling. *Biochim Biophys Acta* 1761:588-598.

Lisanti, M.P., Scherer, P.E., Tang, Z., and Sargiacomo, M. 1994. Caveolae, caveolin and caveolin-rich membrane domains: a signalling hypothesis. *Trends Cell Biol* 4:231-235.

Madore, N., Smith, K.L., Graham, C.H., Jen, A., Brady, K., Hall, S., and Morris, R. 1999. Functionally different GPI proteins are organized in different domains on the neuronal surface. *Embo J* 18:6917-6926.

Manes, S., Mira, E., Gomez-Mouton, C., Lacalle, R.A., Keller, P., Labrador, J.P., and Martinez, A.C. 1999. Membrane raft microdomains mediate front-rear polarity in migrating cells. *Embo J* 18:6211-6220.

Maneta-Peyret, L., Compere, P., Moreau, P., Goffinet, G., and Cassagne, C. 1999. Immunocytochemistry of lipids: chemical fixatives have dramatic effects on the preservation of tissue lipids. *Histochem J* 31:541-547.

Mayor, S., Viola, A., Stan, R.V., and del Pozo, M.A. 2006. Flying kites on slippery slopes at Keystone. Symposium on Lipid Rafts and Cell Function. *EMBO Rep* 7:1089-1093.

McGookey, D.J., Fagerberg, K., and Anderson, R.G. 1983. Filipin-cholesterol complexes form in uncoated vesicle membrane derived from coated vesicles during receptor-mediated endocytosis of low density lipoprotein. *J Cell Biol* 96:1273-1278.

Mukherjee, S., and Maxfield, F.R. 2000. Role of membrane organization and membrane domains in endocytic lipid trafficking. *Traffic* 1:203-211.

Negreiros, E.M., Leao, A.C., Santiago, M.F., and Mendez-Otero, R. 2003. Localization of ganglioside 9-O-acetyl GD3 in point contacts of neuronal growth cones. *J Neurobiol* 57:31-37.

Pagano, R.E., Longmuir, K.J., Martin, O.C., and Struck, D.K. 1981. Metabolism and intracellular localization of a fluorescently labeled intermediate in lipid biosynthesis within cultured fibroblasts. *J Cell Biol* 91:872-877.

Pagano, R.E., Martin, O.C., Kang, H.C., and Haugland, R.P. 1991. A novel fluorescent ceramide analogue for studying membrane traffic in animal cells: accumulation at the Golgi apparatus results in altered spectral properties of the sphingolipid precursor. *J Cell Biol* 113:1267-1279.

Pagano, R.E., and Sleight, R.G. 1985. Defining lipid transport pathways in animal cells. *Science* 229:1051-1057.

Parton, R.G. 1994. Ultrastructural localization of gangliosides; GM1 is concentrated in caveolae. J. Histochem. *Cytochem.* 42:155-166.

Pierce, S.K. 2002. Lipid rafts and B-cell activation. *Nat Rev Immunol* 2:96-105.

Pike, L.J. 2006. Rafts defined: a report on the Keystone Symposium on Lipid Rafts and Cell Function. *J Lipid Res.* 47:1597-8.

Plowman, S.J., Muncke, C., Parton, R.G., and Hancock, J.F. 2005. H-ras, K-ras, and inner plasma membrane raft proteins operate in nanoclusters with differential dependence on the actin cytoskeleton. *PNAS*:0504114102.

Proia, R.L. 2003. Glycosphingolipid functions: insights from engineered mouse models. *Philos Trans R Soc Lond B Biol Sci* 358:879-883.

Rintoul, D.A., and Simoni, R.D. 1977. Incorporation of a naturally occurring fluorescent fatty acid into lipids of cultured mammalian cells. *J Biol Chem* 252:7916-7918.

Rippo, M.R., Malisan, F., Ravagnan, L., Tomassini, B., Condo, I., Costantini, P., Susin, S.A., Rufini, A., Todaro, M., Kroemer, G., et al. 2000. GD3 ganglioside directly targets mitochondria in a bcl-2-controlled fashion. *Faseb J* 14:2047-2054.

Roux, A., Cuvelier, D., Nassoy, P., Prost, J., Bassereau, P., and Goud, B. 2005. Role of curvature and phase transition in lipid sorting and fission of membrane tubules. *Embo J* 24:1537-1545.

Saito, T., and Yokosuka, T. 2006. Immunological synapse and microclusters: the site for recognition and activation of T cells. *Curr Opin Immunol* 18:305-313.

Schulte, S., and Stoffel, W. 1993. Ceramide UDPgalactosyltransferase from myelinating rat brain: purification, cloning, and expression. *Proc Natl Acad Sci USA* 90:10265-10269.

Schwarz, A., and Futerman, A.H. 1997. Determination of the localization of gangliosides using anti-ganglioside antibodies: comparison of fixation methods. *J Histochem Cytochem* 45:611-618.

Selvaraj, V., Asano, A., Buttke, D.E., McElwee, J.L., Nelson, J.L., Wolff, C.A., Merdiushev, T., Fornes, M.W., Cohen, A.W., Lisanti, M.P., et al. 2006. Segregation of micron-scale membrane sub-domains in live murine sperm. *J Cell Physiol* 206:636-646.

Sharma, D.K., Choudhury, A., Singh, R.D., Wheatley, C.L., Marks, D.L., and Pagano, R.E. 2003. Glycosphingolipids internalized via caveolar-related endocytosis rapidly merge with the clathrin pathway in early endosomes and form microdomains for recycling. *J Biol Chem* 278:7564-7572.

Sillence, D.J., Raggers, R.J., and van Meer, G. 2000. Assays for transmembrane movement of sphingolipids. *Methods Enzymol* 312:562-579.

Simons, K., and van Meer, G. 1988. Lipid sorting in epithelial cells. *Biochemistry* 27:6197-6202.

Simpson, M.A., Cross, H., Proukakis, C., Priestman, D.A., Neville, D.C., Reinkensmeier, G., Wang, H., Wiznitzer, M., Gurtz, K., Verganelaki, A., et al. 2004. Infantile-onset symptomatic epilepsy syndrome caused by a homozygous loss-of-function mutation of GM3 synthase. *Nat Genet* 36:1225-1229.

Sklar, L.A., Hudson, B.S., and Simoni, R.D. 1975. Conjugated polyene fatty acids as membrane probes: preliminary characterization. *Proc Natl Acad Sci USA* 72:1649-1653.

Somerharju, P. 2002. Pyrene-labeled lipids as tools in membrane biophysics and cell biology. *Chem Phys Lipids* 116:57-74.

Sorice, M., Parolini, I., Sansolini, T., Garofalo, T., Dolo, V., Sargiacomo, M., Tai, T., Peschle, C., Torrisi, M.R., and Pavan, A. 1997. Evidence for the existence of ganglioside-enriched plasma membrane domains in human peripheral lymphocytes. *J Lipid Res* 38:969-980.

Sorice, M., Molinari, S., Di Marzio, L., Mattei, V., Tasciotti, V., Ciarlo, L., Hiraiwa, M., Garofalo, T., and Misasi, R. 2008. Neurotrophic signalling pathway triggered by prosaposin in PC12 cells occurs through lipid rafts. *FEBS J* 275:4903-4912.

Sorre, B., Callan-Jones, A., Manneville, J.B., Nassoy, P., Joanny, J.F., Prost, J., Goud, B., and Bassereau, P. 2009. Curvature-driven lipid sorting needs proximity to a demixing point and is aided by proteins. *Proc Natl Acad Sci USA* 106:5622-5626.

Spiegel, S., Kassis, S., Wilchek, M., and Fishman, P.H. 1984. Direct visualization of redistribution and capping of fluorescent gangliosides on lymphocytes. *J Cell Biol* 99:1575-1581.

Sprong, H., van der Sluijs, P., and van Meer, G. 2001. How proteins move lipids and lipids move proteins. *Nat Rev Mol Cell Biol* 2:504-513.

Steer, C.J., Bisher, M., Blumenthal, R., and Steven, A.C. 1984. Detection of membrane cholesterol by filipin in isolated rat liver coated vesicles is dependent upon removal of the clathrin coat. *J Cell Biol* 99:315-319.

Sugii, S., Reid, P.C., Ohgami, N., Shimada, Y., Maue, R.A., Ninomiya, H., Ohno-Iwashita, Y., and Chang, T.Y. 2003. Biotinylated theta-toxin derivative as a probe to examine intracellular cholesterol-rich domains in normal and Niemann-Pick type C1 cells. *J Lipid Res* 44:1033-1041.

Tillack, T.W., Allietta, M., Moran, R.E., and Young, J.W.W. 1983. Localization of globoside and forssman glycolipids on erythrocyte membranes. *Biochimica et Biophysica Acta (BBA) - Biomembranes* 733:15.

Uliana, A.S., Giraudo, C.G., and Maccioni, H.J. 2006. Cytoplasmic tails of SialT2 and GalNAcT impose their respective proximal and distal Golgi localization. *Traffic* 7:604-612.

van't Hof, W., Silvius, J., Wieland, F., and van Meer, G. 1992. Epithelial sphingolipid sorting allows for extensive variation of the fatty acyl chain and the sphingosine backbone. *Biochem J* 283 (Pt 3):913-917.

van Genderen, I.L., van Meer, G., Slot, J.W., Geuze, H.J., and Voorhout, W.F. 1991. Subcellular localization of Forssman glycolipid in epithelial MDCK cells by immuno-electronmicroscopy after freeze-substitution. *J Cell Biol* 115:1009-1019.

van Meer, G. 1989. Lipid traffic in animal cells. Annu Rev Cell Biol. 5:247-75.

van Meer, G., and Holthuis, J.C. 2000. Sphingolipid transport in eukaryotic cells. *Biochim Biophys Acta* 1486:145-170.

van Meer, G., and Simons, K. 1986. The function of tight junctions in maintaining differences in lipid composition between the apical and the basolateral cell surface domains of MDCK cells. *Embo J* 5:1455-1464.

van Meer, G., Stelzer, E.H., Wijnaendts-van-Resandt, R.W., and Simons, K. 1987. Sorting of sphingolipids in epithelial (Madin-Darby canine kidney) cells. *J Cell Biol* 105:1623-1635.

Vanier, M.T. 1999. Lipid changes in Niemann-Pick disease type C brain: personal experience and review of the literature. *Neurochem Res* 24:481-489.

Vielhaber, G., Brade, L., Lindner, B., Pfeiffer, S., Wepf, R., Hintze, U., Wittern, K.P., and Brade, H. 2001a. Mouse anti-ceramide antiserum: a specific tool for the detection of endogenous ceramide. *Glycobiology* 11:451-457.

Vielhaber, G., Pfeiffer, S., Brade, L., Lindner, B., Goldmann, T., Vollmer, E., Hintze, U., Wittern, K.P., and Wepf, R. 2001b. Localization of ceramide and glucosylceramide in human epidermis by immunogold electron microscopy. *J Invest Dermatol* 117:1126-1136.

Vyas, K.A., Patel, H.V., Vyas, A.A., and Schnaar, R.L. 2001. Segregation of gangliosides GM1 and GD3 on cell membranes, isolated membrane rafts, and defined supported lipid monolayers. *Biol Chem* 382:241-250.

Wang, T.Y., and Silvius, J.R. 2000. Different sphingolipids show differential partitioning into sphingolipid/cholesterol-rich domains in lipid bilayers. *Biophys J* 79:1478-1489.

Wattenberg, B.W., and Silbert, D.F. 1983. Sterol partitioning among intracellular membranes. Testing a model for cellular sterol distribution. *J Biol Chem* 258:2284-2289.

Wilson, B.S., Steinberg, S.L., Liederman, K., Pfeiffer, J.R., Surviladze, Z., Zhang, J., Samelson, L.E., Yang, L.H., Kotula, P.G., and Oliver, J.M. 2004. Markers for detergent-resistant lipid rafts occupy distinct and dynamic domains in native membranes. *Mol Biol Cell* 15:2580-2592.

Yamashita, T., Hashiramoto, A., Haluzik, M., Mizukami, H., Beck, S., Norton, A., Kono, M., Tsuji, S., Daniotti, J.L., Werth, N., et al. 2003. Enhanced insulin sensitivity in mice lacking ganglioside GM3. *Proc Natl Acad Sci U S A* 100:3445-3449.

Yamashita, T., Wada, R., Sasaki, T., Deng, C., Bierfreund, U., Sandhoff, K., and Proia, R.L. 1999. A vital role for glycosphingolipid synthesis during development and differentiation. *Proc Natl Acad Sci U S A* 96:9142-9147.

Yanagisawa, M., Ariga, T., and Yu, R.K. 2006. Cholera toxin B subunit binding does not correlate with GM1 expression: a study using mouse embryonic neural precursor cells. *Glycobiology* 16:19G-22G.

Chapter 4

GM1 gangliosidosis: Subcellular localization of the ganglioside GM1 in diseased cells

Sandra Hoetzl[1], Bruno Humbel[2], Alessandra d'Azzo[3] and Gerrit van Meer[1]

Manuscript in preparation

[1]Membrane Enzymology, Bijvoet Center and Institute of Biomembranes, Utrecht University, Utrecht, The Netherlands

[2]Dept. of Cellular Architecture and Dynamics, Institute of Biomembranes, Utrecht University, Utrecht, The Netherlands

[3]Dept. of Genetics and Tumor Cell Biology, St. Jude Children's Research Hospital, Memphis, TN, USA

Abstract
GM1 gangliosidosis, or Landing disease, is an autosomal recessive lysosomal storage disorder characterized by the generalized accumulation of GM1 ganglioside, oligosaccharides, and the mucopolysaccharide keratan sulfate (and their derivatives). This storage is due to defects in the lysosomal hydrolase acid β-galactosidase. In this study, different anti-GM1 antibodies were tested for their specificity for GM1 on lipid extracts by TLC immune overlay and on fixed cells by immunofluorescence. All antibodies bound specidically to GM1 and did not show cross-reactivity to other lipids tested, nor to mouse fibroblast (glyco)proteins. Co-localization studies by immunofluorescence showed that the accumulated GM1 in diseased cells localized mainly to lysosomal/endosomal structures. The ultrastructural distribution of the ganglioside GM1 was investigated in β-galactosidase$^{-/-}$ mouse embryonic fibroblasts by electron microscopy. After fixation, the cells were frozen in liquid nitrogen, freeze substituted and then embedded in Lowicryl HM20 at sub-zero temperatures. Using anti-GM1 antibodies, followed by labeling with protein A-gold, accumulated GM1 was shown to be essentially limited to multivesicular endosomes/lysosomes.

Introduction
Complex glycosphingolipids are found on cell surfaces where they are thought to fulfill important roles in recognition and signaling. They have been invoked in lateral domain formation on the cell surface, and may modulate cell surface receptors by promoting or inhibiting their partitioning into domains or by direct glycosphingolipid-protein interactions. A number of complex glycosphingolipids are medically relevant because they are used as receptors by parasites, bacteria, viruses and toxins. One interesting glycosphingolipid is the monosialoganglioside GM1.

GM1 gangliosidosis, or Landing disease, is an autosomal recessive lysosomal storage disorder characterized by the generalized accumulation of GM1 ganglioside, oligosaccharides, and the mucopolysaccharide keratan sulfate (and their derivatives). This storage is due to defects in the lysosomal hydrolase acid β-galactosidase (Figure 1). Interestingly, whereas certain mutations in this enzyme result in GM1 gangliosidosis with storage of primarily GM1, other mutations in the same enzyme result in Morquio B disease which is characterized by the storage of keratan sulfate. This divergence is probably due to the specific effects of each mutation on substrate binding and/or on the interaction of the enzyme with cofactors like saposins or other enzymes (Callahan, 1999). As is the case in other storage diseases, the storage of GM1 results in secondary storage of other material, such as lipids, glycoproteins and carbohydrates. Typically, it is unclear how the storage leads to the typical pathology of these diseases (Futerman and van Meer, 2004). Tessitore et al. (2004) reported that no pathologic effects of a

deficiency in β-galactosidase were found in a mouse model of GM1 gangliosidosis if at the same time the synthesis of GM1 was prevented by knocking out the GalNAc transferase in the pathway (Figure 1). This indicates that GM1 or a derivative is essential for causing the pathology. Substrate reduction therapy had clear beneficial effects in the mouse model (Kasparzyk et al., 2005; Elliot-Smith et al., 2008).

GM1 is monosialoganglioside that is synthesized in the Golgi lumen (Figure 1). From there it travels in the non-cytosolic leaflet of transport vesicles between cellular organelles. In A431 cells, by electron microscopy GM1 was found to be 100-fold enriched at the plasma membrane as compared to the ER (Parton, 1994). The simplest interpretation for this enrichment is the concentration of GM1 in sphingolipid/cholesterol rafts on the lumenal side of the Golgi membrane and preferential inclusion of these rafts into the anterograde secretory pathway (van Meer et al., 2008). In support of this, GM1 is invariably found enriched in detergent-resistant membranes, and has therefore been coined a "lipid raft marker". By electron microscopy GM1 has been found to be concentrated in caveolae on the cell surface (Parton, 1994), and by fluorescence it was found clustered on plasma membranes independent of GM3 (Gómez-Moutón et al., 2001; Fujita et al., 2007; Janich and Corbeil, 2007). One technical difficulty with the fluorescence studies is that GM1 was visualized by labeling with the pentavalent β-subunit of cholera toxin. Binding of the toxin to 5 GM1 molecules (Fishman et al., 1978) may locally order the membrane and can induce raft coalescence (Lingwood et al., 2008). Cholera toxin does therefore not always faithfully report the native organization of GM1.

Apart from a possible role in raft organization, GM1 has been related to the activities of a number of membrane channels, like Ca^{2+} channels and exchangers (see Wu et al., 2009), receptors such as the EGF, NGF and PDGF receptors (Mutoh et al., 1995; Farooqui et al., 1999). Would any of these functions of GM1 be affected when too much GM1 is around? One important observation was that GM1 gangliosidosis in the mouse model resulted in the activation of the unfolded protein response (UPR) pathway and neuronal cell death. From light microscopic localization of GM1 it seemed that embryonic fibroblasts from these mice had a higher concentration of GM1 in their ER membranes, supporting the hypothesis that UPR activation in β-galactosidase$^{-/-}$ cells could be a consequence of the abnormal accumulation of GM1 at the ER membrane that would perturb calcium homeostasis (Tessitore et al., 2004). Because the localization of glycolipids in opened cells by immunofluorescence has a number of potential pitfalls (Hoetzl et al., 2007), we set out in the present work to study the GM1 distribution at higher resolution by electron microscopy after freeze-substitution. To avoid redistribution of lipids in the samples, cells were fixed, frozen in liquid nitrogen, freeze substituted and embedded in Lowicryl at sub-zero temperatures (van Genderen et al. 2001). This technique was combined with post-embedding ("on sections") labeling, which provides accessibility of labeling reagent to the antigen without the need to

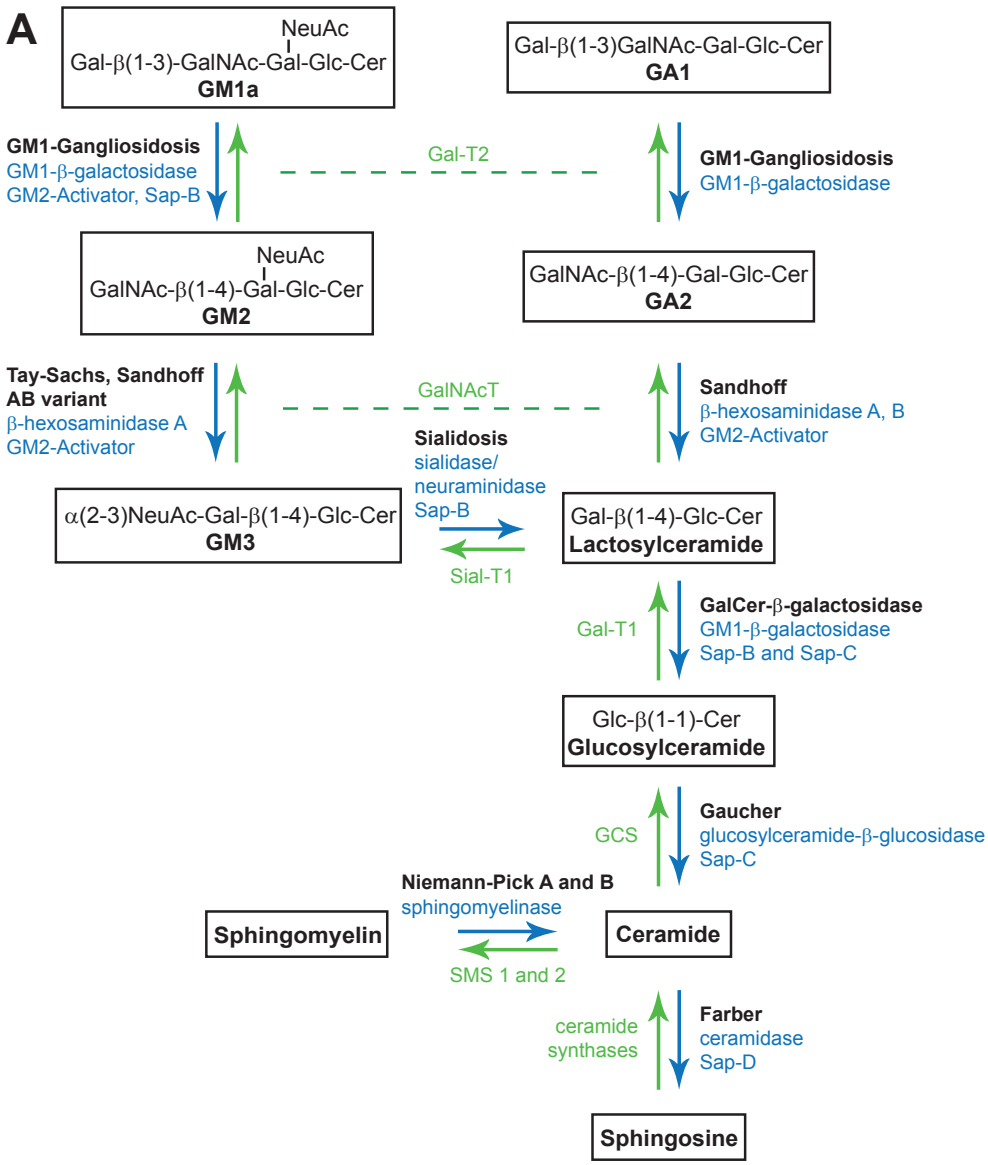

Figure 1. Pathways of GM1 biosynthesis and degradation. (A) Complex glycosphingolipids are synthesized by the stepwise addition of sugars by glycosyltransferases in the lumen of the Golgi. Degradation occurs in the lysosomal lumen by hydrolases that in many cases require saposins (Saps) for their activity (after Schulze et al., 2009). The notation GM1 is generally used to indicate the GM1a isoform. GM1b carries the sialic acid alpha2-3 on the terminal galactose. Glycosyltransferase nomenclature according to Maccioni et al. (1999), see also Hoetzl et al. (2007) and chapter 3 of this thesis. (B) Deficiency of β-galactosidase in GM1 gangliosidosis prevents the degradation of GM1 to GM2 in the lysosomes, leading to an accumulation of GM1. (C) Schematic structures of glycosphingolipids used in this study.

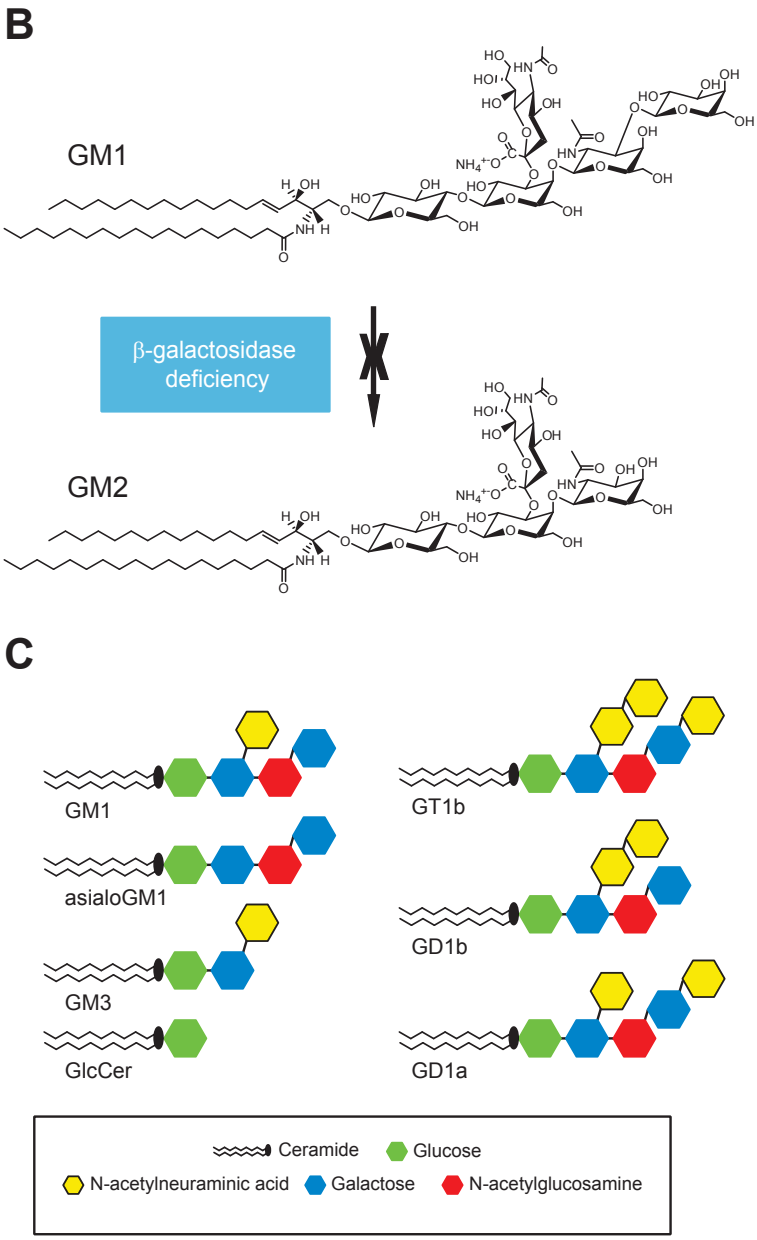

open the cells by detergents of organic solvents. In this study, we show that accumulated GM1 in GM1 gangliosidosis cells was essentially limited to multivesicular endosomes/lysosomes.

Results

Anti-GM1 antibodies bind specifically to GM1 and do not show cross-reactivity to other lipids or (glyco)proteins

One polyclonal and two monoclonal anti-GM1 antibodies (see Table 1) have been tested for their specificity to detect the ganglioside GM1 in ganglioside lipid mixtures. Furthermore we used lipid extracts of various cell types, to see if the antibodies identify specifically the ganglioside in a more complex lipid background and if cross-reactions with other gangliosides can be observed (for GSL structures see Figure 1C). Lipid extracts of wild type mouse embryonic fibroblasts (MEFs) and a melanocytic cell line, MEB4, which is known to lack GM1 (Ichikawa et al., 1994), were used in TLC immune overlay experiments. MEB4 cells contain no GM1, however, they contain the simple glycosphingolipid glucosylceramide (GlcCer) and the ganglioside GM3. These cells acted therefore as a control to test for cross-reactions on other lipids. For TLC immune overlay experiments, cells were collected and lipids were isolated as described in detail in Materials and Methods. Lipid extracts and a standard mixture containing GM1, GA1, lacking the sialic acid of GM1, and the gangliosides GD1a, GD1b and GT1b which contain additional sialic acids at either the proximal or at the distal galactose, were applied in duplicate to TLC plates. After running the TLC plates, the plates were split into sets of parallel plates, and one of the parallel plates was labeled with iodine to control for similar loading and subsequently with orcinol to identify glycolipids (Figure 2A). In MEB4 cells (Figure 2A, lane 2) clearly GlcCer and GM3 were detected by the orcinol stain.

Table 1. Antibodies used in this study

Antibody	Specification	Source	Known cross-reactivity
mouse anti-GM1	IgG subclass 1	Schnaar et al., 2002	GD1a
mouse anti-GM1	IgG subclass 2b	Schnaar et al., 2002	GD1a
rabbit anti-GM1	-	USBiological	GA1

This staining was not as pronounced in the MEFs. However, clearly GM1 and its derivative ganglioside GD1a were identified. Similar amounts of lipid extracts (30 nmol phosphate) were applied to the TLC plates, as shown by the iodine stain of a companion plate. TLC plates for the immune detection of lipids were overlaid with the antibody of interest as described in Materials and Methods. Detection was with HRP-conjugated secondary antibodies and enhanced chemiluminenscence on an X-ray film. All three antibodies tested clearly recognize GM1 in the standard (Figure 2A, lane Std), as well as in the lipid extract of wild type MEFs (Figure 2A, lane 2). In contrast to the literature (Schnaar et al. 2002), cross-reactivity of monoclonal antibodies with the gangliosides GD1a or GD1b was not detected. No further signal on the TLC plate for any of the antibodies was observed in the standard

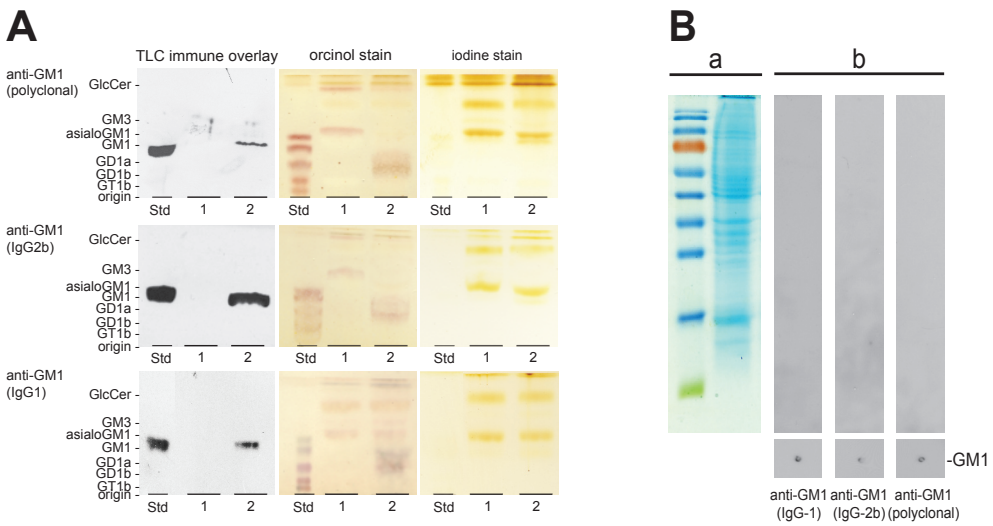

Figure 2. Specificity of anti-GM1 antibodies on lipid and protein extracts of cells. (A) TLC immune overlay staining of major brain gangliosides (lane Std) and lipid extracts of MEB4 (cells lacking GM1, lane 1) and wild type MEFs (lane 2) by anti-ganglioside antibodies. The standard, containing the gangliosides GA1, GM1, GM1, GD1a, GD1b and GT1b (150 pmol), and the lipid extracts (30 nmol phosphate) were spotted in duplicate at the origin of a TLC plate. After development, the plate was cut into 2 replicate sections. One section was immunostained as described in Material and Methods, with the indicated anti-GM1 antibody, the second section was first stained with iodine, and subsequently stained with orcinol/H_2SO_4 reagent. (B) Western blot analysis of anti-GM1 antibodies on total wild type MEF extracts. (a) A portion of the SDS-PAGE gel was coomassie stained. (b) Proteins separated by SDS-PAGE were blotted onto a nitrocellulose membrane and immunostained with the indicated anti-GM1 antibodies. As a positive control the ganglioside GM1 (150 pmol) was spotted on a nitrocellulose membrane and immunostained equally to the protein extract of the cells.

mixture and in the lipid extract of MEB4 cells. Therefore we can conclude that the tested antibodies show high affinity for GM1 and show no cross-reactivity towards other gangliosides. Although the same amounts of lipids were applied on the plates, our results suggested that the labeling intensity of the studied antibodies clearly differed (Figure 2A, TLC immune overlay). The monoclonal anti-GM1 (IgG-2b) showed the strongest signal of the three antibodies on wild type MEF lipid extracts, however the amount of antibodies used for labeling was not determined.

To investigate whether the anti-GM1 antibodies exclusively bind to the cellular lipids, a SDS-PAGE of a cell extract of β-galactosidase$^{-/-}$ MEFs was performed (Figure 2B). The gels were then incubated with the antibody of interest, followed by labeling with secondary antibodies. As a control, 150 pmol of GM1 were spotted onto nitrocellulose membranes and treated equally as the membranes with the cellular extract. Binding activity was only found in the GM1 control, indicating that the antibodies solely bound to glycolipids and not to glycoproteins.

Anti-GM1 antibodies detect accumulation and cellular redistribution of GM1 in diseased cells

Next, we wanted to test if the studied anti-GM1 antibodies are also able to reveal the accumulation of GM1 in β-galactosidase$^{-/-}$ mouse cells. These cells closely resemble the early onset form of human GM1 gangliosidosis (Tessitore et al., 2004). Identical amounts of lipid extract from MEB4 (Figure 3A, lane 1), wild type MEFs (Figure 3A, lane 2) and mutated β-galactosidase$^{-/-}$ cells (Figure 3A, lane 3) were spotted on a TLC plate. Plates were run, and parallel plates were either stained with iodine as a loading control, or immunostained with anti-GM1 (IgG-2b) antibody, as described above. This antibody was chosen for the experiment, because it gave the strongest signal in the experiment we described above (Figure 2A). In contrast to MEB4 cells, antibody binding activity of anti-GM1 (IgG-2b) towards GM1 could be found in MEF lipid extracts (Figure 3A). Clearly, a stronger antibody binding activity could be found in β-galactosidase$^{-/-}$ lipid extracts, indicating a many-fold accumulation of GM1 in diseased β-galactosidase$^{-/-}$ MEFs.

As lipids may be differently presented on a TLC plate from the surface of biological membranes, it is possible that the antibody recognized different epitopes in the cellular context. For that reason, we gathered more information about the cross-reactivity of the anti-GM1 antibodies by using immunofluorescence labeling of GM1 in cells having and lacking glycosphingolipids. Briefly, cells were fixed, opened with saponin and labeled with the primary antibody of interest, followed by labeling with secondary Alexa conjugated antibodies. In wild type MEFs only very weak staining at the plasma membrane (mouse IgG-1 antibody) or only background staining (polyclonal and mouse IgG-2b antibodies) was observed (Figure 3B). An increase of immunofluorescence levels was observed in β-galactosidase$^{-/-}$ cells, this is consistent with the accumulation of GM1 in mutant MEF lipid extracts (Figure 3A). Additionally, a striking redistribution of GM1 from the PM to punctuate structures at the perinuclear area (Figure 3B, right panel) was observed. This was consistently observed with all studied antibodies. Anti-GM1 antibodies did not show background staining in MEB4 cells, which are lacking GM1. However, anti-GM1 (IgG-1) antibodies show clearly higher immunofluorescence signals in these control cells. Although this antibody appears to be very specific for GM1 and does not react against glycoproteins (as shown in Figure 2B), results obtained with this antibody have to be interpreted cautiously.

Accumulated ganglioside GM1 localized mainly to lysosomal/endosomal structures

Figure 3B shows a distribution of GM1 in punctuate structures at the perinuclear area. As the phenotype for GM1 gangliosidosis is described by an accumulation of GM1 in lysosomes, and because of the finding that the central nervous system of mutant mice shows a compressed ER (Tessitore et al., 2004), we co-stained the wild type and mutant MEFs with lysotracker (marker for acidified

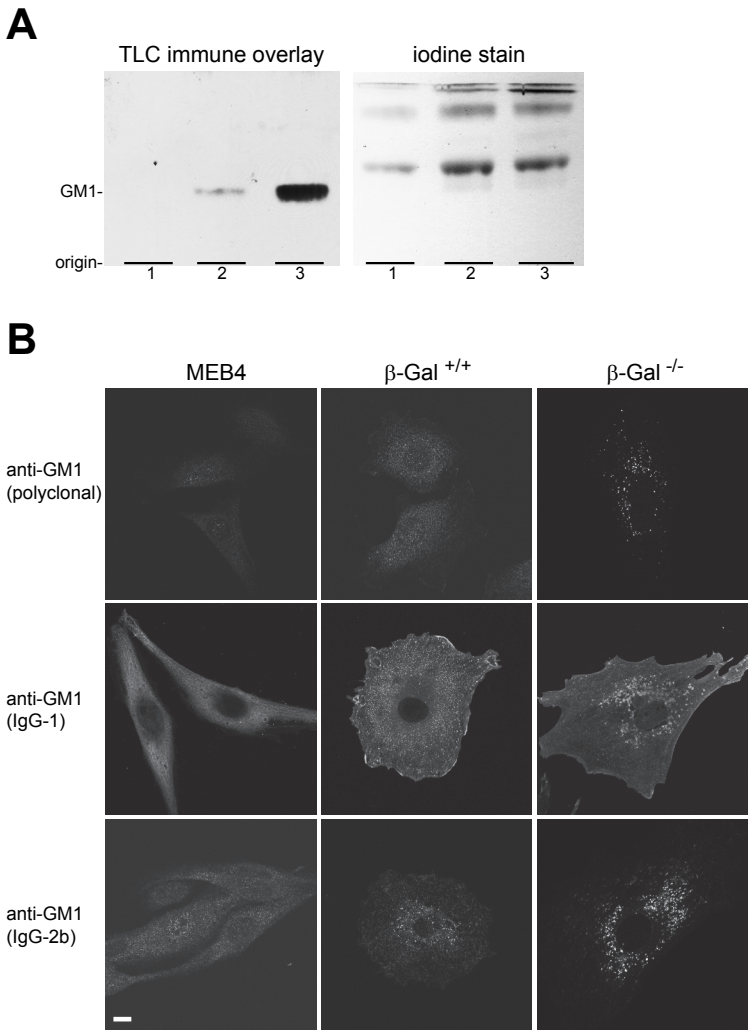

Figure 3. Accumulation and localization of GM1 in MEFs. (A) TLC immunostaining of total lipid extracts of MEB4 cells (lane 1), wild type MEFs (lane 2) and β-galactosidase$^{-/-}$ MEFs, with monoclonal anti-GM1 (IgG-2b) antibody. The same amounts of lipids were spotted on the TLC plate (30 nmol phosphate). As a loading control a parallel plate (prepared as described in Figure 2) stained with iodine is displayed. (B) MEB4 cells, wild type and β-galactosidase$^{-/-}$ MEFs were fixed, opened with saponin and labeled with indicated anti-GM1 antibodies, and Alexa 488 conjugated secondary antibodies. Bar, 10 μm

organelles) and anti-calnexin (ER marker). This staining would help us to get more information about the subcellular localization of this lipid. A clear increase of the number and size of lysosomes in mutant cells is observed in the middle panel of

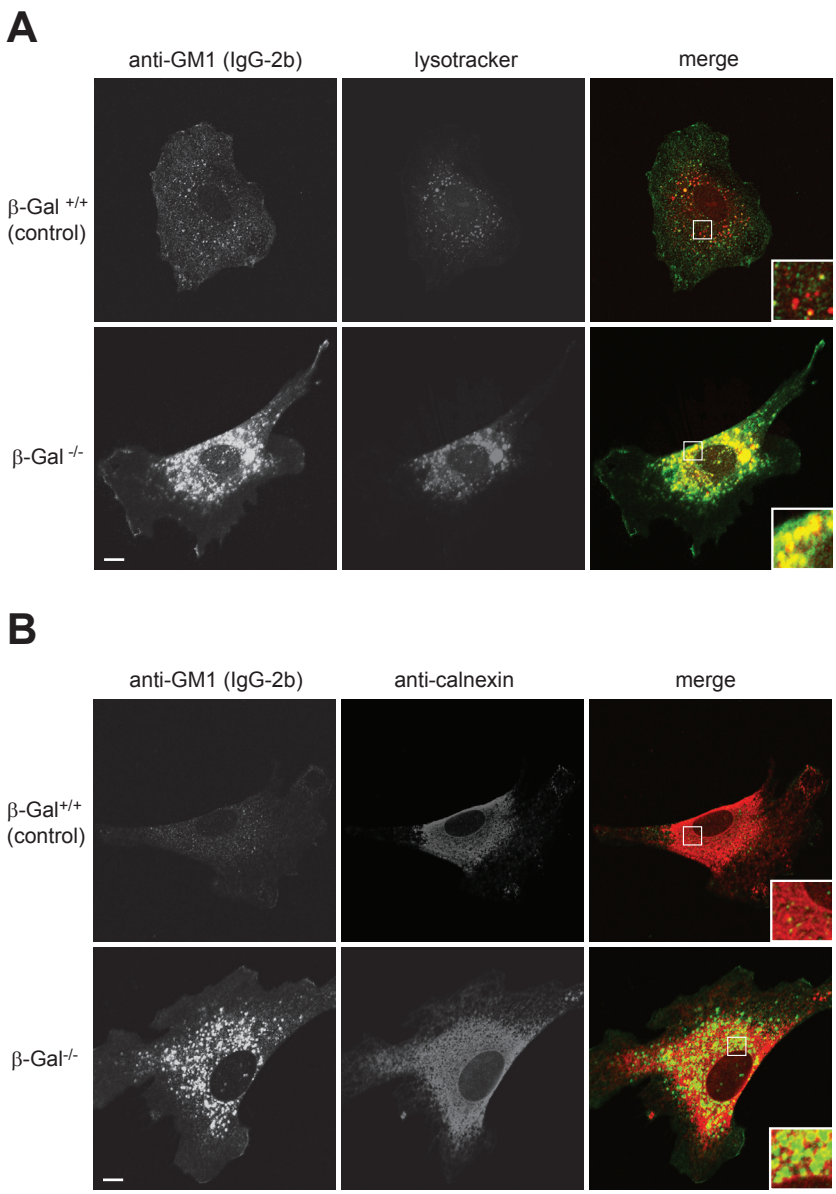

Figure 4. GM1 in MEFs, suffering from GM1 gangliosidosis, colocalizes mainly with lysosomal structures. (A) Confocal microscopy images of wild type and β-galactosidase$^{-/-}$ MEFs. Cells were grown on coverslips, incubated with Lysotracker Red DND-99 for 1 h at 37°C to stain for acidified organelles. After incubation the cells were washed, fixed, opened with saponin and immunostained with anti-GM1 (IgG-2b), followed by Alexa 488 conjugated secondary antibody (green, left panel). (B) Immunostaining of wild type and β-galactosidase$^{-/-}$ MEFs with anti-GM1 (IgG-2b) and the ER marker calnexin (red, middle panel). Bar 10 μm.

Figure 4A, confirming the phenotype of diseased cells. In β-galactosidase$^{-/-}$ MEFs a strong co-localization of the lysosomal marker with GM1 was observed. Such a colocalization was hardly detectable in wild type cells (Figure 4A). Labeling with the ER marker calnexin suggested that the labeling patterns were essentially complementary and that the yellow color, which indicates that green and red signal was present in the same pixel, might be due to insufficient resolution of the signals by the light microscope (Figure 4B). In wild type cells no colocalization of GM1 with calnexin was observed.

Accumulated GM1 is essentially limited to multivesicular endosomes/lysosomes
To overcome the shortcomings of immunofluorescence, we used an immuno electron microscopy approach. Due to the fact that lipids are not fixed by aldehydes, and are known to relocate when using detergents (Heffer-Lauc et al., 2005; see also chapter 3 of this thesis), we used freeze-substitution to be able to get access to the cytoplasm avoiding the use of detergents. Briefly, cells were chemically fixed, cryoprotected and frozen in liquid nitrogen. The samples were embedded in Lowicryl HM20 at sub-zero temperatures, and the resin was subsequently cross-linked by UV. Ultrathin sections were cut and processed for immunolabeling as described in Materials and Methods. Freeze-substituted samples showed an overall excellent morphology, showing well-defined nuclear envelopes, mitochondria, and vesicular membranes. Figure 5 shows representative pictures of wild type MEFs. In contrast, ultrathin sections of mutant cells (Figure 6) displayed a different morphology, showing a higher number and size of lysosomal structures in fibroblast cells. However, from these pictures no compressed ER was obvious, which is in contrast to the literature (Tessitore et al., 2004). Immunolabeling with anti-GM1 (IgG-2b) in control cells (Figures 5A,B), followed by a rabbit anti-mouse IgG antibody and protein A-gold (10 nm), revealed the localization of well-defined gold particles in low levels in endosomal structures, and over the nucleus and mitochondria, as depicted by the arrows. The same labeling pattern was found for the polyclonal anti-GM1 antibody (Figure 5C). In contrast to the low level of labeling in control cells, mutant MEFs showed high amounts of gold particles in lysosomal structures that were packed with membranous material (see Figure 6B,C). In addition, also in these cells some label was found over the nucleus and mitochondria, and at the PM (Figure 6B). The endoplasmic reticulum, however, also seemed to be labeled only in minor amounts.

In summary, we can conclude that freeze-substitution of samples is an excellent tool to localize specific lipids by using anti-lipid antibodies, avoiding redistribution of lipids due to detergents or organic solvents for opening the cells. Anti-GM1 antibodies confirmed an increasing level of GM1 in diseased cells, mainly located to lysosomal structures. Levels of labeled GM1 on the ER are comparable with those at the PM or over the nucleus. Further investigations have to exclude

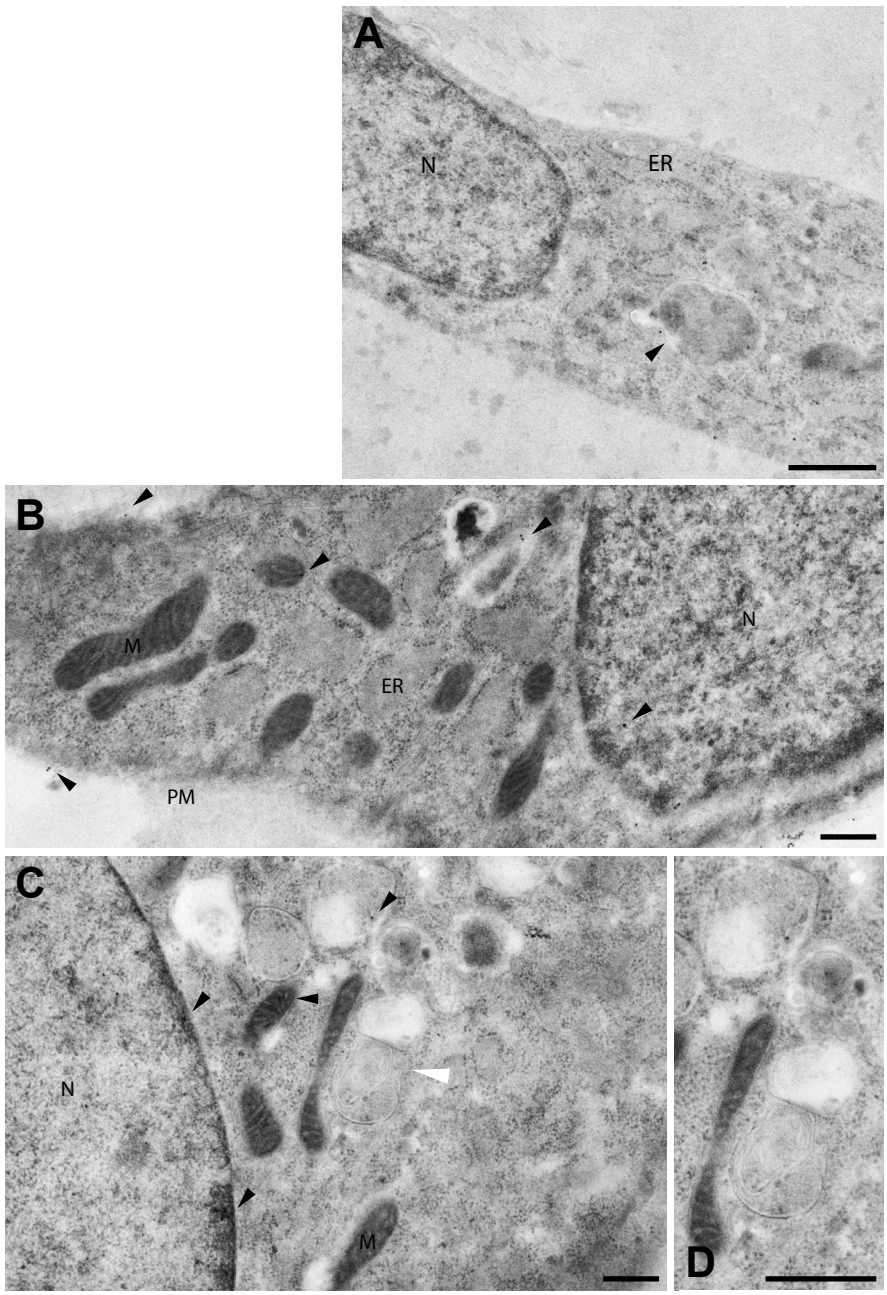
A
N
ER
B
M
ER
N
PM
C
N
M
D

background staining (by labeling of GM1 lacking cells), in order to see whether the localization of low levels of GM1 at the ER, mitochondria and in the nucleus are really due to an increased level of GM1 in these membranes.

Discussion

Storage of glycosphingolipids invariably results in severe diseases. Although some therapies, such as enzyme replacement therapy, substrate reduction therapy and even gene therapy hold promise in alleviating the pathology (Boomkamp and Butters, 2008), it will be very important to elucidate how the storage in the lumen of late endosomes and lysosomes leads to the disease pathology. One idea is that the stored lipid "leaks out" of the storage compartment and disarranges other cellular membranes, notably the ER membrane. This was postulated for Gaucher disease, where glucosylceramide accumulates, and where it was shown that artificial accumulation of glucosylceramide in hippocampal neurons resulted in enhanced Ca^{2+} release from the ER via the ryanodine receptor Ca^{2+} channel (Korkotian et al., 1999). A similar effect has been observed in the case of GM1 gangliosidosis, where it has been reported that GM1 forms a complex with the Na^{+}/Ca^{2+} exchanger in the nuclear membrane (see Wu et al., 2009). This alteration of the calcium content in the ER has been proposed to lead to an accumulation of misfolded proteins in the ER (Tessitore et al. 2004). Although this data suggest that GM1 can be found in lysosomes and in parts of the ER, the lack of resolution of the fluorescence experiments and the possibility that some GM1 had redistributed due to the presence of the detergent saponin did not allow a critical assessment of whether or not GM1 can spill over from the storage compartment to other membranes.

The mutant β-galactosidase$^{-/-}$ MEFs clearly contained a lot more GM1 than the control wild type cells (Figure 3A). This was not immediately clear from the immunofluorescence of GM1 (Figure 3B). First of all the IgG-1 antibody gave quite a bit of background labeling even in MEB4, which do not contain (or contain very little) GM1 (Ichikawa et al., 1994). Also the polyclonal antibody and the IgG-2b did not give the overall impression of a strongly increased GM1 content in the mutant

◄ **Figure 5. Immunogold labeling of GM1 in wild type MEFs.** Murine embryonic fibroblasts were fixed, cryoprotected and frozen in liquid nitrogen before freeze-substitution and embedding in Lowricryl HM20 at -40°C. (A,B) Sections were labeled with mouse anti-GM1 (IgG-2b), followed by rabbit anti-mouse bridging IgG antibody and protein A-gold (10 nm). In (A), labeling is located to endosomal vesicles and the plasma membrane (PM; as indicated by the arrowhead). (B) In addition, labeling is visible at the nucleus (N) and mitochondria (M). (C) Sections were labeled with polyclonal anti-GM1 and protein A-gold (10 nm). Labeling is visible in mitochondria, at the nucleus and in endosomal organelles. (D) A section (higher magnification of C) labeled by polyclonal anti-GM1 and protein A-gold (10 nm). Labeling was found in endosomal organelles, the nucleus and mitochondria (indicated by arrowheads). Note the unlabeled lysosome, packed with membranous material. Bars, 0.5 µm.

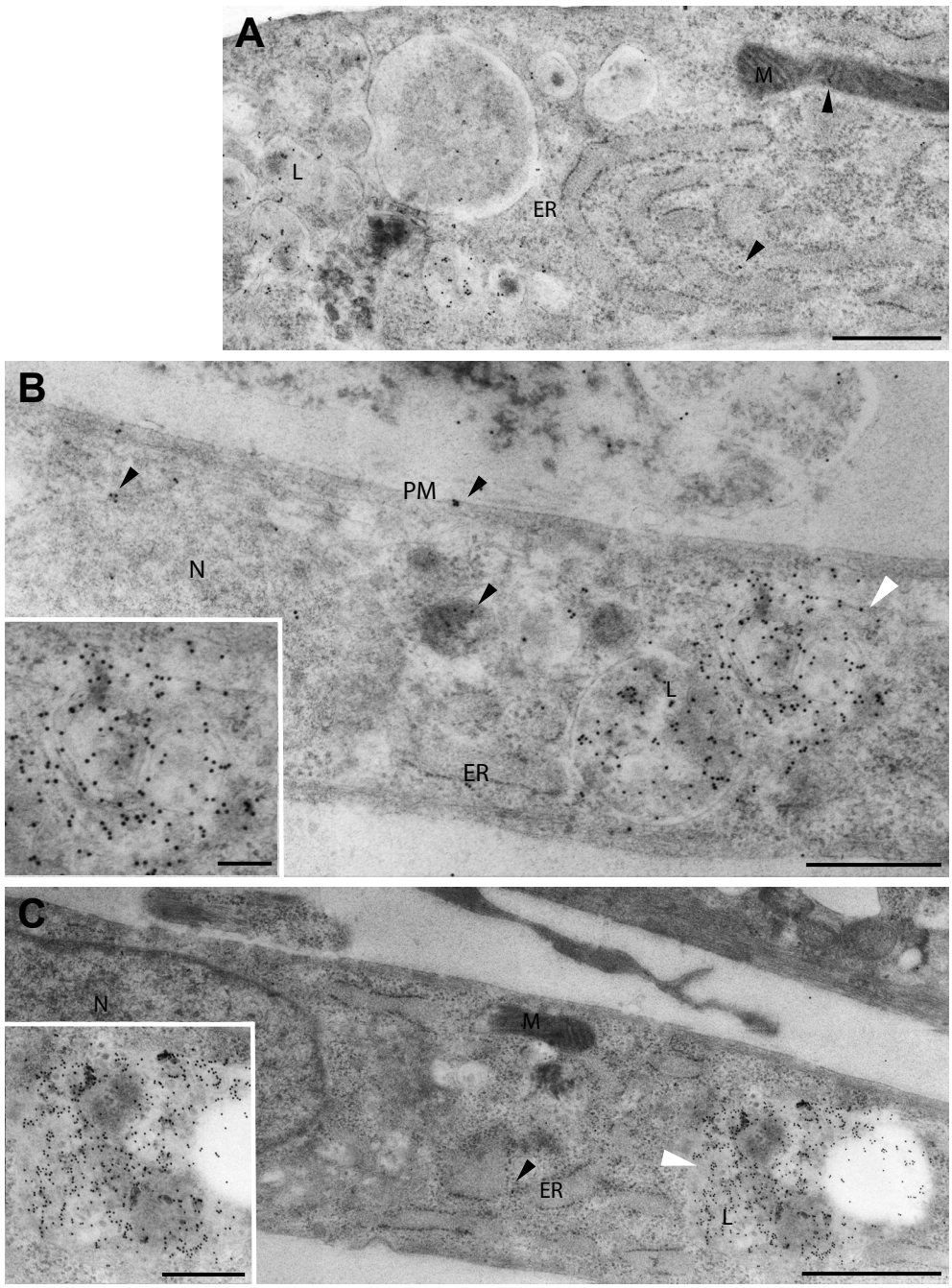
A
M
L
ER
B
PM
N
L
ER
C
N
M
ER
L

cells. However, the pattern of staining was very different between mutant and wild type cells. Whereas the wild type cells had a more homogeneous distribution of the label, the mutant cells clearly displayed a punctuate pattern. This is in itself remarkable because the membranes had been opened by the detergent saponin in order to make GM1 accessible to the antibody: clearly GM1 was not readily mobilized and was not distributed over the whole cell. Figure 4A shows that GM1 in wild type cells did not colocalize with acidic compartments stained by the lysotracker. However, we cannot exclude the possibility that part of the organelles lost the lysotracker due to the subsequent opening of the cells and washing steps during the antibody labeling protocol. Anyway, the GM1 staining did not co-localize with the ER marker calnexin, which fits the fact that no nuclear membrane staining of GM1 was evident. In contrast, in the β-galactosidase$^{-/-}$ cells we saw extensive co-localization of the bulk of the GM1 staining with the lysotracker (Figure 4A). However, there was still a significant fraction of the GM1 that did not co-localize with lysotracker positive organelles. Once again, part of the organelles may have lost the lysotracker. Part of the GM1 stain was on the plasma membrane. Although some yellow staining was observed which indicates that both GM1 and calnexin staining were recorded for these pixels, these pixels were located at sites where the bright green of a GM1 containing organelle touched the bright red of the calnexin-containing ER. A method with higher resolution than the conventional light microscope is required to resolve to what extent GM1 resided in the ER. Nuclear membrane staining was not observed for GM1.

In wild type fibroblasts, only a low level of gold labeling was observed (Figure 5). Label was located to endosomes and the plasma membrane. In addition, labeling is visible at the nucleus and mitochondria. A dramatic increase in the labeling density was observed in the mutant cells. Most amazing, the GM1 labeling was essentially limited to the multivesicular endosomes/lysosomes without a rise in label density over ER and nucleus. Thus, the present study does not provide evidence for a significant rise in the level of GM1 in the ER of GM1 gangliosidosis cells. However, because the labeling may not be quantitative at the low level of labeling in the ER, and because we have no idea how much GM1 would be required to damage the ER membrane, we cannot fully exclude the hypothesis that spill-over

◄ **Figure 6. Immunogold labeling of GM1 in β-galactosidase$^{-/-}$ MEFs.** Mutant MEFs were fixed, cryoprotected and frozen in liquid nitrogen before freeze-substitution and embedding in Lowricryl HM20 at -40°C. (A,B) Sections were labeled with mouse anti-GM1 (IgG-2b), followed by rabbit anti-mouse bridging IgG antibody and protein A-gold (10 nm). In A and B enlarged endosomal/lysosomal structures (L) are visible and highly labeled for GM1. Note the highly labeled endosomal/lysosomal structures, packed with membranous material. Some labeling is also associated with the plasma membrane (PM) and the nucleus (N). (C) Section was labeled by polyclonal anti-GM1 and protein A-gold (10 nm). Enlarged endosomal/lysosomal structures are highly labeled without labeling over other membranes such as ER and mitochondria (M). Bars, 0.5 µm. Insets in B and C show higher magnification images of areas indicated by white arrowheads. Scale bars in inset are 0.1 µm.

of GM1 to the ER causes the disease pathology. An alternative hypothesis is that lyso-GM1 would be produced in β-galactosidase$^{-/-}$ lysosomes, escape and cause the pathology. Very high levels of externally added lyso-GM1 (10-100 μM) caused neuronal apoptosis (Sueyoshi et al., 2001). Indeed, lyso-GM1 has been found in the brain of GM1 gangliosidosis patients (Kobayashi et al., 1992), but at levels 1,000x lower than GM1, so this issue remains to be resolved.

Although lysosomes are generally considered to be the endpoint of the endocytotic pathway, and a point of no return, work by Pagano and colleagues has suggested that there is a vesicular pathway out of the cholesterol storage compartment in Niemann-Pick type C cells, and that overexpression of Rab7 or Rab9 can dramatically reduce storage (Choudhury et al., 2002). Rab 7 and 9 are involved in the transport from early to late endosomes/lysosomes and from late endosomes to the trans Golgi network, respectively (see Mackiewicz and Wyroba, 2009). Interestingly, it has been demonstrated that cholera toxin-GM1 is endocytosed and targeted to the Golgi apparatus of normal cells, but to punctate structures in GM1 gangliosidosis fibroblasts (Puri et al., 2001) and Niemann-Pick type C cells (Sugimoto et al., 2001; Choudhuri et al., 2002). Trafficking of cholera toxin-GM1 to the Golgi of Niemann-Pick type C cells was restored when Rab7 or Rab9 was overexpressed (Choudhuri et al., 2002), bringing up the question whether transport to the Golgi would also be restored by overexpression of Rab7 or Rab9 in GM1 gangliosidosis fibroblasts. However, it has to be kept in mind that although cholera toxin has been used as a "probe" to monitor GM1 transport (Sugimoto et al., 2001), the binding of the pentavalent toxin to 5 GM1 molecules may affect its trafficking because cholera toxin has been shown to cluster GM1 on the cell surface and result in raft coalescence (Lingwood et al., 2008). Biotinylated GM1 was preferentially transported to the lumenal membranes of multivesicular endosomes in control fibroblasts, but the presence of a biotin label on the sialic acid in the GM1 headgroup may have affected the regular transport of GM1 in the cell (Möbius et al., 1999). So, the questions what are the normal transport pathways of GM1 in cells, how are they affected in β-galactosidase$^{-/-}$ cells, and can storage be prevented or cured by manipulating specific vesicular pathways remain to be resolved.

In summary, we have demonstrated that the accumulation of GM1 in multivesicular endo-/lysosomes of β-galactosidase$^{-/-}$ fibroblasts is not accompanied by a significant rise in the GM1 content of other cellular membranes, notably the ER membrane. Whether this is also true for other cell types, especially neuronal cells, remains to be established. This is important for finding out how GM1 storage causes the gangliosidosis pathology and what can be done about it.

Acknowledgements
We thank Ronald L. Schnaar for providing hybridoma cells. This work was supported by a grant of the The Netherlands Organization for Scientific Research (NWO/ALW MtC).

Materials and Methods

Materials

Chemicals, if not indicated otherwise, were from Sigma-Aldrich (St. Louis, Missouri) and used in the highest purity available. Lysotracker Red DND-99 was purchased from Invitrogen (Breda, The Netherlands). Silica TLC plates were from Merck (Darmstadt, Germany), organic solvents were from Riedel de Haën (Darmstadt, Germany). Cell culture media, reagents and FCS were from PAA (Pasching, Austria). Cell culture plastics were from Greiner Bio-One (Frickenhausen, Germany), and gangliotetraosylceramide and sialosyl derivatives mixlipid standards were from Matreya Inc. (Distrilab BV, The Netherlands).

Antibodies

Anti-GM1 polyclonal antibody was from USBiological (Swampscott, MA). GM1-1 and GM1-2b hybridoma cells were kind gifts from Ronald L. Schnaar (The Johns Hopkins School of Medicine, Baltimore, MD) and are described in Schnaar et al. (2002). The hybridoma clones were grown in Hybridoma-SFM (1x, from Invitrogen). Cell culture supernatants of secreted anti-GM1 (IgG subclass 2b) were used directly; anti-GM1 (IgG subclass 1) monoclonal antibodies were purified from cell culture supernatants via affinity chromatography using immobilized goat anti-mouse IgG agarose (Sigma). Polyclonal anti-calnexin antibody was obtained from Santa Cruz (Santa Cruz, CA), fluorescent secondary goat antibodies were obtained from Pierce (Perbio, The Netherlands). Horseradish peroxidase-conjugated secondary goat anti rabbit and mouse IgGs were from Dako (Glostrup, Denmark).

Cells

MEB4 cells were from RIKEN Cell Bank (Saitama, Japan). Embryonic fibroblasts from wild type and β-Gal$^{-/-}$ mice were kindly provided by Alessandra d'Azzo (St. Jude Children's Research Hospital, Memphis, TN) and used at low passage number (maximum four). All cells were grown in DMEM, stable glutamine, 4.5 g/l glucose, 10 % heat inactivated FCS at 37°C with 5% CO_2.

Lipid extraction

Lipids were extracted by a modified Bligh and Dyer extraction (Bligh and Dyer, 1959). In brief, cells were collected and 3 ml of chloroform/methanol/H_2O (1:4.4:0.2, v/v/v) were added to the cells. After 10 min extraction at room temperature, phase

separation was conducted by adding 1.5 ml of chloroform and 1.9 ml 10 mM HAc/120 mM KCl. After spinning for 10 min at 3,000 g in a table top centrifuge, the lower (chloroform) phase was removed and combined with the organic wash phase from an additional washing step. To collect higher gangliosides, which are also partly dissolved in the water phase, the water phase was applied to a Sep-Pak C18 cartridge (Waters, Millford, MA), washed once with water and eluted with 5 ml methanol. This methanolic solution was combined with the organic phases and the lipids were dried under N_2. Dried lipids were taken up with a solution of chloroform/methanol (2:1, v/v). Total phospholipids were quantified by phosphate determination according to Rouser et al. (1970).

TLC immune overlay

TLC immune overlay was performed as described by Schnaar and Needham (1994). 150 pmol of a ganglioside standard (GA1, GM1, GD1a, GD1b, and GT1b; 150 pmol each) and lipid extracts of cells (30 nmol phosphate) were spotted on replicate silica gel TLC plates (Merck, Darmstadt, Germany) and resolved using chloroform:methanol:0.2% aqueous $CaCl_2$ (55:45:10, v/v/v). After development, the plates were thoroughly dried then immersed in 2 mg/ml polyisobutylmethacrylate in hexane for 60 s. The plates were dried for 15 min, and then immersed in 5% Protifar (Nutricia, Zoetermeer, The Netherlands) in PBS (blocking buffer) for 30 min to inhibit nonspecific antibody binding. After that, the plates were overlaid with polyclonal anti-GM1 (1:500 in blocking buffer), or with mouse anti-GM1 (IgG-1) purified antibodies or anti GM1 (IgG-2b) hybridoma culture supernatants (1:5, respectively) for 1 h at room temperature. After incubation with primary antibodies, the plates were washed three times with blocking buffer. roteins were detected by overlaying with HRP-conjugated secondary antibodies and enhanced chemiluminescence (Amersham, Roosendaal, The Netherlands). Parallel plates were treated with orcinol/H_2SO_4 for chemical detection of gangliosides.

SDS-PAGE and Western blotting

Cells were washed 3 times with PBS and were resuspended in a protein sample buffer (200 mM Tris-HCl pH 6.8, 3% (w/v) SDS, 12% (v/v) glycerol, 1 mM EDTA, 0.003% (w/v) bromophenol blue, 50 mM dithiothreitol). Samples were heated for 5 min at 95°C and resolved by SDS-PAGE on 12% minigels. For Western blotting nitrocellulose transfers were blocked for 1 h with 5% Protifar in PBS (blocking buffer). Primary antibody incubations were for 1 h in blocking buffer. Detection was with HRP-conjugated secondary antibodies and enhanced chemiluminescence (Amersham, Rosendaal, The Netherlands).

Immunofluorescence microscopy
Cells were grown on glass coverslips (20% confluency) and fixed with 4% (w/v) freshly prepared paraformaldehyde in PBS for 20 min at RT. Cells were permeabilized with saponin and incubated with primary antibodies of interest for 1 h. After washing, cells were incubated with Alexa-conjugated secondary antibodies for 1 h and mounted in Mowiol and stored at -20°C till further use.
For staining of acidic organelles, cells were incubated for 1 h with 1 µM Lysotracker Red DND-99 in growth medium before fixation. Further steps and co-staining with antibodies follow the protocol described above.

Freeze substitution
Confluent 10 cm dishes of cells were rinsed shortly with 0.1 M phosphate buffer (pH 7.4) and fixed for 2 h in 2% paraformaldehyde and 0.2% glutaraldehyde in 0.1 M phosphate buffer at room temperature followed by an overnight incubation at 4°C. Fixed cells were washed twice with phosphate buffer containing 0.02 M glycine, cells were scraped and pelleted in 12% gelatin. Small blocks of the embedded cell pellets were infiltrated overnight in 2.3 M sucrose. Sucrose-protected blocks were frozen in liquid nitrogen. Frozen samples were transferred (under liquid nitrogen) into a Reichert Cs-auto freeze-substitution unit (Leica, Vienna, Austria). Freeze-substitution was carried out at -90°C in methanol supplemented with 0.5% uranyl acetate for 32 h. After raising the temperature to -40°C at a rate of 4°C/h, samples were kept at -40°C for 3 h. After several washes with pure methanol, the samples were infiltrated with Lowicryl HM20. Infiltration was done in the following graded series of Lowicryl/methanol mixtures: 1:3 for 2 h, 3:2 for 2 h, pure Lowicryl for 3h, and pure Lowicryl overnight (18 h). The samples were transferred, inside the Reichert Cs-auto, to a flat embedding mold filled with pure Lowicryl HM20 and polymerized by UV light at -30°C for 50 h. After that the temperature was raised to 0°C within 5 h. UV polymerization was continued for 24 h at room temperature.

Immunolabeling of Lowicryl Sections
Ultrathin Lowicryl sections were cut, nonspecific binding sites were blocked by incubating the sections for 20 min on a drop of 0.1 % BSA and 0.045% fish skin gelatin (Sigma) in PBS. Sections were incubated at room temperature with anti-GM1 antibodies diluted in BSA/fish skin gelatin in PBS. Sections, labeled with mouse anti-GM1 antibodies, were labeled with rabbit anti mouse-IgG antibody for 30 min in 0.1% BSA/fish skin gelatin in PBS, followed by labeling with protein A-gold (10 nm) for 20 min. Sections, labeled with polyclonal anti-GM1 antibody were directly labeled with protein A-gold (10 nm). Colloidal gold particles were prepared according to Slot and Geuze (1985) and conjugated to protein A (Roth et al. 1978). Sections were stained for 10 min with 2% uranyl acetate and viewed in a Tecnai 10 electron microscope (FEI company, Eindhoven, The Netherlands) at 80 kV.

References

Bligh, E.G., and Dyer, W.J. 1959. A rapid method of total lipid extraction and purification. *Can J Biochem Physiol* 37:911-917.

Boomkamp, S.D., and Butters, T.D. 2008. Glycosphingolipid disorders of the brain. *Subcell Biochem* 49:441-467.

Callahan, J.W. 1999. Molecular basis of GM1 gangliosidosis and Morquio disease, type B. Structure-function studies of lysosomal β-galactosidase and the non-lysosomal β-galactosidase-like protein. *Biochim Biophys Acta* 1455:85-103.

Choudhury, A., Dominguez, M., Puri, V., Sharma, D.K., Narita, K., Wheatley, C.L., Marks, D.L., and Pagano, R.E. 2002. Rab proteins mediate Golgi transport of caveola-internalized glycosphingolipids and correct lipid trafficking in Niemann-Pick C cells. *J Clin Invest* 109:1541-1550.

Elliot-Smith, E., Speak, A.O., Lloyd-Evans, E., Smith, D.A., van der Spoel, A.C., Jeyakumar, M., Butters, T.D., Dwek, R.A., d'Azzo, A., and Platt, F.M. 2008. Beneficial effects of substrate reduction therapy in a mouse model of GM1 gangliosidosis. *Mol Genet Metab* 94:204-211.

Farooqui, T., Kelley, T., Coggeshall, K.M., Rampersaud, A.A., and Yates, A.J. 1999. GM1 inhibits early signaling events mediated by PDGF receptor in cultured human glioma cells. *Anticancer Res* 19:5007-5013.

Fishman, P.H., Moss, J., and Osborne, J.C., Jr. 1978. Interaction of choleragen with the oligosaccharide of ganglioside GM1: evidence for multiple oligosaccharide binding sites. *Biochemistry* 17:711-716.

Fujita, A., Cheng, J., Hirakawa, M., Furukawa, K., Kusunoki, S., and Fujimoto, T. 2007. Gangliosides GM1 and GM3 in the living cell membrane form clusters susceptible to cholesterol depletion and chilling. *Mol Biol Cell* 18:2112-2122.

Futerman, A.H., and van Meer, G. 2004. The cell biology of lysosomal storage disorders. *Nat Rev Mol Cell Biol* 5:554-565.

Gómez-Moutón, C., Abad, J.L., Mira, E., Lacalle, R.A., Gallardo, E., Jiménez-Baranda, S., Illa, I., Bernad, A., Mañes, S., and Martínez-A., C. 2001. Segregation of leading-edge and uropod components into specific lipid rafts during T cell polarization. *Proc Natl Acad Sci USA* 98:9642-9647.

Heffer-Lauc, M., Lauc, G., Nimrichter, L., Fromholt, S.E., and Schnaar, R.L. 2005. Membrane redistribution of gangliosides and glycosylphosphatidylinositol-anchored proteins in brain tissue sections under conditions of lipid raft isolation. *Biochim Biophys Acta* 1686 3:200-208.

Hoetzl, S., Sprong, H., and van Meer, G. 2007. The way we view cellular (glyco)sphingolipids. *J Neurochem* 103 Suppl 1:3-13.

Ichikawa, S., Nakajo, N., Sakiyama, H., and Hirabayashi, Y. 1994. A mouse B16 melanoma mutant deficient in glycolipids. *Proc. Natl. Acad. Sci. USA* 91:2703-2707.

Janich, P., and Corbeil, D. 2007. GM1 and GM3 gangliosides highlight distinct lipid microdomains within the apical domain of epithelial cells. *FEBS Lett* 581:1783-1787.

Kasperzyk, J.L., d'Azzo, A., Platt, F.M., Alroy, J., and Seyfried, T.N. 2005. Substrate reduction reduces gangliosides in postnatal cerebrum-brainstem and cerebellum in GM1 gangliosidosis mice. J *Lipid Res* 46:744-751.

Kobayashi, T., Goto, I., Okada, S., Orii, T., Ohno, K., and Nakano, T. 1992. Accumulation of lysosphingolipids in tissues from patients with GM1 and GM2 gangliosidoses. *J Neurochem* 59:1452-1458.

Korkotian, E., Schwarz, A., Pelled, D., Schwarzmann, G., Segal, M., and Futerman, A.H. 1999. Elevation of intracellular glucosylceramide levels results in an increase in endoplasmic reticulum density and in functional calcium stores in cultured neurons. *J Biol Chem* 274:21673-21678.

Lingwood, D., Ries, J., Schwille, P., and Simons, K. 2008. Plasma membranes are poised for activation of raft phase coalescence at physiological temperature. *Proc Natl Acad Sci USA* 105:10005-10010.

Maccioni, H.J., Daniotti, J.L., and Martina, J.A. 1999. Organization of ganglioside synthesis in the Golgi apparatus. *Biochim. Biophys. Acta* 1437:101-118.

Mackiewicz, P., and Wyroba, E. 2009. Phylogeny and evolution of Rab7 and Rab9 proteins. *BMC Evol Biol* 9:101.

Möbius, W., Herzog, V., Sandhoff, K., and Schwarzmann, G. 1999. Intracellular distribution of a biotin-labeled ganglioside, GM1, by immunoelectron microscopy after endocytosis in fibroblasts. *J Histochem Cytochem* 47:1005-1014.

Mutoh, T., Tokuda, A., Miyadai, T., Hamaguchi, M., and Fujiki, N. 1995. Ganglioside GM1 binds to the Trk protein and regulates receptor function. *Proc Natl Acad Sci US*A 92:5087-5091.

Parton, R.G. 1994. Ultrastructural localization of gangliosides; GM1 is concentrated in caveolae. J. Histochem. Cytochem. 42:155-166.

Puri, V., Watanabe, R., Singh, R.D., Dominguez, M., Brown, J.C., Wheatley, C.L., Marks, D.L., and Pagano, R.E. 2001. Clathrin-dependent and -independent internalization of plasma membrane sphingolipids initiates two Golgi targeting pathways. *J Cell Biol* 154:535-548.

Roth, J., Bendayan, M., and Orci, L. 1978. Ultrastructural localization of intracellular antigens by the use of protein A-gold complex. *J Histochem Cytochem* 26:1074-1081.

Rouser, G., Fleischer, S., and Yamamoto, A. 1970. Two dimensional then layer chromatographic separation of polar lipids and determination of phospholipids by phosphorus analysis of spots. *Lipids* 5:494-496.

Schnaar, R.L., Fromholt, S.E., Gong, Y., Vyas, A.A., Laroy, W., Wayman, D.M., Heffer-Lauc, M., Ito, H., Ishida, H., Kiso, M., et al. 2002. Immunoglobulin G-class mouse monoclonal antibodies to major brain gangliosides. *Anal Biochem* 302:276-284.

Schnaar, R.L., and Needham, L.K. 1994. Thin-layer chromatography of glycosphingolipids. *Methods Enzymol* 230:371-389.

Schulze, H., Kolter, T., and Sandhoff, K. 2009. Principles of lysosomal membrane degradation: Cellular topology and biochemistry of lysosomal lipid degradation. *Biochim Biophys Acta* 1793:674-683.

Slot, J.W., and Geuze, H.J. 1985. A new method of preparing gold probes for multiple-labeling cytochemistry. *Eur J Cell Biol* 38:87-93.

Sueyoshi, N., Maehara, T., and Ito, M. 2001. Apoptosis of Neuro2a cells induced by lysosphingolipids with naturally occurring stereochemical configurations. *J Lipid Res* 42:1197-1202.

Sugimoto, Y., Ninomiya, H., Ohsaki, Y., Higaki, K., Davies, J.P., Ioannou, Y.A., and Ohno, K. 2001. Accumulation of cholera toxin and GM1 ganglioside in the early endosome of Niemann-Pick C1-deficient cells. *Proc Natl Acad Sci USA* 98:12391-12396.

Tessitore, A., del P. Martin, M., Sano, R., Ma, Y., Mann, L., Ingrassia, A., Laywell, E.D., Steindler, D.A., Hendershot, L.M., and d'Azzo, A. 2004. GM1-ganglioside-mediated activation of the unfolded protein response causes neuronal death in a neurodegenerative gangliosidosis. *Mol Cell* 15:753-766.

van Meer, G., Voelker, D.R., and Feigenson, G.W. 2008. Membrane lipids: where they are and how they behave. *Nat Rev Mol Cell Biol* 9:112-124.

Wu, G., Xie, X., Lu, Z.H., and Ledeen, R.W. 2009. Sodium-calcium exchanger complexed with GM1 ganglioside in nuclear membrane transfers calcium from nucleoplasm to endoplasmic reticulum. *Proc Natl Acad Sci USA.*

Chapter 5

Glycosphingolipids stabilize nanodomains of lipid-anchored proteins at the plasma membrane

Sandra Hoetzl[1], Arjen N. Bader[2], Dave van den Heuvel[2], Hein Sprong[3], Sarah J. Plowman[4], John F. Hancock[4], Hans C. Gerritsen[2] and Gerrit van Meer[1]

Manuscript in preparation

[1]Membrane Enzymology, Bijvoet Center and Institute of Biomembranes, Utrecht University, Utrecht, The Netherlands

[2]Department of Molecular Biophysics, Utrecht University, Utrecht, The Netherlands

[3]Present address: National Institute of Public Health and Environment (RIVM), Bilthoven, The Netherlands

[4]Department of Integrative Biology and Pharmacology, University of Texas Medical School at Houston, Houston, TX, USA

Abstract
(Glyco)sphingolipids and cholesterol play an important role in the functional organization of eukaryotic cell membranes as main components of lipid rafts in the exoplasmic leaflet. Coupling exoplasmic leaflet rafts with inner leaflet nanodomains could have important functional relevance, allowing the coupling of events outside to signaling pathways within the cell. Here, we tested the role of glycosphingolipids on the nanoscale organization of different lipid-anchored proteins at inner leaflet of the plasma membrane using electron microscopy and homo-FRET imaging. Electron microscopy showed that in melanoma cells GFP-labeled lipidation sequences of H-ras (GFP-truncated H-ras; GFP-tH) and K-ras (GFP-tK), as well as GFP-EGFR, were organized in nanodomains with radii of 8-14 nm. The average size of nanodomains was not significantly affected by the depletion of glycosphingolipids in GM95 cells. However, in GM95 cells the number of proteins per cluster was significantly decreased for cells expressing GFP-tH (from 3.0 to 1.8 proteins per cluster). Homo-FRET measurements showed that GFP-tH containing monomeric GFP (mGFP-tH) and mGFP-tK displayed nanoscale organization also at the molecular level (<5 nm radius). These small nanoclusters primarily consisted of dimers ($N_{av} \approx 2$). Depletion of glycosphingolipids resulted in significantly higher molecular clustering for both mGFP-tH and mGFP-tK, where the relative anisotropy dropped from 0.83 to 0.78 and from 0.87 to 0.83, respectively ($p=0.05$). In conclusion, glycosphingolipids did not affect the diameter of GFP-tH and GFP-tK clusters. However, they increased the number of GFP-tH and GFP-tK molecules per cluster. At the same time, the glycosphingolipids lowered the level of molecular interaction between these molecules.

Introduction
Glycosphingolipids (GSLs), sphingomyelin and cholesterol are thought to play an important role in the functional organization of membranes in eukaryotic cells as main components of lipid rafts. There is abundant evidence for the potential of sphingolipids and cholesterol to segregate from glycerophospholipids into domains of different fluidity (liquid-ordered, l_o, and liquid-disordered, l_d, respectively) in model membranes that mimic the lipid composition of the outer leaflet of eukaryotic plasma membranes. In addition, ordered lipid domains can be induced in lipid compositions that are typical for the inner leaflet of mammalian plasma membranes by having outer leaflet lipids in the opposed bilayer leaflet (reviewed in van Meer et al., 2008; Kiessling et al., 2009). Still, the occurrence, size and lifetime of lipid rafts in biomembranes have been the subject of heated debate over the last 20 years. A critical assessment of the literature suggested lipid rafts are small, <10-20 nm diameter, transient (<ms) and can be stabilized by lipid-anchored or transmembrane proteins (Hancock, 2006).

Recent developments in fluorescence microscopy have greatly improved the resolution of fluorescence light microscopy, and using this technology it has now been reported that in contrast to glycerophospholipids, sphingolipids are transiently trapped in cholesterol-mediated molecular complexes dwelling within <20-nm diameter areas, and the same behavior was observed for glycosyl-phosphatidylinositol anchored (GPI-) proteins (Eggeling et al., 2009), which lends strong support to the lipid raft model.

Lipid microdomains, or rafts, were originally proposed to be required for the sorting, in vesicular membrane traffic, of lipids and defined proteins (van Meer and Simons, 1988; reviewed in Hanzal-Bayer et al., 2007; van Meer et al., 2008), including glycosylphosphatidylinositol (GPI)-anchored proteins (Lisanti et al., 1989). While for a long time the size of rafts was only defined by their invisibility under the light microscope, FRET studies suggested that GPI-proteins occur as nanoscale clusters (Sharma et al., 2004). These probably coalesce when transport carriers bud from the membrane and a large-scale phase separation is stabilized by curvature and/or protein-protein interactions (Sorre et al., 2009; Tian et al., 2009). The major impact of the lipid raft model, however, has been in signal transduction, triggered by the notion that some lipid-anchored GTPases

Table 1. Constructs used

Membrane targeting motif	Protein	Motif sequence	Construct name	Reference
Inner leaflet				
Farnesylation/double palmitoylation	H-ras	CMSCK**CVLS**-Cterm	GFP-tH	Apolloni et al. (2000)
		CMSCK**CVLS**-Cterm	mGFP-tH	this study
Farnesylation/polybasic	K-ras	KKKKKSKTK**CVIM**-Cterm	GFP-tK	Apolloni et al. (2000)
		KKKKKSKTK**CVIM**-Cterm	mGFP-tK	this study
Geranylgeranylation/polybasic	K-ras	KKKKKSKTK**CCIL**-Cterm	GFP-tKCCIL	Prior et al. (2001), Hancock et al. (1991)
Membrane spanning				
	EGFR	not shown	EGFR-GFP	Paul van Bergen en Henegouwen, UU
			EGFR-mGFP	Erik Hofman, UU

preferentially associate with the rafts (Sargiacomo et al., 1993). Extensive studies have been carried out on the organization and kinase activity of the small GTPases H-ras and K-ras (its 4B splice variant), highly homologous key regulators of signal transduction, which are significantly different only in their C-terminal sequences that determine how they are anchored to the inner leaflet of the plasma membrane. Both proteins are farnesylated on a methylated C-terminal cysteine, but H-ras carries

two palmitoyl chains on cysteines at positions -2 and -5, whereas K-ras has a polybasic domain of 6 lysines in a row starting at position -5 of the processed protein. These studies have resulted in revised models for the organization of proteins in lipid rafts, suggesting that the H-ras lipid anchor itself drives the formation or stabilization of cholesterol-dependent nanoclusters, whereas K-ras is organized in a different type of cholesterol-independent domain (Hancock, 2006; Henis et al., 2009).

Because sphingomyelin and the complex GSLs are synthesized on the lumenal surface of the Golgi complex, from where they reach the plasma membrane by vesicular traffic, they are supposed to be present in the exoplasmic leaflet of the plasma membrane (van Meer et al., 2008). In most cells, sphingomyelin is the major sphingolipid and, therefore, the most likely contributor to raft formation. In contrast, every mammalian cell synthesizes the simple glycolipid glucosylceramide on the cytosolic side of the Golgi. From there it may have access to the inner leaflet of the plasma membrane via monomeric transfer across the cytosol (Warnock et al., 1994; Halter et al., 2007), where it may be involved in lipid segregation. In addition, complex GSLs may organize in discrete nanoclusters on the cell surface and regulate specific receptors (Gómez-Moutón et al., 2001; Fujita et al., 2007). It is therefore an interesting question whether the presence of glycosphingolipids is relevant for the nanoscale organization of proteins on the outer and inner surfaces of the plasma membrane. To address this question, we have used a melanoma mutant cell line that lacks the glucosyltransferase activity needed for the first step in regular glycolipid synthesis, the synthesis of glucosylceramide (Ichikawa et al., 1994). Like many other cells, melanoma cells lack the capability to synthesize galactosylceramide, and therefore this mutant lacks all glycolipid synthesis. Knockout mice for the glucosyltransferase die as embryos (Yamashita et al., 1999) but the mutant melanoma cell line only displays a hypopigmentation phenotype (Sprong et al., 2001). In this paper we report effects of the absence of glycosphingolipids on the organization of lipid-anchored proteins on the cytosolic surface of the plasma membrane.

Results

Clustering of lipid anchored proteins in cells with or without glycosphingolipids

First we wanted to test whether the type of lipid anchor determines the localization of lipid-anchored proteins at the cytosolic side of the plasma membrane of melanoma cells, and, second, whether the presence of GSLs plays a role in this organization. For this, GFP was coupled to the minimal membrane-targeting motifs of the Ras proteins H-ras and K-ras (the 4B splice variant; see Table 1), which differ in the lipid modification of their C-terminus. Both H-ras and K-ras are farnesylated, but H-ras is dually palmitoylated whereas K-ras contains a polybasic domain.

The constructs have been reported to be located in different nanodomains (Prior et al., 2003). As a control we included the GFP-labeled minimal membrane-targeting motif of K-ras where the farnesylation motif had been replaced by a geranylgeranylation motif, which abolished clustering (Prior et al., 2003). The different constructs were expressed in melanoma MEB4 cells and its derivative GM95 that lacks GSLs (Ichikawa et al., 1994).

The GFP-labeled targeting motif of K-ras, GFP-tK, and its geranylgeranylated analog GFP-tKCCIL, were mainly expressed at the plasma membrane of both MEB4 and GM95 cells (Figure 1A). Due to its low resolution, conventional fluorescence microscopy does not allow the characterization of lipid rafts or other microdomains. Therefore, we studied the microlocalization of the cytosolic lipid-anchored constructs by examining 2D sheets of plasma membrane. These were ripped off from adherent cells directly onto EM grids (Sanan and Anderson, 1991; Parton and Hancock, 2001). GFP-tK and GFP-tKCCIL were visualized in plasma membrane sheets using anti-GFP-4.5nm gold. In both cell types, each construct was distributed in small, morphologically featureless patches, as shown here for GM95 cells (Figure 1B). Due to the staining with uranyl acetate, the edges of plasma membrane sheets were clearly visible. Anti-GFP-4.5nm gold labeling was specific, localized within a plasma membrane sheet (Figure 1C).

To evaluate the complete gold patterns statistically, we analyzed point patterns using Ripley's K-function (Materials and Methods; Box 1). The variable L(r)-r is an index of clustering. It equals 0 when the gold particles have a complete spatial randomness (CSR) as assessed on length scale r. A value for L(r)-r > 1, the 99% confidence interval for CSR, indicates statistically significant clustering at that value of r, and the r value where maximal clustering is observed represents the mean radius of nanoclusters for that specific protein. The analysis of GFP-tK sheets showed that the gold particles were clustered in both MEB4 and GM95 cells (Figures 1D,E; dark gray line), i.e. the curves showed a significantly positive deviation from the L(r)-r value that would be expected for a random point pattern (Figures 1D,E; any value above the dashed line is significantly non-random). When the wild-type K-ras CVIM motif was replaced with CCIL, resulting in geranylgeranylation rather than farnesylation of the protein, clustering was reduced (Figures 1D,E; light gray line), most strongly in the mutant GM95 cells. A direct comparison between the mean K-function curves for MEB4 and GM95 demonstrated a significantly stronger clustering of GFP-tK in cells lacking GSLs ($p = 0.001$).

GFP-tH contains the minimal plasma membrane targeting motif of H-ras. With GFP-tK, it shares the farnesyl chain, but it lacks the polybasic domain and is dually palmitoylated instead. In contrast to GFP-tK, GFP-tH has been found to localize to cholesterol-dependent lipid rafts (Prior et al., 2001; 2003). So we tested

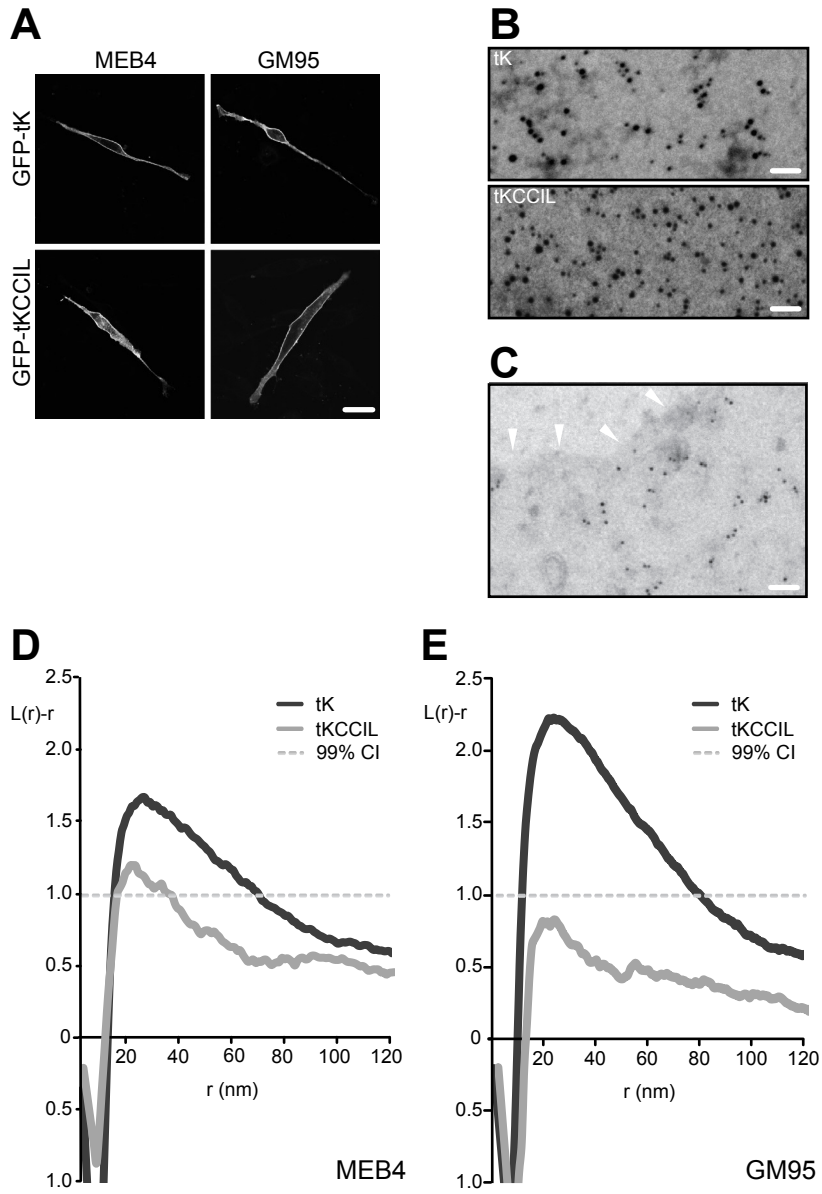
A
MEB4
GM95
GFP-tK
GFP-tKCCIL
B
tK
tKCCIL
C
D
L(r)-r
tK
tKCCIL
99% CI
r (nm)
MEB4
E
L(r)-r
tK
tKCCIL
99% CI
r (nm)
GM95

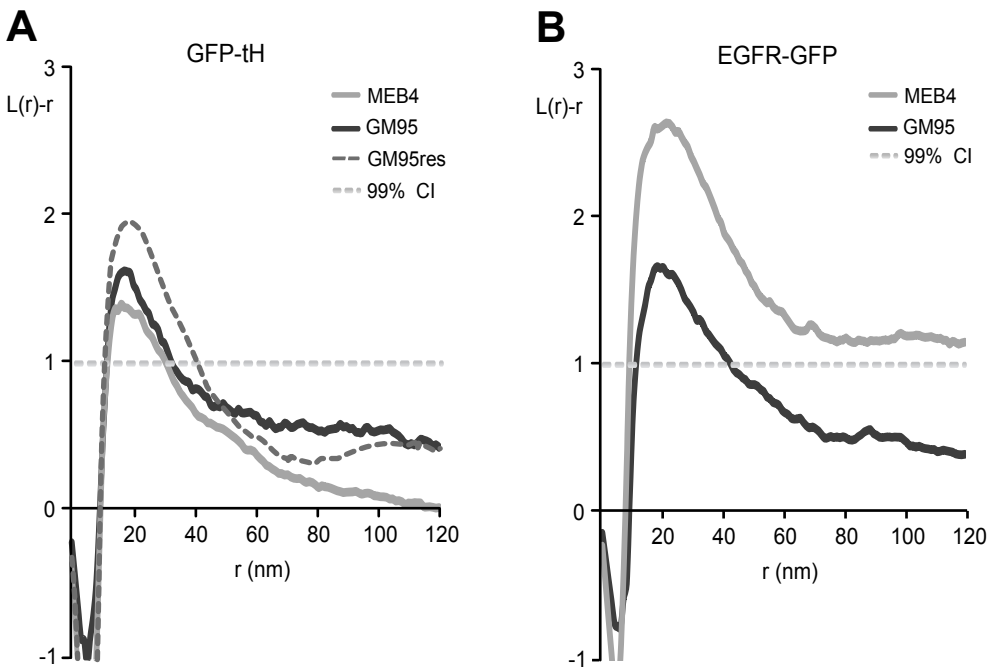

Figure 2. Clustering of a palmitoylated ras protein construct, GFP-tH, and of the transmembrane raft protein EGFR in MEB4 and GM95 cells. Plasma membrane sheets from cells expressing GFP-tH and EGFR-GFP were labeled with anti-GFP antibodies conjugated to 4.5 nm gold, and the spatial distribution of the gold particles analyzed. The K-function curves are weighted means (n ≥ 7). (A) No significant difference of clustering in MEB4 and GM95 cells was detected for GFP-tH (p = 0.747). (B) In MEB4 cells clustering of EGFR-GFP is increased, however, not significantly.

◄ **Figure 1. Lipid anchor dependence of plasma membrane nanoclusters in melanoma MEB4 cells and in mutant GM95 cells, which do not synthesize glycosphingolipids.** (A) Fluorescence pictures of cells transfected with GFP-tK and GFP-tKCCIL. Bar: 25 µm. (B) Plasma membrane sheets were prepared from cells expressing GFP-tK and GFP-tKCCIL. Sheets were labeled with anti-GFP antibodies conjugated to 4.5 nm gold. Representative electron microscopic images of GFP-tK and GFP-tKCCIL in GM95 cells. (C) Anti-GFP-4.5nm-gold labeling was specific, ending at the edge of a typical GFP-tK sheet (white arrowhead). EM bar 50 nm. (D, E) The spatial distributions of the gold particles were analyzed. Each L(r)-r curve represents a weighted mean K function analysis (n ≥ 10 replicates) and the total number of gold particles analyzed for each curve was ≥ 1800. L(r)- r values above the 99% confidence interval (99% CI; dashed line) for complete spatial randomness indicate statistically significant clustering at that value of r. tK was significantly clustered in both MEB4 (D) and GM95 cells (E) whereby GFP-tK clustering was significantly higher in GM95 cells than in MEB4 cells (p = 0.001). Replacement of the farnesyl anchor of GFP-tK with a geranylgeranyl anchor in GFP-tKCCIL resulted in a reduction in clustering. The reduction was significant in GM95 cells, which lack GSLs (p = 0.001).

whether GSLs play a role in the distribution of GFP-tH proteins in the melanoma cells. K-function analysis of gold-labeled GFP-tH plasma membrane sheets of GM95 and MEB4 cells showed significant positive deviation from the L(r)-r curve (Figure 2A). Significant clustering of GFP-tH was also observed in GM95res cells (Figure 2A, dashed gray line). No significant differences of clustering were observed for GFP-tH in cells having or lacking GSLs.

Membrane spanning proteins may be influenced by the lipid environment in both the outer and inner leaflet of the membrane. To determine whether the distribution of a transmembrane protein is influenced by GSLs, we investigated the distribution of a GFP-tagged version of the EGF receptor (EGFR-GFP), a known lipid raft protein (Hofman et al., 2008). Significant deviation of the L(r)-r curve from complete spatial randomness (CSR) was also observed for EGFR-GFP (Figure 2B). Although there was a higher probability of clusters in MEB4 cells, the difference with GM95 cells was not statistically significant.

Nanoclusters of lipid anchored proteins in cells measured by electron microscopy
An analysis of the radius of the nanoclusters (Table 2) shows that in MEB4 and GM95 cells clusters of GFP-tK were significantly bigger (26.5 nm and 25.8 nm, respectively) than for GFP-tH (19.4 nm and 18.1 nm) and EGFR-GFP (21.5 nm and 20.3 nm). If nanocluster size was compared in MEB4 and GM95, consistently larger clusters were observed in cells having GSLs. This difference was however not significant. As described in Materials and Methods, we also analyzed the mean

Table 2. Apparent cluster size (radius, nm) of lipid-anchored proteins[1]

	MEB4	GM95	GM95res
GFP-tK	26.5±2.7	25.8±1.6	-
GFP-tH	19.4±1.0	18.1±1.0	20.4±0.8
EGFR-GFP	21.5±1.3	20.3±0.9	-

[1] Numbers are the values for the radius, r, in nm where the deviation of the L(r)-r curves from CSR is maximal. They represent the mean values of 10 (GFP-tK) or 7 (GFP-tH and EGFR-GFP) individual K-function curves, ± SEM. For GFP-tH in BHK cells, the apparent cluster size of 20-22 nm resulted in an estimated real cluster size of 10-12 nm when a correction for antibody spacer distance was introduced (Plowman et al., 2005). Application of the calibration curve generated in that paper yields r values of 8-10 nm for GFP-tH, about 14 nm for GFP-tK and about 10 nm for EGFR-GFP. Because the correction introduces uncertainties by itself, and because the aim of the present work was not to calculate absolute domain sizes but to compare distribution patterns between cell types, the primary, uncorrected data are provided in this table.

number of molecules per cluster. Table 3 clearly shows, that compared to GM95 cells the number of proteins per cluster for cells expressing GFP-tH was significantly increased in MEB4 cells (from 1.8 to 3.0 molecules per cluster, $p < 0.05$). In GM95res cells this effect was even more drastic (4.3 molecules per cluster, $p < 0.05$).

Table 3. Number of lipid-anchored proteins per nanocluster[1]

	MEB4	GM95	GM95res
GFP-tK	6.2±1.0	5.4±0.9	-
GFP-tH	3.0±0.5	1.8±0.5	4.3±1.1
EGFR-GFP	4.8±1.0	3.3±0.8	-

[1] Numbers represent the mean values of 10 (GFP-tK) or 7 (GFP-tH and EGFR-GFP) K-function curves. They were calculated according to Parton and Hancock (2004), and are followed by the SEM. An antibody-gold labeling efficiency of 0.42 (see Plowman et al. 2005) was included into the calculations. When divided by the apparent cluster sizes (Table 2), the densities of GFP-tK in MEB4 and GM95 cells were 2.8 and 2.6 $x10^{-3}/nm^2$. For GFP-tH the densities in MEB4, GM95 and GM95res cells were 2.5, 1.7 and 3.3 $x10^{-3}/nm^2$, respectively. Finally, for EGFR-GFP, the densities in MEB4 and GM95 cells were 3.3 and 2.5 $x10^{-3}/nm^2$, respectively. After correction for antibody spacer distance the real densities are about 4x higher, around $10^{-2}/nm^2$. For comparison, the density of cholesterol/phospholipid pairs with a surface area of some 90 $Å^2$ is about $1/nm^2$.

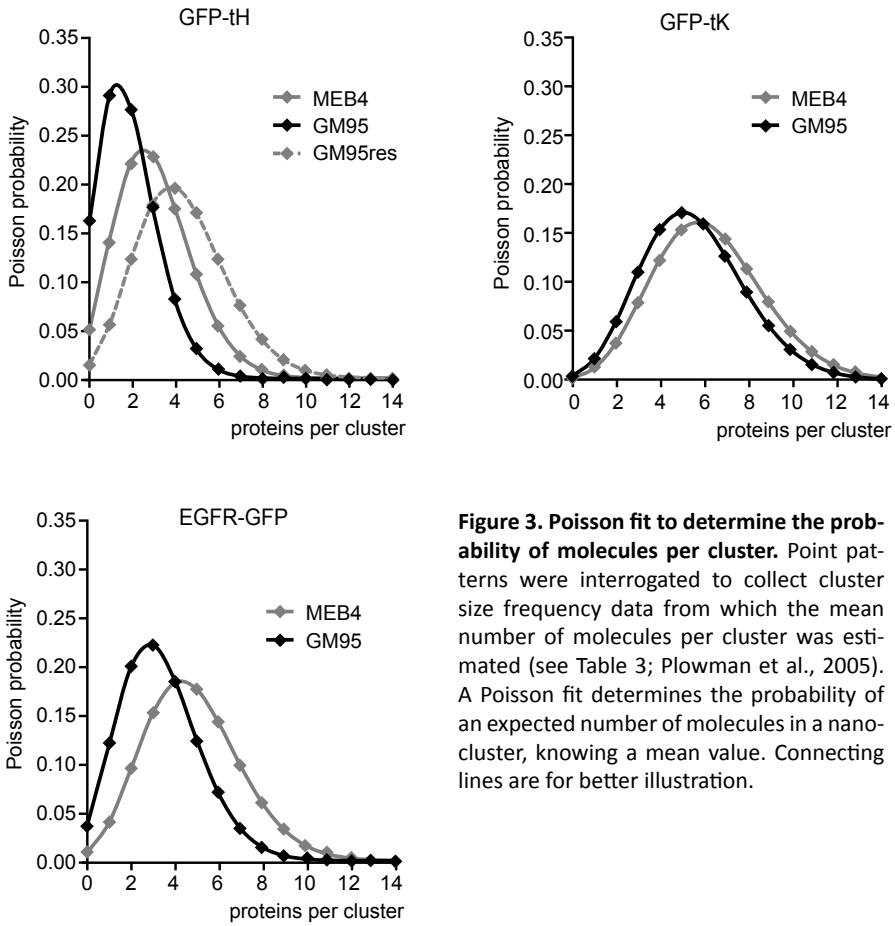

Figure 3. Poisson fit to determine the probability of molecules per cluster. Point patterns were interrogated to collect cluster size frequency data from which the mean number of molecules per cluster was estimated (see Table 3; Plowman et al., 2005). A Poisson fit determines the probability of an expected number of molecules in a nanocluster, knowing a mean value. Connecting lines are for better illustration.

Although the increase of proteins per cluster is also observed in GM95 and MEB4 cells expressing GFP-tK (5.4 to 6.2 molecules) and the membrane spanning protein EGFR-GFP (3.3 to 4.8 molecules), these differences were not significant. A different representation of the data is provided in Figure 3. A Poisson fit was used to determine the probability of molecules per cluster. In MEB4 cells, 80% of clusters contained 2 to 14 mGFP-tH molecules. This value decreased to 55% in GM95 cells. For GFP-tK no significant difference were found (MEB4, 93%; GM95, 95%).
However, also for EGFR-GFP the fraction of clusters, which consists of 2 to 14 molecules decreased from 94% in MEB4 cells to 85% in GM95 cells. Clearly, more proteins per nanocluster were found in cells containing GSLs, suggesting that the presence of GSLs changes the lipid-protein interactions leading to a steady state with a higher number of GFP-tH (and other palmitoylated proteins?) per cluster.

Molecular scale interaction of lipid anchored proteins assessed by homo-FRET
Various methods, like immuno-electron microscopy, FRET, and single-fluorophore tracking microscopy, have been used to investigate nanodomain organization on the plasma membrane of intact cells. Each of these has its spatial and temporal limitations. Electron microscopic analysis provides information on clustering on length scales ≤ 200 nm, but the antibody spacer distance precludes studies on a nm length scale. To get a better insight into the clustering of molecules in their direct molecular neighborhood (≤ 10nm), we studied the clustering of identical proteins at the plasma membrane by confocal time-resolved fluorescence anisotropy imaging microscopy (CTR-FAIM). This technique can be used to observe FRET between identical fluorophores (homo-FRET): after excitation with polarized light, the fluorophores that are monomers or act as donors exhibit a high anisotropy ($r_{mono} \approx 0.4$), whereas for the fluorophores that act as acceptor the anisotropy is much lower (also see Box 2). Therefore, CTR-FAIM is able to detect proximity between identical fluorescent reporters (e.g. GFP) at the nm level.

Previously, it has been shown that by utilizing anisotropy, the number of identical fluorophores within a cluster can be quantitatively imaged (Bader et

► **Figure 4. Time-resolved fluorescence anisotropy imaging of lipid anchored proteins in melanosomal cells.** Confocal steady-state intensity, fluorescence anisotropy and cluster size images of MEB4 and GM95 cells, expressing mGFP-tH (A) and mGFP-tK (B). (C) Histogram of the average anisotropy values of the samples in (A) and (B). Per sample at least 4 cells were imaged. The intensity values of all significant pixels were added together for each of the two emission channels and the overall anisotropy per cell (r_{inf}) was calculated. The initial anisotropy value (r_{mono}) for GFP in solution was 0.38. The dashed lines give the borders of the anisotropy ranges for average cluster sizes N_{av} = 1, 2 and ≥ 3. (D) Time-gated anisotropy decays of the mGFP-tH and mGFP-tK in MEB-4 and GM95 cells. The black line shows the decay of GFP monomers in glycerol/buffer (50/50). The error bars give the standard error of the mean (SEM), statistical differences were determined by student t-test (*$p < 0.05$). r_{inf} values are expressed as a fraction of r_{mono}.

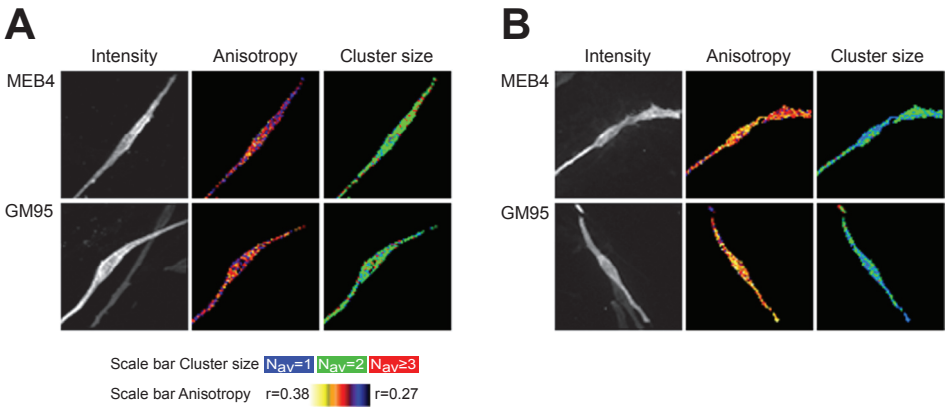
A
Intensity
Anisotropy
Cluster size
MEB4
GM95
B
Intensity
Anisotropy
Cluster size
MEB4
GM95
Scale bar Cluster size Nav=1 Nav=2 Nav≥3
Scale bar Anisotropy r=0.38 r=0.27

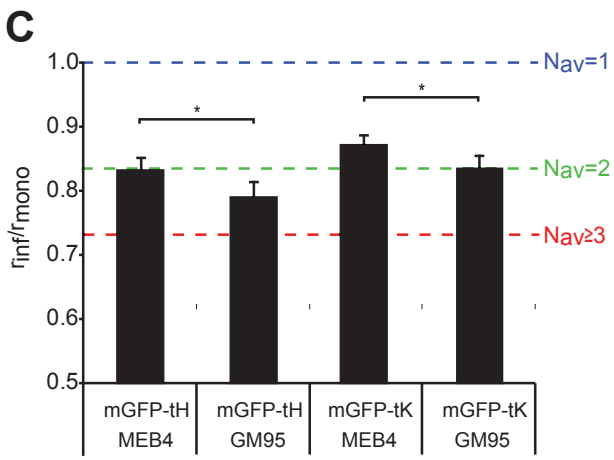
C
1.0
0.9
0.8
0.7
0.6
0.5
rinf/rmono
Nav=1
Nav=2
Nav≥3
*
*
mGFP-tH MEB4
mGFP-tH GM95
mGFP-tK MEB4
mGFP-tK GM95

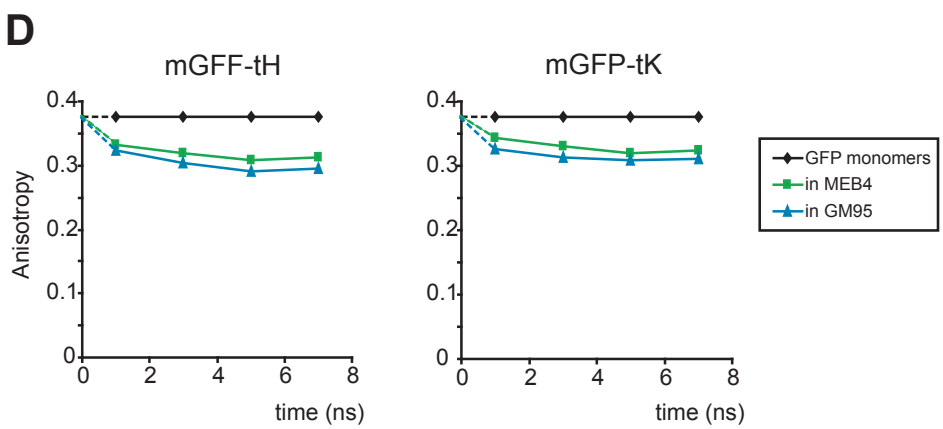
D
mGFF-tH
mGFP-tK
Anisotropy
0.4
0.3
0.2
0.1
0
0
2
4
6
8
time (ns)
GFP monomers
in MEB4
in GM95

al., 2007b). A number of conditions have to be fulfilled in homo-FRET based clustering studies. First, the fluorophores should not lower their anisotropy by rotation. For bulky fluorophores like fluorescent proteins, the time resolved anisotropy decay shows that the anisotropy remains high. In case of homo-FRET, however, it rapidly decays and stays constant afterwards. A decay that occurs within a nanosecond means that the efficiency of the transfer is high and consequently that the distance between the fluorophores is short (less than 5 nm).Such a short distance is the result of intermolecular forces between the GFP barrels. When the GFP is fused with a flexible linker, these interactions result in preferential relative orientations. Provided that this is the case, the experimentally calibrated anisotropy values for N_{av}=1, N_{av}=2 and N_{av}≥3. Preferably, the limiting anisotropy in the time-resolved anisotropy decay (r_{inf}) is used since it is not impeded by fluctuations in the energy transfer efficiency, unlike steady-state anisotropy. Moreover, fluctuations in r_{mono} are compensated for by presenting the degree of depolarization (r_{inf}/r_{mono}). The reference values of r_{inf}/r_{mono} are plotted as dashed lines in Figure 4C (1, 0.82 and 0.72 for N_{av}=1, 2 ≥3, respectively).

For measuring the effect of glycosphingolipids on the oligomerization of lipid-anchored proteins by CTR-FAIM, constructs encoding mGFP-tH and mGFP-tK (Supplementary Table 1) were transiently expressed in MEB4 and GM95 (Figures 4A,B; intensity pictures) cells. Cells expressing these constructs display GFP fluorescence on various locations throughout the cell, but the plasma membrane is the most prominent site. The r_{mono} is 0.38, as determined using a strictly monomeric reference sample (10 μM GFP in glycerol/buffer (50/50)). Compared to this value, a reduction in anisotropy is observed in the image. Furthermore, clear heterogeneities in anisotropy values can be distinguished (Figures 4A,B; anisotropy images). The intensity values of all significant pixels of at least 4 cells were summed

► **Figure 5. Intensity dependence of depolarization in melanosomal cells.** Possible results of depolarization experiments with fluorescently labeled reporter molecules in a microscope pixel (adapted from Varma and Mayor, 1998). (A) The average distance between individual molecules decreases by a factor of two upon a fourfold increase in fluorescence density. The depolarization (or anisotropy) value in two pixels with different fluorescence intensities changes if the fluorophores are within energy-transfer distance of each other. (B) If the fluorophores are arranged in subpixel-sized domains with fixed protein/domain ratios, the local fluorophore density would be proportional to the number of domains in a given pixel. Therefore, the distance between fluorophores would be independent of the fluorophore density. For microdomains at nm scale that means that the anisotropy values of two pixels differing in fluorescence intensities will be independent of fluorophore intensity. (C) Possible outcomes of anisotropy experiments described in (A) and (B). MEB4 and GM95 cells have been transfected with mGFP-tH (D) and mGFP-tK (E), respectively. CTR-FAIM data values of a representative cell were sorted on intensity. The intensities and anisotropy values were averaged per 50 pixels. A scatter plot of the obtained averaged data was plotted. The error bars give the standard error of the mean (SEM), n = 8, r_{mono} = 0.38.

for each of the two emission channels and the overall anisotropy per cell was calculated. mGFP-tH and mGFP-tK expressed in MEB4 cells show depolarization compared to the monomer anisotropy: r_{inf}/r_{mono} values of 0.83 and 0.87, respectively are determined (Figure 4C). Also in cells lacking GSLs depolarization was observed, for mGFP-tH a relative anisotropy value of 0.78 was found. For mGFP-tK expressed in GM95 cells nanoscale organization was also observed, with a r_{inf}/r_{mono} value of 0.83.

The time-resolved anisotropy decay shows a typical homo-FRET profile (Figure 4D), confirming that the reduction in anisotropy is due to nanoscale organi-

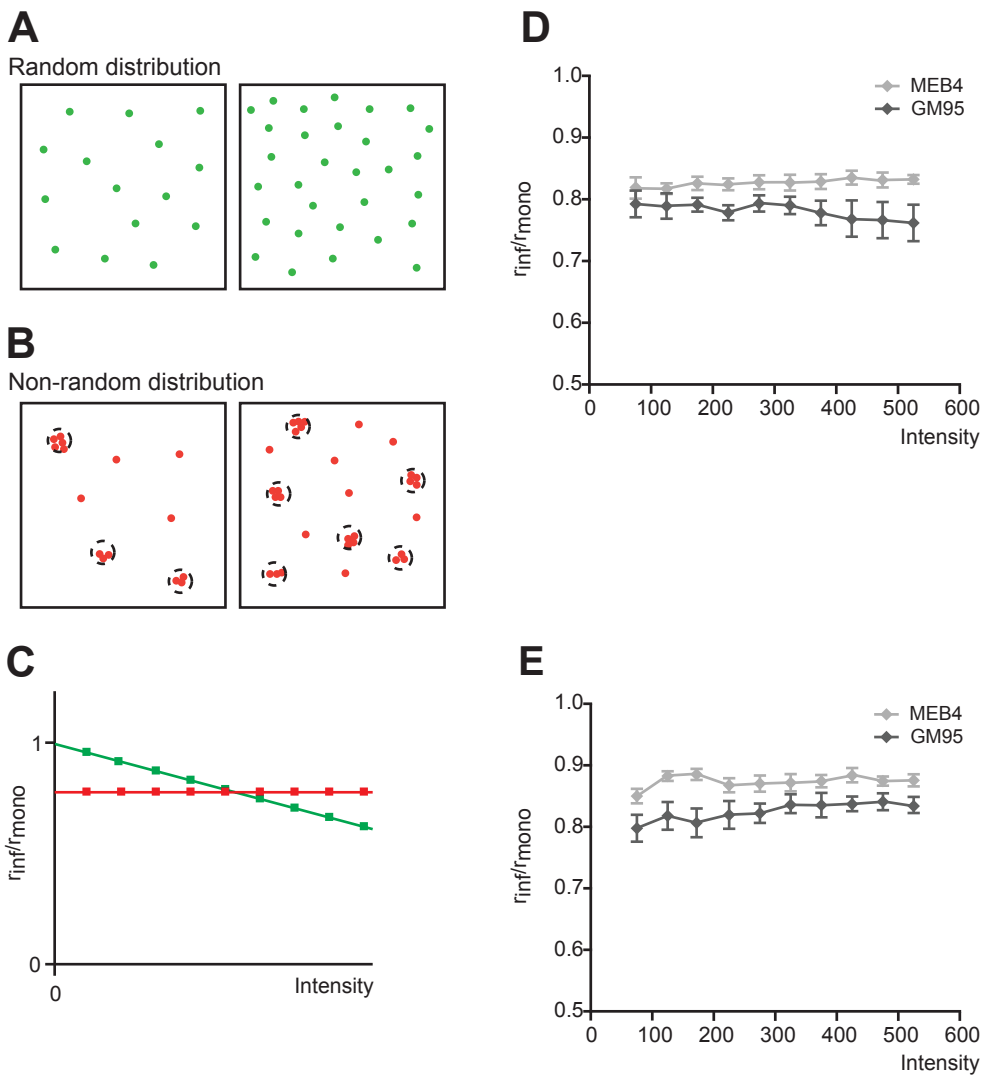

zation of ras. Moreover, a cluster size analysis can be performed. In all samples, the conclusion can be drawn that clusters have an average size of 2. Probably they consist of a mixture of monomers, dimers and larger scale clusters. However, clearly a significant difference between cells having or lacking GSLs can be found. For mGFP-tH as well as mGFP-tK more clustering is observed in GM95 cells. Anisotropy values decrease in GM95 cells to 0.78 (from 0.83 in MEB4 cells) for mGFP-tH, and to 0.83 (from 0.87 in MEB4 cells) for mGFP-tK ($p < 0.05$).

To exclude the possibility of concentration-induced homo-FRET, scatter plots of intensity versus anisotropy were made. In Figure 5C possible outcomes of depolarization experiments with fluorescently labeled reporter molecules are shown based on two models (Figure 5A,B), as discussed by Varma and Mayor (1998) and Hancock (2006). In case of concentration induced homo-FRET a correlation between intensity and anisotropy is expected. Data values of representative cells were sorted on intensity. For defined intensity ranges (i.e. 50-100 counts, 100-150 counts etc.) the anisotropy values (r_{inf}/r_{mono}) were averaged. Figure 5D shows MEB4 (light gray line) and GM95 (dark gray line) expressing mGFP-tH. Nanoscale organization can be observed, displayed by relative anisotropy values of around 0.8. No significant correlation between intensity and anisotropy values was found. That indicates that the intensity is only a measure for the number of clusters, not of the number of GFPs per cluster. Also for cells expressing mGFP-tK no concentration-induced homo-FRET was observed (Figure 5E).

Discussion

In the present paper we have determined the size and density of H-ras in domains by electron microscopy. In wild type MEB4 melanoma cells H-ras, as measured by GFP on the H-ras lipid anchor, was found in clusters of roughly 40 nm diameter (Table 2; uncorrected). GFP-tH reflected the distribution of the GDP form of the full length Ras (Prior et al. 2001). Upon nucleotide exchange GDP-H-ras redistributes to cholesterol independent domains, by a clustering process dependent on the scaffold protein Galectin-1 (Belanis et al. 2008). When corrected for antibody dimensions and a capture ratio of 42% (Plowman et al., 2005) the GFP-tH clusters had a diameter of roughly 18 nm and contained 3 GFP-tH molecules (Table 3). This is comparable with the dimension of GFP-tH clusters measured for BHK cells of 44 nm diameter uncorrected (Prior et al., 2003) and a corrected number of 6 GFP-tH molecules per cluster (Plowman et al., 2005).

Interestingly, also for K-ras nanoscale clusters are observed. In the case of K-ras the behavoir of GFP-tK reflects the behavior of the native full length K-ras protein (Prior et al. 2001). GFP-tK clusters had a corrected diameter of 24 nm and a corrected number of 6 per cluster. This yields a density not much different from

that of GFP-tH, which is unexpected as the basis of clustering for these molecules is thought to be very different, and a 2-fold higher density for GFP-tK was found in BHK cells (Plowman et al., 2005). It is presently not clear what causes this difference in K-ras density cluster size between BHK and MEB4 cells.

We investigated the effect of glycolipids on the protein clustering in lipid domains. It is shown that the absence of glycolipids had remarkably little effect on the observed cluster sizes of the various molecules, but that there was a remarkable two-fold reduction in the density of GFP-tH in the clusters. This may imply that the presence of glycolipids does change the lipid composition of the nanodomains that harbor the tH and thereby shift the steady-state equilibrium between the lipid-anchored proteins and the lipids. A similar but less pronounced shift was observed for GFP-EGFR, which has also been shown to be present in sphingolipid-cholesterol dependent domain. Hardly any effect was observed for GFP-tK, which seems to confirm the notion that cluster formation of GFP-tK has a different molecular basis from the other two. When interpreting these data in signaling terms it has to be kept in mind that the clustering of full-length H-ras is different for the GTP- and GDP-loaded form, which shows that the main relevance of the present study is to unravel the principles underlying the biological process, but not to describe the signaling processes themselves.

One important function of the plasma membrane is the processing of incoming signals. This involves the transduction of signals received on the outside of the cell into the cell interior and the conversion of molecular interactions on the cell surface to molecular interactions on the cytosolic side of the membrane. However, there is more than that. The cell also integrates information received from various sources. One mechanism includes changes in the lipid organization in the plasma membrane. Like proteins, the many different lipids in the plasma membrane are not homogeneously distributed in the plane of the membrane: lateral domains of different lipid composition are found in plasma membranes due to preferential lipid-lipid interactions and probably stabilized by distinct membrane proteins. This has been most convincingly demonstrated for proteins anchored to the outer leaflet of the plasma membrane bilayer by a GPI-tail (Varma and Mayor, 1998; Sharma et al., 2004). These domains, which are generally thought to be small and transient and to be enriched in sphingolipids and cholesterol (van Meer et al., 2008), will be enriched in proteins that preferentially partition into such microdomains. There is evidence that various types of microdomains can coexist, each having a unique lipid composition and being enriched in a specific (set of) GPI-proteins (Madore et al., 1999; Brügger et al., 2004). Changes in the lipid organization have been invoked as a crucial step in some signal transduction processes, such as domain coalescence in B-cell and T-cell activation (Sohn et al., 2008; Zech et al., 2009) and in EGF signaling (Hofman et al., 2008), and changes in domain organization due to the hydrolysis of sphingomyelin to ceramide (Zhang et al., 2009).

Many signal transduction events involve kinases on the cytosolic surface of the plasma membrane, and after the original observation by Sargiacomo et al. (1993), suggesting the presence of Src in lipid rafts, many studies have connected the activation of a number of these signaling kinases, such as Src, Lyn, and Akt to lipid rafts. This is also the case for one isoform of the small GTPase Ras, H-ras. H-ras partitioned into detergent-resistant membranes in its GDP-bound form, but it was chased out of the detergent-resistant membranes by GTP-loading. The truncated minimal membrane-targeting motif of H-ras behaved like the GDP-form (Prior et al., 2001). K-ras with its polybasic domain instead of the H-ras double palmitoylation did not partition into detergent-resistant membranes, and did not colocalize with H-ras in electron microscopic studies (Prior et al., 2003). Interestingly, K-ras still distributed non-randomly in the membrane in clusters that probably depended on (negatively charged) lipids (Prior et al., 2003). Our observation that also the monomeric form of GFP on the K-ras membrane anchor (mGFP-tK), which should not display protein-protein binding, displayed nanoscale clustering supports the notion of lipid-dependent K-ras clustering. Similar observations were reported previously for mYFP and mCFP on a sole geranylgeranyl anchor in MDCK cells (Zacharias et al., 2002). Remarkably, in our case the geranylgeranylated K-ras anchor did not result in clustering (Prior et al., 2003; Figure 1). All in all, apparently, the cytosolic leaflet of the plasma membrane contains a number of different lipidic microdomains, that are differentially recognized or even organized by the various GTPases and kinases, which has important implications for signal processing via these mediators (Henis et al., 2009).

In the present study we have combined two techniques that have recently been successfully used in visualizing lipid domains: EM and homo-FRET. It should be realized that both techniques are complementary. EM is used to determine the size of the raft and density of proteins in it. Homo-FRET, on the other hand, shows whether the proteins in the raft are interacting with each other on a molecular level. Our observation that fewer GFP-tH molecules were found per cluster in GM95 cells by electron microscopy (Figure 3; Table 3), whereas the level of clustering as measured by a loss of fluorescence anisotropy was higher (Figure 4) can possibly be explained by the different characteristics of clustering measured by each method (Figure 6). Whereas immuno-electron microscopy measures whether molecules are close together on a length scale of >10 nm, it provides no information on whether or not molecules are within 10 nm of each other. The opposite is true for the loss of fluorescence anisotropy. This method provides information on whether or not molecules are within some 5 nm of one another but if they are not, the method cannot say anything about their proximity on scales >5 nm. In the absence of glycolipids, in GM95 cells, fewer GFP-tH molecules appear to be present per 20-40 nm diameter cluster, but within each cluster the mGFP-tH molecules are apparently closer together than in the presence of GSLs.

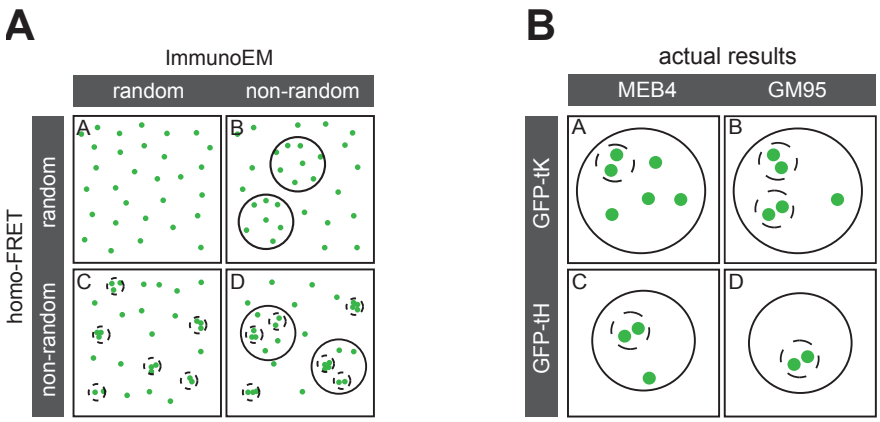

Figure 6. Combination of immuno-electron microscopy and homo-FRET for the investigation of nanodomain organization. Immuno electron microscopy and homo-FRET show different limitations in their ability to discriminate between random and non-random organization of proteins at the plasma membrane. Immuno-electron microscopy is able to discriminate nanoclusters ≤ 200 nm. However, because of the labeling of the antigen with gold particles conjugated to a bivalent antibody, very small nanoclusters on molecular level, e.g. dimers, can not be recognized. Immuno-electron microscopy is therefore able to discriminate between condition A and B, however it is not able to discriminate B from D. Subclusters on molecular level (smaller than 5 nm) are not detectable (C). In contrast, homo-FRET is able to detect nanoclustering on a scale ≤ 10 nm. Therefore, homo-FRET discriminates condition A from C. In contrast to immuno electron microscopy, homo-FRET is neither able to discriminate A from B, nor C from D. To get a more accurate picture of the nano-scale organization of proteins at the plasma membrane, a combination of both techniques is required. (B) Schematic representation of actual results, observed in this study. Glycosphingolipids do not significantly affect the diameter of nanoclusters in melanosomal cells for GFP-tH and GFP-tK, respectively. However, in cells containing GSLs the number of proteins, which reside in nanoclusters was increased. Molecular nanoclustering did not depend on the density of proteins per nanocluster, on the contrary, in MEB4 cells lower levels of clustering at the molecular level were observed.

The bulk of the sphingolipids in most cellular plasma membranes is made up of the phosphosphingolipid sphingomyelin. GSLs sphingomyelin as the bulk sphingolipid only in rare cases like the apical surface of epithelial cells and the plasma membrane of myelinating cells and, maybe, neurons. The lipid raft hypothesis was originally based on glycosphingolipid clustering in epithelial cells (van Meer and Simons, 1988), and prominent roles for GSLs have also been proposed in so-called glycosynapses, complexes on the cell surface involved in cell-cell and cell-matrix recognition events (Todeschini et al., 2008). Apart from that, the complex glycosphingolipid GM3 has been reported to inhibit EGF-induced signal transduction, whereas GM1 had a stimulatory effect (see Hofman et al., 2008). Inhibition of the synthesis of GM3 and GM1 reduced EGF activation by 50% (Liu et al., 2008). Interestingly, GM3 and GM1 have been found to reside in different types of lipid rafts (Gómez-Moutón et al., 2001; Fujita et al., 2007; Janich and

Corbeil, 2007). Because complex glycosphingolipids are thought to reside only on the exoplasmic suface of membranes, their absence might affect the organization of the EGFR, but less likely that of lipid-anchored proteins on the cytosolic surface. In contrast the first glycolipid, glucosylceramide, is synthesized on the cytosolic surface of the Golgi and has access to the cytosolic side of the plasma membrane (Warnock et al., 1994). How this glycolipid affects the lipid organization in the cytosolic leaflet is unclear. The present data would suggest that glucosylceramide containing domains would require fewer H-ras molecules for stability and would render the lipid distribution within lipid rafts more homogeneous. Physio-chemical studies will have to elucidate the organizational principles underlying the structure of lipid rafts on the cytosolic surface.

Also the number of GFP-EGFR per cluster was reduced in GM95 cells. Because MEB4 cells contain significant amounts of the glycolipids glucosylceramide and GM3 only, these are the candidate molecules that are responsible for this effect. As in the case of the cytosolic rafts, it is presently not obvious, what the effect of the individual GSLs on raft structure is. The presence of lipid-based signaling microdomains on both the exoplasmic and cytosolic surface of the plasma membrane has brought up the question whether domains in one leaflet are related to domains on the opposite side. When GPI-proteins in the exoplasmic leaflet were induced to patch by cross-linking, co-patching was observed for the Src-like protein tyrosine kinase fyn on the cytosolic surface (Harder et al., 1998), and indeed, clustering of raft-associated proteins in the external membrane leaflet was found to modulate internal leaflet H-ras diffusion and signaling (Eisenberg et al., 2006). First *in vitro* experiments in asymmetric lipid bilayers have shown that ordered lipid domains can be induced in lipid compositions that are typical for the inner leaflet by lipid compositions that are typical for the outer leaflet of mammalian plasma membranes (Kiessling et al., 2009). However, it seems unlikely that the multitude of small transient nanodomains thought to exist in the exoplasmic leaflet under non-signaling conditions (Hancock, 2006) would all be connected to similar structures in the cytosolic leaflet.

Materials and Methods

Materials

Chemicals, if not indicated otherwise, were from Sigma-Aldrich (St. Louis, MI) and used in the highest purity available. Cell culture media, reagents and fetal calf serum (FCS) were from PAA Laboratories GmbH (Pasching, Austria). Cell culture plastics were from Greiner Bio-One (Frickenhausen, Germany) and Lipofectamine 2000 was from Invitrogen (Carlsbad, CA).

DNA constructs

GFP-tH, GFP-tK, and GFP-tKCCIL have been described in Prior et al. (2003). EGFR-GFP, EGFR-mGFP and monomeric GFP in pEGFP-N3 (Clontech, Mountain View, CA) were provided by Paul van Bergen en Henegouwen and Erik Hofman (Utrecht University, Utrecht, The Netherlands). The mutation A206K is in accordance with Zacharias et al. (2002). mGFP was amplified from pEGFR-N3 by PCR. High fidelity DNA polymerase Phusion (Finnzymes, Espoo, Finland) was used for all PCR reactions. For the construction of mGFP-tH, a PCR reaction was performed using the forward primer and the mGFP-tH reverse primer (see Supplementary Table 1), and using mGFP in pEGFP-N3 as template. mGFP-tK was constructed by two separate PCR reactions. First, a PCR reaction using the forward primer and the reverse primer 1, and mGFP in pEGFP-N3 as a template (see Supplementary Table 1) was performed. On the amplified PCR products a second PCR reaction was performed using the forward primer and the mGFP-tK reverse primer 2. The final PCR products of mGFP-tH and mGFP-tK were inserted into pcDNA3.1/hygro(+) from Invitrogen, via HindIII and XhoI restriction sites. All constructs were verified by DNA sequencing.

Supplementary Table 1. Primers used in this study

	Primer (restriction sites are indicated in bold)
mGFP forward	5'-AC**AAGCTT**ATGGTGACGAAGGGCGAG-3'
mGFP-tK reverse1	5'-CTTCTTTTTCTTCTTTTTCTTGTACGATGCCCTACTGCCG-3'
mGFP-tK reverse2	5'-GCT**CTCGAG**TTACATAATTACACACTTTGTCTTTGACTTCTTTCTTTTCTTTTT-3'
mGFP-tH reverse	5'-GCT**CTCGAG**TTAGGAGAGCACACACTTGCAGCTCTTGTACAGCTCGTCCATGCCG-3'

Cell culture and sample preparation

GM95 and MEB4 cells from RIKEN Cell Bank (Saitama, Japan) were cultured in Dulbecco's modified Eagle's medium supplied with stable glutamine, 4.5 g/l glucose, 10% FCS, or in Optimem I (PAA) supplemented with 5% delipidated FCS from Hyclone (Perbio Science Nederland, The Netherlands) at 37°C at 5% CO_2. A stable retransfectant GM95 cell line (GM95res) expressing a ceramide glucosyltransferase was generated as before (Sprong et al., 2001). Cells were transfected using 1 µl Lipofectamine 2000 and ~0.3 µg DNA per cm^2 cells. Expression of proteins was induced by adding 5 mM butyrate 16 h prior to experiments. For imaging, cells were seeded on 18 mm coverslips, grown for 24 h after transfection till 40% confluency. Cells were washed with PBS, fixed with freshly prepared 4% paraformaldehyde at room temperature for 20 min, and quenched with 50 mM glycine for 10 min. Coverslips were mounted with Mowiol and stored at -20°C until further use.

Preparation of antibody-conjugated colloidal gold

4.5 nm gold-conjugated antibodies were prepared by the tannic acid/citrate method (Slot and Geuze, 1985). Affinity-purified polyclonal anti-GFP antibodies have been described previously (Prior et al., 2001). Briefly, 10 ml of reducing solution (2 ml 1% trisodium citrate, 0.75 ml 1% tannic acid, 0.75 ml 25 mM potassium carbonate, 6.5 ml deionized water) and 40 ml of 1% gold chloride were heated to 60°C, mixed together, stirred and boiled for 5 min to obtain deep red gold colloids. The gold solution was cooled on ice and the pH was adjusted to about 8.5 with 0.5 M NaOH. After that, the optimal antibody-gold concentration was titrated. For this, 0 to 5 μg of antibody (in total volumes of 20 μl) were added to 250 μl of the gold colloid. After 5 min of incubation at room temperature, 100 μl of 10% NaCl were added. The lowest concentration of antibody that prevented the color change to blue was taken to be the lowest concentration that stabilized the gold (typically 7 to 10 μg/ml gold) and was used for the experiments. The gold was incubated with the optimal antibody concentration for 10 min and 10% BSA was added to a final concentration of 0.1%. To remove unbound antibody and to concentrate the gold, the 4.5-nm gold was centrifuged at 100,000 g_{av} for 1 h at 4°C. The loose part of the pellet was harvested as soon as the centrifugation step was stopped to avoid resuspension of the more compact pellet, which contains gold aggregates. Gold-conjugated antibody was stored at 4°C.

Electron microscopy and image analysis

Transfected cells on 18 mm glass coverslips (70-80% confluent, grown in DMEM with 10% FCS) were washed with 0.1 M phosphate buffer, pH 7.4, and the coverslips were firmly pressed face-down onto poly-L-lysine-coated carbon-coated copper grids. The grids were floated off the coverslips using potassium acetate buffer (25 mM HEPES, pH 7.4, 115 mM potassium acetate, 2.5 mM $MgCl_2$) and fixed with 4% paraformaldehyde, 0.1% glutaraldehyde in potassium acetate buffer, pH 7.4, for 20 min at room temperature. Ripped-off plasma membranes were labeled with affinity-purified anti-GFP antisera coupled directly to 5 nm gold as described in detail in Prior et al. (2003), stained with 0.6% aqueous uranyl acetate, 1.8% methyl cellulose and viewed (Tecnai 10, FEI Company, Eindhoven, The Netherlands). Digital images of immunogold-labeled plasma membrane sheets were taken at 39,000x magnification. The (x,y) coordinates of gold particles over intact 1 μm^2 areas of the plasma membrane sheet were identified by using ImageJ (version 1.38x, http://rsb.info.nih.gov/ij) and analyzed by using Ripley's K-function. K-function curves were calculated for the immunogold point patterns as described (Prior et al., 2003; Hancock and Parton, 2005; Plowman et al., 2005). Gold densities were comparable between experiments, typically between 300-600 gold/μm^2 in labeled areas. The K-function curves were standardized on a 99% confidence interval, and statistics including bootstrap tests for evaluating differences between

the weighted mean K-function curves were performed all as described by Prior at al. (2003). The mean number of labeled molecules that are clustered in a nanodomain can also be estimated by K-function analysis (Parton and Hancock 2004, see also theoretical background in the Appendix). For this, the antibody-gold labeling efficiency ε towards individual molecules was estimated to be 0.42 (see Plowman et al., 2005).

Statistics (Poisson distribution)
The Poisson distribution was used to predict the numbers of molecules in a specific nanocluster. Equation 1 shows the formula used, where the mean λ is the mean number of proteins (see Table 3) in a nanocluster and x is the number of proteins expected.

$$Poisson = (e^{-\lambda}\lambda^{x}) / x! \qquad \text{(Eq. 1)}$$

Confocal time-resolved fluorescence anisotropy imaging microscopy (CTR-FAIM)
The average number of proteins per cluster (N_{av}) can be determined using fluorescence anisotropy based techniques. Here, we utilize a time resolved fluorescence anisotropy imaging approach which has the advantage of providing a measure (r_{inf}) for cluster size that is independent on the efficiency of the transfer (Bader et al., 2007a). A 473 nm pulsed diode laser (Becker and Hickl BDL-473, Berlin, Germany) operating at 50 MHz was directly coupled to the modified confocal scan head (C1, Nikon Instruments, Badhoevedorp, The Netherlands). No optical fibres were used to avoid complication of polarization dependent measurements due to broadening of the laser pulse. A linear polarizer (Meadowlark, Frederick, CO) was positioned in the laser beam to define the excitation polarization direction. The microscope was equipped with a 60x, NA = 1.20 water immersion objective (Plan Apo, Nikon), but, because the excitation beam did not fill the whole back aperture of the objective, the effective excitation NA amounted to approximately 0.5, causing a small loss of microscopic resolution. The emission light was split into a parallel and a perpendicular channel with a broadband polarizing beam splitter cube (OptoSigma, Santa Ana, CA). Each emission channel was fiber-coupled to a detection system consisting of a fluorescence lifetime imaging module (LIMO, Nikon), as described by De Grauw and Gerritsen (2001), equipped with an internal photon counting photomultiplier tube. The LIMOs collect photons in four 2 ns wide consecutive time gates. By employing two synchronized LIMOs, one for each polarization direction, a four channel time-resolved anisotropy decay is acquired for each pixel in the image. An acquisition time of 3 ms per pixel was applied. All images were recorded over 80x80 pixels, covering an area of 50x50 μm^2. Data analysis, synchronization and correction for sensitivity differences between the two channels were based on using reference dyes, as described in detail before (Bader et al., 2007a;b).

Data handling

Cluster size images were obtained by extracting r_{inf}-values from the time-gated fluorescence anisotropy images. These values of r_{inf} were calculated using I_{par} and I_{per} summed over the last three gates. The relative decreases in anisotropy (r_{inf}/r_{mono}) for $N_{av} = 1$, $N_{av} = 2$ and $N_{av} \geq 3$ have been experimentally determined in previous work . Four-gate anisotropy decays were created by binning the intensities I_{par} and I_{per} per gate for all significant pixels. In the anisotropy imaging experiments a threshold of $I_{par, inf} + 2I_{per, inf} > 300$ counts was applied to all images. In theory, this number of counts corresponds to a standard deviation in the anisotropy of 0.05 (Lidke et al., 2005).

Acknowledgements

We thank Erik Hofman and Paul van Bergen en Henegouwen for providing DNA constructs. This work is financially supported by the NWO/ALW MtC program.

References

Apolloni, A., Prior, I.A., Lindsay, M., Parton, R.G., and Hancock, J.F. 2000. H-ras but not K-ras traffics to the plasma membrane through the exocytic pathway. *Mol Cell Biol* 20:2475-2487.

Bader, A.N., Hofman, E.G., van Bergen en Henegouwen, P.M., and Gerritsen, H.C. 2007a. Confocal time-resolved fluorescence anisotropy imaging. *Imaging, Manipulation, and Analysis of Biomolecules, Cell, and Tissues* V 6441.

Bader, A.N., Hofman, E.G., van Bergen en Henegouwen, P.M.P., and Gerritsen, H.C. 2007b. Imaging of protein cluster sizes by means of confocal time-gated fluorescence anisotropy microscopy. *Opt. Express* 15:6934-6945.

Bader, A. N., E. G. Hofman, J. Voortman, P. M. P. van Bergen en Henegouwen, and H. C. Gerritsen. 2009. Homo-FRET imaging enables quantification of protein cluster sizes with sub-cellular resolution. *Biophys. J*., submitted.

Belanis, L., Plowman, S.J., Rotblat, B., Hancock, J.F., and Kloog, Y. 2008. Galectin-1 Is a Novel Structural Component and a Major Regulator of H-Ras Nanoclusters. *Mol. Biol. Cell* 19:1404-1414.

Besag, J.E. 1977. Contribution to the discussion of Dr. Ripley's paper. *J. R. Statist. Soc.* B39:193-195.

Brügger, B., Graham, C., Leibrecht, I., Mombelli, E., Jen, A., Wieland, F., and Morris, R. 2004. The membrane domains occupied by glycosylphosphatidylinositol-anchored prion protein and Thy-1 differ in lipid composition. *J Biol Chem* 279:7530-7536.

de Grauw, C.J., and Gerritsen, H.C. 2001. Multiple time-gate module for fluorescence lifetime imaging. *Appl. Spectrosc.* 55:655-805.

Eggeling, C., Ringemann, C., Medda, R., Schwarzmann, G., Sandhoff, K., Polyakova, S., Belov, V.N., Hein, B., von Middendorff, C., Schonle, A., et al. 2009. Direct observation of the nanoscale dynamics of membrane lipids in a living cell. *Nature* 457:1159-1162.

Eisenberg, S., Shvartsman, D.E., Ehrlich, M., and Henis, Y.I. 2006. Clustering of raft-associated proteins in the external membrane leaflet modulates internal leaflet H-ras diffusion and signaling. *Mol Cell Biol* 26:7190-7200.

Fujita, A., Cheng, J., Hirakawa, M., Furukawa, K., Kusunoki, S., and Fujimoto, T. 2007. Gangliosides GM1 and GM3 in the living cell membrane form clusters susceptible to cholesterol depletion and chilling. *Mol Biol Cell* 18:2112-2122.

Gautier, I., Tramier, M., Durieux, C., Coppey, J., Pansu, R.B., Nicolas, J.C., Kemnitz, K. and Coppey-Moisan, M. 2001. Homo-FRET microscopy in living cells to measure monomer-dimer transition of GFP-tagged proteins. *Biophys J* 80:3000-3008.

Gómez-Moutón, C., Abad, J.L., Mira, E., Lacalle, R.A., Gallardo, E., Jiménez-Baranda, S., Illa, I., Bernad, A., Mañes, S., and Martínez-A., C. 2001. Segregation of leading-edge and uropod components into specific lipid rafts during T cell polarization. *Proc Natl Acad Sci USA* 98:9642-9647.

Halter, D., Neumann, S., van Dijk, S.M., Wolthoorn, J., de Maziere, A.M., Vieira, O.V., Mattjus, P., Klumperman, J., van Meer, G., and Sprong, H. 2007. Pre- and post-Golgi translocation of glucosylceramide in glycosphingolipid synthesis. *J Cell Biol* 179:101-115.

Hancock, J.F. 2006. Lipid rafts: contentious only from simplistic standpoints. *Nat Rev Mol Cell Biol* 7:456-462.

Hancock, J.F., Cadwallader, K., Paterson, H., and Marshall, C.J. 1991. A CAAX or a CAAL motif and a second signal are sufficient for plasma membrane targeting of ras proteins. *EMBO J* 10:4033-4039.

Hancock, J.F., and Parton, R.G. 2005. Ras plasma membrane signalling platforms. Biochem J 389:1-11.

Hanzal-Bayer, M.F., and Hancock, J.F. 2007. Lipid rafts and membrane traffic. *FEBS Lett* 581:2098-2104.

Harder, T., Scheiffele, P., Verkade, P., and Simons, K. 1998. Lipid domain structure of the plasma membrane revealed by patching of membrane components. *J Cell Biol* 141:929-942.

Henis, Y.I., Hancock, J.F., and Prior, I.A. 2009. Ras acylation, compartmentalization and signaling nanoclusters. *Mol Membr Biol* 26:80-92.

Hofman, E.G., Ruonala, M.O., Bader, A.N., van den Heuvel, D., Voortman, J., Roovers, R.C., Verkleij, A.J., Gerritsen, H.C., and van Bergen En Henegouwen, P.M. 2008. EGF induces coalescence of different lipid rafts. *J Cell Sci* 121:2519-2528.

Ichikawa, S., Nakajo, N., Sakiyama, H., and Hirabayashi, Y. 1994. A mouse B16 melanoma mutant deficient in glycolipids. *Proc. Natl. Acad. Sci. USA* 91:2703-2707.

Janich, P., and Corbeil, D. 2007. GM1 and GM3 gangliosides highlight distinct lipid microdomains within the apical domain of epithelial cells. *FEBS Lett* 581:1783-1787.

Jares-Erijman, E.A. and Jovin, T.M. 2003. FRET imaging. Nat Biotechnol 21:1387-1395.

Kiessling, V., Wan, C., and Tamm, L.K. 2009. Domain coupling in asymmetric lipid bilayers. *Biochim Biophys Acta* 1788:64-71.

Lidke, D.S., Nagy, P., Barisas, B.G., Heintzmann, R., Post, J.N., Lidke, K.A., Clayton, A.H., Arndt-Jovin, D.J. and Jovin, T. M. 2003. Imaging molecular interactions in cells by dynamic and static fluorescence anisotropy (rFLIM and emFRET). *Biochem Soc Trans* 31:1020-1027.

Lidke, K.A., Rieger, B., Lidke, D.S., and Jovin, T.M. 2005. The role of photon statistics in fluorescence anisotropy imaging. *IEEE Trans Image Proc*ess 14:1237-1245.

Lisanti, M.P., Caras, I.W., Davitz, M.A., and Rodriguez-Boulan, E. 1989. A glycophospholipid membrane anchor acts as an apical targeting signal in polarized epithelial cells. *J Cell Biol* 109:2145-2156.

Liu, Y., Su, Y., Wiznitzer, M., Epifano, O., and Ladisch, S. 2008. Ganglioside depletion and EGF responses of human GM3 synthase-deficient fibroblasts. *Glycobiology* 18:593-601.

Madore, N., Smith, K.L., Graham, C.H., Jen, A., Brady, K., Hall, S., and Morris, R. 1999. Functionally different GPI proteins are organized in different domains on the neuronal surface. *EMBO J*. 18:6917-6926.

Parton, R.G., and Hancock, J.F. 2001. Caveolin and Ras function. *Methods Enzymol* 333:172-183.

Parton, R.G., and Hancock, J.F. 2004. Lipid rafts and plasma membrane microorganization: insights from Ras. *Trends Cell Biol* 14:141-147.

Plowman, S.J., Muncke, C., Parton, R.G., and Hancock, J.F. 2005. H-ras, K-ras, and inner plasma membrane raft proteins operate in nanoclusters with differential dependence on the actin cytoskeleton. *PNAS*:0504114102.

Prior, I.A., Harding, A., Yan, J., Sluimer, J., Parton, R.G., and Hancock, J.F. 2001. GTP-dependent segregation of H-ras from lipid rafts is required for biological activity. *Nat Cell Biol* 3:368-375.

Prior, I.A., Parton, R.G., and Hancock, J.F. 2003. Observing cell surface signaling domains using electron microscopy. *Sci STKE* 2003:PL9.

Ripley, B.D. 1977. Modelling spatial patterns. *J. R. Statist. Soc.* B 39:172-192.

Runnels, L.W., and Scarlata, S.F. 1995. Theory and application of fluorescence homotransfer to melittin oligomerization. *Biophys J* 69:1569-1583.

Sanan, D.A., and Anderson, R.G. 1991. Simultaneous visualization of LDL receptor distribution and clathrin lattices on membranes torn from the upper surface of cultured cells. *J Histochem Cytochem* 39:1017-1024.

Sargiacomo, M., Sudol, M., Tang, Z.L., and Lisanti, M.P. 1993. Signal transducing molecules and glycosyl-phosphatidylinositol-linked proteins form a caveolin-rich insoluble complex in MDCK cells. *J. Cell Biol.* 122:789-807.

Sharma, P., Varma, R., Sarasij, R.C., Ira, Gousset, K., Krishnamoorthy, G., Rao, M., and Mayor, S. 2004. Nanoscale organization of multiple GPI-anchored proteins in living cell membranes. *Cell* 116:577-589.

Slot, J.W., and Geuze, H.J. 1985. A new method of preparing gold probes for multiple-labeling cytochemistry. *Eur J Cell Biol* 38:87-93.

Sohn, H.W., Tolar, P., and Pierce, S.K. 2008. Membrane heterogeneities in the formation of B cell receptor-Lyn kinase microclusters and the immune synapse. *J Cell Biol* 182:367-379.

Sorre, B., Callan-Jones, A., Manneville, J.B., Nassoy, P., Joanny, J.F., Prost, J., Goud, B., and Bassereau, P. 2009. Curvature-driven lipid sorting needs proximity to a demixing point and is aided by proteins. *Proc Natl Acad Sci USA* 106:5622-5626.

Sprong, H., Degroote, S., Claessens, T., van Drunen, J., Oorschot, V., Westerink, B.H., Hirabayashi, Y., Klumperman, J., van der Sluijs, P., and van Meer, G. 2001. Glycosphingolipids are required for sorting melanosomal proteins in the Golgi complex. *J. Cell Biol.* 155:369-380.

Tian, A., and Baumgart, T. 2009. Sorting of lipids and proteins in membrane curvature gradients. *Biophys J* 96:2676-2688.

Todeschini, A.R., and Hakomori, S.I. 2008. Functional role of glycosphingolipids and gangliosides in control of cell adhesion, motility, and growth, through glycosynaptic microdomains. *Biochim Biophys Acta* 1780:421-433.

van Meer, G., and Simons, K. 1988. Lipid polarity and sorting in epithelial cells. *J Cell Biochem* 36:51-58.

van Meer, G., Voelker, D.R., and Feigenson, G.W. 2008. Membrane lipids: where they are and how they behave. *Nat Rev Mol Cell Biol* 9:112-124.

Varma, R., and Mayor, S. 1998. GPI-anchored proteins are organized in submicron domains at the cell surface. *Nature* 394:798-801.

Warnock, D.E., Lutz, M.S., Blackburn, W.A., Young, W.W., Jr., and Baenziger, J.U. 1994. Transport of newly synthesized glucosylceramide to the plasma membrane by a non-Golgi pathway. *Proc. Natl. Acad. Sci. USA* 91:2708-2712.

Yamashita, T., Wada, R., Sasaki, T., Deng, C., Bierfreund, U., Sandhoff, K., and Proia, R.L. 1999. A vital role for glycosphingolipid synthesis during development and differentiation. *Proc. Natl. Acad. Sci. USA* 96:9142-9147.

Yeow, E.K.L. and Clayton, A.H.A. 2007. Enumeration of Oligomerization States of Membrane Proteins in Living Cells by Homo-FRET Spectroscopy and Microscopy: Theory and Application. *Biophys. J.* 92:3098-3104.

Zacharias, D.A., Violin, J.D., Newton, A.C., and Tsien, R.Y. 2002. Partitioning of lipid-modified monomeric GFPs into membrane microdomains of live cells. *Science* 296:913-916.

Zech, T., Ejsing, C.S., Gaus, K., de Wet, B., Shevchenko, A., Simons, K., and Harder, T. 2009. Accumulation of raft lipids in T-cell plasma membrane domains engaged in TCR signalling. *EMBO J* 28:466-476.

Zhang, Y., Li, X., Becker, K.A., and Gulbins, E. 2009. Ceramide-enriched membrane domains--structure and function. *Biochim Biophys Acta* 1788:178-183.

Appendix

Immuno-EM combined with statistical analysis

Combination of immunogold electron microscopy with a statistical analysis of gold patterns allows the visualization of membrane protein nanoclusters at the plasma membrane. Plasma membrane sheets of cells expressing the protein of interest were prepared accordingly to Prior et al. (2003), fixed and labeled with gold-conjugated anti GFP antibody. Electron microscopy images of labeled plasma membrane sheets are processed to determine the (x, y) coordinates of the gold particles.

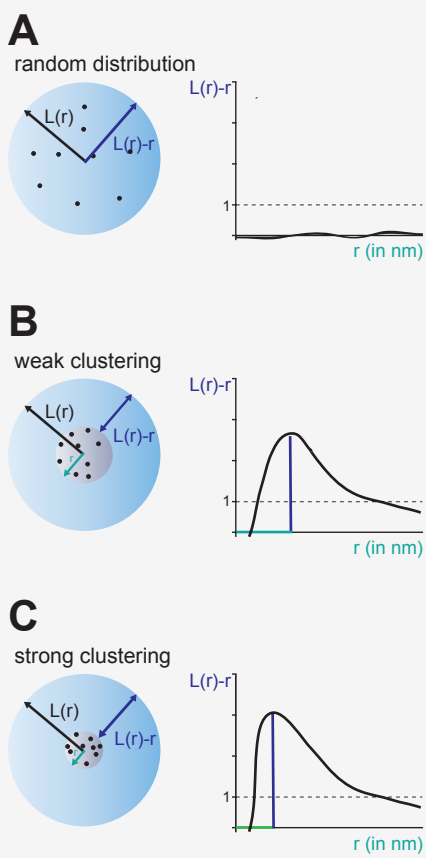

Box 1. Cluster analysis by statistical evaluation of immuno electron microscopy data. Analysis of anti GFP-4.5 nm gold labeled plasma membrane sheets has been described in Parton and Hancock (2004). If a protein pattern is clustered, the spatial distance between labeled proteins is shorter than under random conditions. Therefore, the radius r in which the proteins are found is smaller than L(r), representing random conditions. Here, we show three situations: random distribution, weak clustering and strong clustering. The right panel displays the change in the statistical analysis due to a change in protein distribution. In the graph, the difference between r and L(r) is displayed on the y-axis. The value L(r)-r is a measure for the degree (probability) of clustering at a certain radius r. (A) Under complete spatial randomness (CSR), L(r)-r = 0. This means, that the radius r equals the radius L(r). In (B) weak clustering is indicated, therefore, the radius r of the clustered pattern is clearly reduced compared to the random situation L(r). (C) The pattern, of a strongly clustered sample, shows an even bigger difference between r and L(r), indicating a higher degree of clustering, and a reduced radius r of the clustered domain.

Ripley's K-function is used to determine the extent of clustering
The first order property of a point pattern is its intensity, λ (=N/A), where N equals the number of points in the studied area A. Ripley's K-function K(r) characterizes the second order property, where the expected number of neighbors N(r) within a distance r of any point in A is given by N(r) = λK(r). In random patterns, the expected value of N(r) is $\lambda\pi r^2$, at any distance r (so K(r) = πr^2). If the gold is clustered, the gold particle will have more neighbors than expected for complete spatial randomness (CSR) thus K(r) > πr^2.

$$L(r) - r = \sqrt{K(r)/\pi} - r \qquad \text{(Eq. A1)}$$

L(r)-r is a linear transformation of K(r), see Besag (1977). Under the null hypothesis of complete spatial randomness, L(r)-r has an expected value of 0 for all values of r. N(r) was estimated as the mean value calculated over A, taking into account border effects (Ripley, 1977). For the cluster analysis experiments this means that the value of r at which the deviation of L(r) - r is maximal indicates the radius of clusters (see Box 1). K-functions were standardized on a 99% confidence interval (Prior et al., 2003).

The estimation of the mean number of labeled molecules that are clustered in a nanodomain (M_c) can also be determined by K-function analysis (Parton and Hancock, 2004).

$$M_c = (1 + (L_{\max} + r)^2 \pi\lambda)/\varepsilon \qquad \text{(Eq. A2)}$$

$$L_{\max} = \sup_r \left| L(r) - r \right| \qquad \text{(Eq. A2a)}$$

Where ε is the antibody-gold labeling efficiency towards individual molecules and equation A2a is valid for a pattern with a density of λ. L_{max} is defined as the supremum of L(r)-r, also referred to as the least upper bound of L(r)-r.

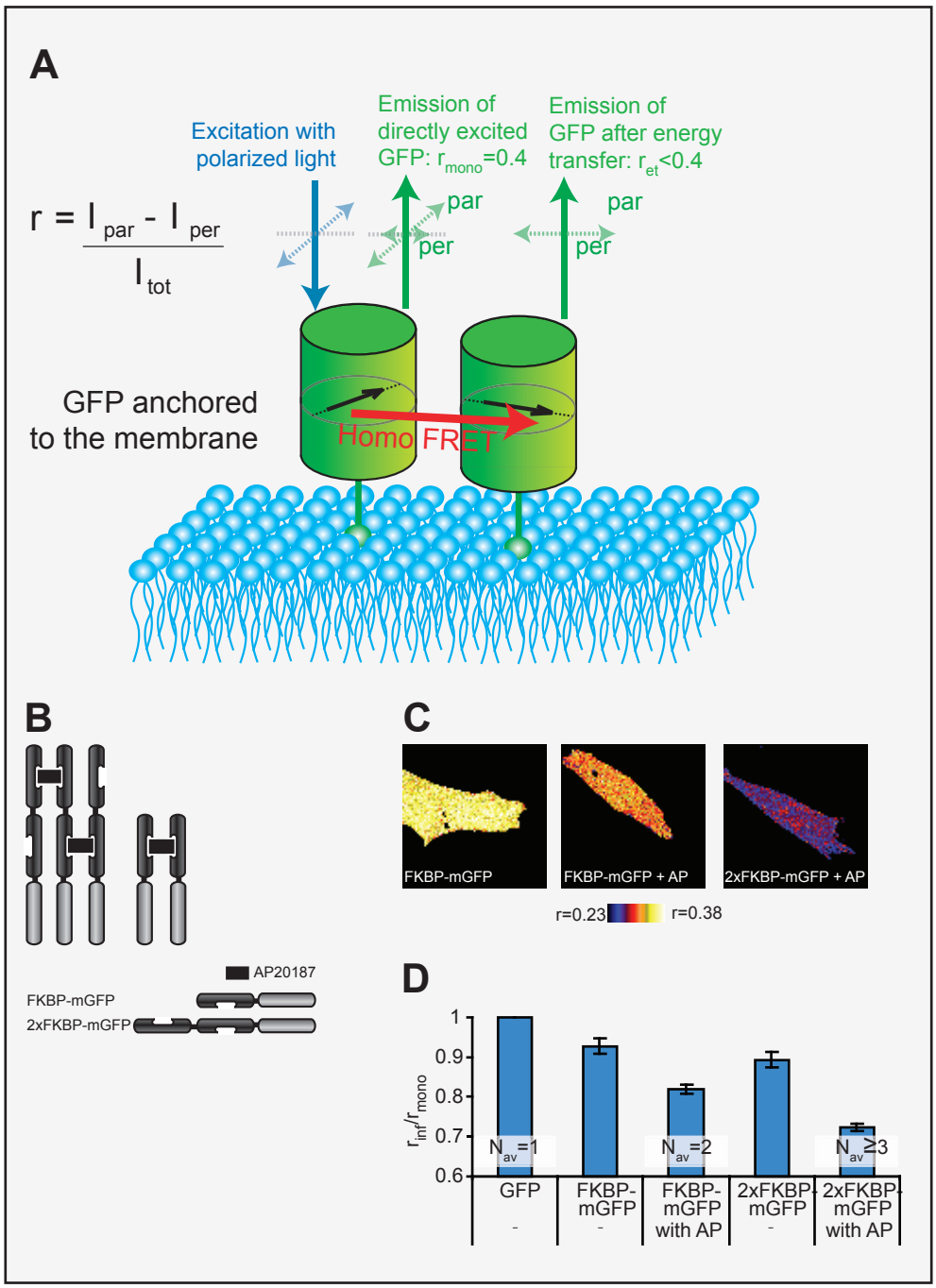
A
Excitation with polarized light
Emission of directly excited GFP: r_{mono}=0.4
Emission of GFP after energy transfer: r_{et}<0.4
$r = \frac{I_{par} - I_{per}}{I_{tot}}$
par
per
par
per
GFP anchored to the membrane
Homo FRET
B
AP20187
FKBP-mGFP
2xFKBP-mGFP
C
FKBP-mGFP
FKBP-mGFP + AP
2xFKBP-mGFP + AP
r=0.23
r=0.38
D
r_{int}/r_{mono}
1
0.9
0.8
0.7
0.6
N_{av}=1
N_{av}=2
$N_{av}\geq3$
GFP
FKBP-mGFP
FKBP-mGFP with AP
2xFKBP-mGFP
2xFKBP-mGFP with AP

Homo-FRET based protein cluster size determination

The relation between homo-FRET and fluorescence anisotropy has been extensively described in literature (Bader et al., 2007b; Gautier et al., 2001; Jares-Erijman and Jovin, 2003; Lidke et al., 2003; Runnels and Scarlata, 1995; Yeow and Clayton, 2007). Briefly, the fluorescence anisotropy r is defined as the intensity corrected difference between the emission parallel (I_{par}) and perpendicular (I_{per}) to the excitation polarization direction:

$$r(t) = \frac{I_{par} - I_{per}}{I_{par} + 2I_{per}} \qquad \text{(Eq. A3)}$$

In homo-FRET studies fluorophores are used that exhibit minimal rotation during the fluorescence lifetime. After photo selection with polarized light, the donor fluorophores (D) exhibit a high anisotropy ($r_{mono} \approx 0.4$, r_{mono} is defined as the anisotropy of monomeric fluorophores in absence of rotation). In contrast, after homo-FRET the fluorophores that act as acceptor (A) have a more random orientation and therefore lower anisotropy (r_{et}, defined as the anisotropy of fluorophores that are indirectly excited after homo-FRET). The measured anisotropy of clusters of fluorophores therefore contains contributions of both donor and acceptor fluorophores. Runnels and Scarlata related the steady state anisotropy (r_{ss}) to the cluster size *N* (i.e., the average number of fluorophores per cluster), the relative orientation of the fluorophores (determines value of r_{et}) and homo-FRET efficiency *E*. The latter is included as the product of the homo-FRET rate ω and fluorescence lifetime τ ($\omega\tau = E/(E\text{-}1)$).

◄ **Box 2. Imaging of protein cluster sizes by means of confocal time-resolved fluorescence anisotropy imaging microscopy (CTR-FAIM).** (A) Schematic diagram of energy transfer in a dimer (modified from Bader et al., 2007b). An important feature of homo-FRET is that it can provide information about the number of fluorophores (N) per cluster (Runnels and Scarlata, 1995). For a monomer, in the absence of rotation the average anisotropy amounts to r_{mono} = 0.4. For a dimer, however, the initial anisotropy of the excited donor equals r = 0.4 whereas the fluorophore that acts as an acceptor has a more random orientation and therefore lower anisotropy (r_{et}, defined as the anisotropy of fluorophores that are indirectly excited after homo-FRET). The measured anisotropy of clusters of fluorophores therefore contains contributions of both donor and acceptor fluorophores. The relation between anisotropy and the number of fluorophores in a cluster is determined experimentally using mGFP tagged FKBP reference constructs. (B) Schematic representation of constructs used for the dimerization and oligomerization of FKBP-mGFP and 2xFKBP-mGFP by the ligand AP20187. (C) Anisotropy images of cells expressing FKBP-mGFP (in presence/absence of AP20187) or 2xFKBP-mGFP (in presence of AP20187). (D) Histograms of the relative decrease in anisotropy (r_{inf}/r_{mono}) for the FKBP reference constructs. The graph shows the r_{inf}/r_{mono} values for N_{av}=1, 2 and ≥ 3. For a detailed description see Bader et al. (2009, submitted).

$$r_{ss} = r_{mono}\frac{1+\omega\tau}{1+N\omega\tau} + r_{et}\frac{(N-1)\omega\tau}{1+N\omega\tau} \qquad \text{(Eq. A4)}$$

Equation A4 is valid for measurements of a large number of fluorophores to average out the orientations of individual fluorophores in clusters. In fluorescence anisotropy imaging, typically hundreds of fluorophores are needed for sufficient signal. Application of Equation A4 requires even more signal. Both the homo-FRET rate ω and the anisotropy r_{et} need to be known to obtain quantitative information about the cluster size N.

In steady-state fluorescence anisotropy imaging ω is either estimated or assumed to be much faster than the rate of fluorescence. In the latter case, ωτ approaches infinity which effectively means that the homo-FRET efficiency is one.
Now, equation A4 simplifies to:

$$r_{ss}(E=1) = r_{mono}\frac{1}{N} + r_{et}\frac{N-1}{N} \qquad \text{(Eq. A5)}$$

Alternatively, the rate ω can be derived from the time-resolved anisotropy decay. In the absence of rotation, the anisotropy decay due to homo-FRET can be written as:

$$r_{\text{homo-FRET}}(t) = (r_{mono} - r_{inf})e^{-2\omega t} + r_{inf} \qquad \text{(Eq. A6)}$$

Fitting the measured anisotropy decay using Equation A6 yields the value of the homo-FRET rate. However, in imaging experiments the number of photons that are typically collected per pixel is in practice not sufficient for a reasonable estimation of ω. Within nanoseconds after the excitation pulse, the anisotropy levels off at the limiting anisotropy r_{inf}. Homo-FRET has occurred multiple times and all fluorophores have equal probability of emitting a photon. This limiting anisotropy is identical to the steady-state anisotropy when fast and reversible homo-FRET takes place (E = 1, Equation A5). As described in previous work (Bader et al. 2007b), the limiting anisotropy is therefore a direct measure of the cluster size N that is independent of the efficiency of homo-FRET and can be written as:

$$r_{inf} = r_{ss}(E=1) = r_{mono}\frac{1}{N} + r_{et}\frac{N-1}{N} \qquad \text{(Eq. A7)}$$

The value of r_{inf} is always lower than or equal to the steady state anisotropy r_{ss} and the reduction in r_{inf} due to clustering is often more pronounced than the reduction in r_{ss}. Consequently, variations in the degree of clustering can be more accurately determined by measuring r_{inf}. The extent of this improvement depends on the homo-FRET efficiency.

For randomly oriented fluorophores, the limiting anisotropy is approximately zero (r_{et} = 0.016), but for non-random orientations r_{et} will be higher. The value of r_{et} should therefore be experimentally determined. Recently, it has been shown that the relative orientation of the fluorophores, and consequently r_{et}, depends on the GFP probe, i.e., not on the fused protein (Bader et al. 2009, submitted). This means that the relation between anisotropy and cluster size can be experimentally calibrated using GFP fusions where controlled dimerization or oligomerization can be induced. This dimerization or oligomerization was achieved by the fusion of monomeric GFP (mGFP) with the FK506-binding protein (FKBP12) that can be dimerized by binding of its ligand AP20187. The main prerequisite is that there is a flexible linker between the protein and (m)GFP, so that the (m)GFPs can have their 'preferred' relative orientation. This aspect can be verified from the FRET efficiency: when E > 0.7, the inter-fluorophore distance is less than 4 nm and the (m) GFPs experience molecular interactions . If so, the relative depolarization r_{inf}/r_{mono} = 0.312/0.382 = 0.82 for dimers and r_{inf}/r_{mono} = 0.276/0.382 = 0.72 for oligomers.

Chapter 6

Sphingolipid topology and membrane protein nanoclusters

Summary

Introduction

Sphingolipids are an essential class of membrane lipids in eukaryotes. Due to their high packing density and their affinity for cholesterol, sphingolipids are able to promote bilayer rigidity and impermeability. Apart from its ability to maintain biomembrane integrity, sphingomyelin (SM) is also a major source for ceramide, involved in signal transduction. Thus, by balancing the formation of ceramide and diacylglycerol (DAG), which is known to act as second messenger, SM synthesis and degradation may play a fundamental role in cell growth and survival. Due to the incomplete knowledge about the enzymes involved in synthesis and degradation of sphingolipids, only little evidence could be gathered to prove the organizing and regulatory capacity of these lipids. Previously, multiple SM synthase (SMS) genes in each organism capable to produce SM were discovered (Huitema et al., 2004). In addition to the two isoforms of SM synthase (SMS1 in the Golgi and SMS2 at the plasma membrane, Huitema et al., 2004) in the human genome, a third SM synthase-related (SMSr) gene was identified. This enzyme catalyses the production of the SM analog ceramide phosphoethanolamine (CPE) in the ER (Ternes et al., 2009; Vacaru et al., 2009).

The SMS family in the context *of C. elegans*

The genome of the nematode *C. elegans* encodes five SMS family members. So far, none of these enzymes has been characterized in any detail. In **chapter 2** we describe a first systematic analysis of this SMS family. Due to its easy manipulation of gene function by mutation and RNAi, the *C. elegans* animal model offers an attractive model to study the implications of SM synthase activity on the molecular level in animal physiology. *C. elegans* has been instructive in many situations where the mammalian systems are too complicated, and where e.g. the molecular ordering of signaling pathways could not be unraveled. V5-tagged versions of four SMS homologues of *C. elegans* were expressed in either budding yeast or insect cells, organisms lacking endogenous SM (both) and CPE (yeast). We identified two proteins of the multigenic protein family as SM synthases and one enzyme as a CPE synthase. To address the contribution of each of these enzymes to the total SM synthase activity, deletion mutants of the respective gene were monitored for the formation of NBD-labeled SM by TLC. Both deletion strains show a significantreduction of SM synthase activity; however none of the two enzymes wiped out the total activity. To clarify if these two enzymes are the only SM synthases in *C. elegans*, a double mutant, showing a disruption in both SM synthases, SMSα and SMSβ, was created. SM synthase activity was strongly reduced in this double mutant, however, still a clearly detectable SM synthase activity was found, indicating that *C. elegans* contains at least one other SM synthase. The identity of this enzyme remains to be unraveled.

SMS proteins in mammals display essential roles in cell growth and survival, as shown e.g. by the reduced growth of human HeLa cells, after depletion of SMS1 and SMS2 (Tafesse et al., 2007). Surprisingly, the depletion of both SMSα and SMSβ in *C. elegans* did not show any obvious morphological or behavioral defects. This observation may be explained by an activation of pro-mitogenic/anti-apoptotic pathways. On the other hand, residual levels of SM and CPE activity may be sufficient to sustain growth and survival, or nematodes simply do not rely on SMS proteins for their vital function, a possibility which cannot be excluded. Novel mutant strains carrying multiple SMS family members combined with RNAi approaches will help to address these possibilities.

C. elegans contains more SMS homologues than any other SM and/or CPE-producing organism. While SMSα, SMSβ and SMSr synthesize SM or CPE, SMSγ and SMSδ may have different functions. A highly interesting option is that SMSγ and/or SMSδ may function as PC:oligosaccharide cholinephosphoryl transferase synthase, as this reaction is mechanistically very similar to SM and EPC synthesis. The production of cholinephosphoryl-substituted oligosaccharides (CPOs) is used by parasitic nematodes to avoid the host immune response (Houston and Harnett, 2004) and was also shown in *C. elegans* (Cipollo et al., 2004). Due to the fact that the CPO synthase is absent in humans, the identification of the CPO synthase in *C. elegans* will help to find an ideal possibility to treat filarial infections.

Cellular localization of (glyco)sphingolipids

Glycosphingolipids (GSLs), the other class of sphingolipids, contain polar headgroups that consist of one or more carbohydrate moieties. Glycosphingolipids containing sialic acids are termed gangliosides. The observation that the knockout of the GlcCer synthase in mice leads to the death of the embryos (Yamashita et al., 1999), indicates the essential role of GSLs in mammalian development. The synthesis of the complex GSLs occurs on the inner, non-cytosolic surface of Golgi cisternae. GSLs travel from there towards the outer, non-cytosolic surface of the plasma membrane and can be recycled into endosomal/lysosomal structures, where they are eventually degraded. Sphingolipids selfaggregate together with cholesterol into microdomains called 'lipid rafts'. These microdomains appear to be transient and small, unless they coalesce and are stabilized by for example curvature, membrane stress or signaling. Apart from their structural role in lipid and protein sorting, they are thought to fulfill essential functions as scaffolds for various signaling domains of different protein and lipid composition.

In the past years, various genetic and biochemical findings have drawn the organization of (glyco)sphingolipids in cells into focus. To unravel the functions and underlying molecular interactions of GSLs within specialized domains of cellular membranes and in their interaction with proteins in, on and outside membranes, combinations of biological, physical and chemical approaches are

required. However, till today the elucidation of the nanoscale organization of GSLs is restrained by complex technical issues. The specificity of the tools (Yanagisawa et al., 2006) and especially the redistribution of lipids during fixation procedures (Schwarz and Futerman, 1997; Heffer-Lauc et al., 2005) have been problematic. In *chapter 3* of this thesis we critically evaluated the published data and discussed the various possibilities to improve the available techniques.

Complex GSLs, such as gangliosides, fulfill important roles in recognition and signaling at the plasma membrane and are also used as receptors by parasites, bacteria, viruses and toxins. GM1, a monosialoganglioside, has been shown to be involved in the regulation and activation of the epidermal growth factor receptor, and acts as a receptor for cholera toxin. A defect in the degradation of this interesting lipid leads to its accumulation and storage in the lysosomes, displaying a clinical phenotype, Landing disease or GM1 gangliosidosis. Different forms of this disease include early encephalopathy, facial and skeletal deformations and parkinsonian features. Unfortunately, as for most storage diseases, it is not clear how the molecular defect is connected to the disease. Recently, the accumulation of GM1 was found to activate different ion-channels (Wang et al., 2009), and it was suggested that GM1 may accumulate at the ER, eventually leading to a perturbation of calcium homeostasis (Tessitore et al., 2004). It was shown that GM1 gangliosidosis in the mouse model resulted in the upregulation of the unfolded protein response (UPR) pathway and concomitantly neuronal cell death. Light microscopic localization of GM1 in embryonic fibroblasts suggested that these mice had a higher concentration of GM1 in their ER membranes, supporting the hypothesis that the UPR activation would be a consequence of the abnormal accumulation of GM1 at ER membranes. In **chapter 4** we study the GM1 distribution at higher resolution by electron microscopy after freeze-substitution, avoiding pitfalls described in **chapter 3** of this thesis. First, different anti-GM1 antibodies were tested for their specificity for GM1 on lipid extracts by TLC immune overlay and on fixed cells by immunofluorescence. All antibodies bound specifically to GM1 and did not show cross-reactivity to other lipids tested, nor to mouse fibroblast (glyco)proteins. Co-localization studies by immunofluorescence showed that the accumulated GM1 in diseased cells localized mainly to lysosomal/endosomal structures. The ultrastructural distribution of the ganglioside GM1 was investigated in β-galactosidase$^{-/-}$ mouse embryonic fibroblasts by electron microscopy. To avoid redistribution of lipids in the samples, cells were fixed, frozen in liquid nitrogen, freeze substituted and embedded in Lowicryl at sub-zero temperatures (van Genderen et al. 2001). This technique was combined with post-embedding ("on sections") labeling, which provides accessibility of labeling reagent to the antigen without the need to open the cells by detergents or organic solvents. Here, we show that accumulated GM1 in GM1 gangliosidosis cells was essentially limited to multivesicular endosomes/lysosomes, and is not accompanied by a significant

rise in the GM1 content of other cellular membranes, notably the ER membrane. Whether this is also valid for other cell types, e.g. neuronal cells, remains to be established.

A number of complex glycosphingolipids are medically relevant and are involved in various severe diseases. The further development of techniques to study the nanoscale organization of these lipids, in combination with biochemical and genetic approaches, is therefore required to unravel the molecular interactions underlying these diseases.

Influence of GSLs on the organization of cytosolic lipid-anchored proteins

Glycosphingolipids, together with SM and cholesterol, are thought to play an essential role in the formation of microdomains, called lipid rafts. The lateral organization of biomembranes was proposed to be required for the sorting of lipids and specialized proteins, and has been shown lately to play a fundamental role in signal transduction, leading to extensive studies on the organization and activation of the small GTPases H-ras and K-ras. Although complex GSLs and SM are found predominantly on the exoplasmic leaflet of the plasma membrane, the simple GSL glucosylceramide (GlcCer) is synthesized at the cytosolic side of the Golgi, from were it may have access to the inner leaflet of the plasma membrane by monomeric transport. Coupling exoplasmic leaflet rafts with inner leaflet nanodomains could have important functional relevance, allowing the coupling of events outside to signaling pathways within the cell. In **chapter 5** of this thesis we tested the role of GSLs on the nanoscale organization of different lipid-anchored proteins at the inner leaflet of the plasma membrane using electron microscopy and homo-FRET imaging. These techniques have both been previously used successfully to study the nanoscale organization at the plasma membrane. Here, we combine them for the first time, exploiting the complementary ranges of the two techniques. To study whether the presence of GSLs is relevant for the nanoscale organization of proteins we used a melanoma mutant cell line that lacks the glucosyltranferase activity needed for the synthesis of GlcCer (Ichikawa et al. 1994). Electron microscopy showed that in melanoma cells GFP-labeled lipidation sequences of H-ras (GFP-tH) and K-ras (GFP-tK), as well as GFP-EGFR, were organized in nanodomains with radii of 8-14 nm. The average size of nanodomains was not significantly affected by the depletion of GSLs in GM95 cells. However, in GM95 cells the number of proteins per cluster was decreased for cells expressing GFP-tH. Homo-FRET measurements show that small nanoclusters consist mainly of dimers. Molecular clustering was also increased when GSLs were depleted. In conclusion, GSLs did not affect the diameter of GFP-tH and GFP-tK clusters. However, GSLs increased the number of molecules per cluster, and lowered at the same time the level of molecular interaction between these molecules. Because melanosomal MEB4 cells only contain significant amounts of the glycolipids GlcCer and GM3, these are the

candidate molecules that are responsible for these effects. GlcCer is synthesized at the cytosolic surface of the Golgi and has, in contrast to the complex ganglioside GM3, access to the cytosolic side of the plasma membrane (Warnock et al., 1994). However, how this lipid affects the lipid and protein organization in the cytosolic leaflet is unclear. The data presented in this thesis would suggest that GlcCer containing domains would require fewer H-ras molecules for stability and would render the lipid distribution within lipid rafts more homogeneous. Physio-chemical studies will have to elucidate the organizational principles underlying the structure of lipid rafts on the cytosolic surface.

Perspectives

Sphingolipids are evolutionary old lipids, and they are applied by eukaryotic cells for a number of basic structural functions, for general physiological signaling pathways like survival and apoptosis, and for a number of more specific signaling functions like modulating interactions with receptors and integrins. It is a challenge to unravel the biophysical and chemical backgrounds of these functions and to find out the molecular mechanisms by which cells and organisms utilize these molecules for their vital functions. Whereas so far most efforts have been directed at mapping the basic physical principles that govern sphingolipid behavior, the location of the various sphingolipids, and the identification of the enzymes and transporters involved, the major challenge for the next years is to find out how cells and organisms sense and vary the concentration of the various sphingolipids to suit their local needs and how they are still able to integrate their sphingolipid metabolism and transport at the cellular or whole body level.

References

Cipollo, J.F., Awad, A., Costello, C.E., Robbins, P.W., and Hirschberg, C.B. 2004. Biosynthesis in vitro of Caenorhabditis elegans phosphorylcholine oligosaccharides. Proc Natl Acad Sci U S A 101:3404-3408.

Heffer-Lauc, M., Lauc, G., Nimrichter, L., Fromholt, S.E., and Schnaar, R.L. 2005. Membrane redistribution of gangliosides and glycosylphosphatidylinositol-anchored proteins in brain tissue sections under conditions of lipid raft isolation. *Biochim Biophys Acta* 1686 3:200-208.

Houston, K.M., and Harnett, W. 2004. Structure and synthesis of nematode phosphorylcholine-containing glycoconjugates. *Parasitology* 129:655-661.

Huitema, K., van den Dikkenberg, J., Brouwers, J.F., and Holthuis, J.C. 2004. Identification of a family of animal sphingomyelin synthases. *Embo J* 23:33-44.

Ichikawa, S., Nakajo, N., Sakiyama, H., and Hirabayashi, Y. 1994. A mouse B16 melanoma mutant deficient in glycolipids. *Proc Natl Acad Sci U S A* 91:2703-2707.

Schwarz, A., and Futerman, A.H. 1997. Determination of the localization of gangliosides using anti-ganglioside antibodies: comparison of fixation methods. *J Histochem Cytochem* 45:611-618.

Tafesse, F.G., Huitema, K., Hermansson, M., van der Poel, S., van den Dikkenberg, J., Uphoff, A., Somerharju, P., and Holthuis, J.C. 2007. Both sphingomyelin synthases SMS1 and SMS2 are required for sphingomyelin homeostasis and growth in human HeLa cells. *J Biol Chem* 282:17537-17547.

Ternes, P., Brouwers, J.F., van den Dikkenberg, J., and Holthuis, J.C. 2009. Sphingomyelin synthase SMS2 displays dual activity as ceramide phosphoethanolamine synthase. *J Lipid Res.*

Tessitore, A., del, P.M.M., Sano, R., Ma, Y., Mann, L., Ingrassia, A., Laywell, E.D., Steindler, D.A., Hendershot, L.M., and d'Azzo, A. 2004. GM1-ganglioside-mediated activation of the unfolded protein response causes neuronal death in a neurodegenerative gangliosidosis. *Mol Cell* 15:753-766.

Vacaru, A.M., Tafesse, F.G., Ternes, P., Kondylis, V., Hermansson, M., Brouwers, J.F., Somerharju, P., Rabouille, C., and Holthuis, J.C. 2009. Sphingomyelin synthase-related protein SMSr controls ceramide homeostasis in the ER. *J Cell Biol* 185:1013-1027.

van Genderen, I.L., van Meer, G., Slot, J.W., Geuze, H.J., and Voorhout, W.F. 1991. Subcellular localization of Forssman glycolipid in epithelial MDCK cells by immuno-electronmicroscopy after freeze-substitution. *J Cell Biol* 115:1009-1019.

Wang, J., Lu, Z.H., Gabius, H.J., Rohowsky-Kochan, C., Ledeen, R.W., and Wu, G. 2009. Cross-linking of GM1 ganglioside by galectin-1 mediates regulatory T cell activity involving TRPC5 channel activation: possible role in suppressing experimental autoimmune encephalomyelitis. *J Immunol* 182:4036-4045.

Warnock, D.E., Lutz, M.S., Blackburn, W.A., Young, W.W., Jr., and Baenziger, J.U. 1994. Transport of newly synthesized glucosylceramide to the plasma membrane by a non-Golgi pathway. *Proc Natl Acad Sci U S A* 91:2708-2712.

Yamashita, T., Wada, R., Sasaki, T., Deng, C., Bierfreund, U., Sandhoff, K., and Proia, R.L. 1999. A vital role for glycosphingolipid synthesis during development and differentiation. *Proc Natl Acad Sci U S A* 96:9142-9147.

Yanagisawa, M., Ariga, T., and Yu, R.K. 2006. Cholera toxin B subunit binding does not correlate with GM1 expression: a study using mouse embryonic neural precursor cells. *Glycobiology* 16:19G-22G.

Summary in Dutch
Acknowledgements
Curriculum vitae

Nederlandse Samenvatting

Een cel is de kleinste functionele levende eenheid waaruit alle organismen zijn opgebouwd. Tegenwoordig bestaan er organismen die uit vele miljarden cellen zijn opgebouwd. Zoogdiercellen worden van hun omgeving gescheiden door het plasmamembraan die als een waterdichte barrière dient. Verder zijn er ook in de cel processen die door middel van een membraan van elkaar gescheiden moeten worden. De hierdoor ontstane afzonderlijke compartimenten worden organellen genoemd. Plasmamembranen en membranen van organellen bestaan uit lipiden, oftewel vetten. Lipiden spelen een belangrijke rol als structureel onderdeel van het membraan met zijn barrière functie, maar hebben ook als moleculen een actieve functie in een veelvoud aan verschillende cellulaire processen. Na het ontstaan van interne membranen zijn cellen begonnen sfingolipiden and sterolen te synthetiseren. Op basis van de fysieke verschillen tussen deze en de glycerofosfolipiden, kunnen cellen lipiden sorteren binnen een membraan en daarmee membranen van verschillende lipidensamenstelling creëren. Membraaneiwitten kunnen op deze manier gesorteerd worden en dus hebben simpele sfingolipiden belangrijke functies gekregen in het doorgeven van signalen en de uitvoering van essentiële fysiologische functies.

Sfingolipiden zijn een essentiële klasse van membraanlipiden in zoogdiercellen. Ceramide, dat de lipide ruggengraat van de sfingolipiden vormt, wordt getransformeerd naar sfingomyeline (SM) door de additie van een fosfocholine kopgroep. Naast barrièrefunctie vormt SM ook een hoofdbron van ceramide, dat betrokken is bij signaaltransductie. Dus, door de vorming van ceramide en het bijproduct diacylglycerol (DAG), spelen SM synthese en afbraak een essentiële rol in de groei en overleving van de cel. In **hoofdstuk 2** gebruiken wij de worm *C. elegans* om de verschillende SM synthase eiwitten te karakteriseren. Dit diermodel is gemakkelijk te manipuleren door genmutaties, en daardoor is het een attractief model om de invloed van SM synthase activiteit te bestuderen. In dit onderzoek hebben wij twee eiwitten als lid van de SM synthase familie en één als een ceramide fosfoethanolamine synthase geïdentificeerd. Verrassend tonen de wormen die een knock-out van de belangrijkste SM synthases hebben geen groei- of gedragdefecten.

Glycosfingolipiden (GSLs) vormen de andere klasse van sfingolipiden en hebben polaire kopgroepen, die uit één of meerdere suikergroepen bestaan. Deze lipiden worden in het Golgi gesynthetiseerd, waarna zij naar de plasmamembraan worden getransporteerd. GSLs kunnen in alle membranen van het endocytotische systeem gevonden worden, waar ook de afbraak van deze lipiden plaatsvindt. De functie van deze lipiden is ook afhankelijk van de plaats waar het lipide zit. In welke membraan, en aan welke kant van het membraan een lipide aanwezig is, en ook of de lipiden heterogeen verdeeld zijn in het vlak van het membraan, zijn vragen die sinds lange jaren in de focus van het onderzoek gestaan hebben en tot nu toe

nog steeds niet helemaal beantwoord zijn. In **hoofdstuk 3** bediscussiëren wij de technische problemen die het moeilijk maken om deze vragen te beantwoorden. Gangliosiden, een bepaalde subgroep van complexe GSLs, spelen een belangrijke rol in het doorgeven van signalen in het plasmamembraan. Verder gebruiken vele parasieten, toxines en bacteriën gangliosiden als receptoren. GM1, een van de gangliosiden, is betrokken bij de regulatie en activatie van de epidermale groeifactorreceptor, en daarnaast dient dit lipide zelf als receptor voor cholera toxine. In gezonde cellen wordt GM1 door een enzym in lysosomen afgebroken. In de ziekte GM1 gangliosidose, ook Landing ziekte genoemd, wordt GM1 in de lysosomen niet afgebroken maar opgeslagen wat tot accumulatie leidt. Tot nu is het niet bekend hoe dit leidt tot ziekte. Nieuwe gegevens tonen aan dat de accumulatie van GM1 tot een activatie van verschillende ionkanalen leidt, en dat GM1 misschien accumuleert in het endoplasmatisch reticulum (ER), waar het de homeostase van calcium verstoort. Om deze vraag te beantwoorden, hebben wij in **hoofdstuk 4** de lokalisatie van GM1 bepaald met behulp van electronenmicroscopie na monstervoorbereiding met vriessubstitutie. Deze methode zal het aantal technische problemen beschreven in Hoofdstuk 3, verkleinen. In zieke cellen werd een accumulatie van GM1 alleen waargenomen in lysosomale/endosomale structuren. In tegenstelling tot gezonde cellen werd geen toename van GM1 moleculen in andere organellen geobserveerd.

Glycosfingolipiden spelen samen met cholesterol en SM een essentiële rol in de vorming van microdomeinen, ook “lipid rafts” genoemd. De laterale organisatie van membranen is noodzakelijk voor het sorteren van lipiden en specifieke eiwitten, en is ook van groot belang voor het doorgeven van signalen van de buitenkant naar de binnenkant van het plasmamembraan. Enerzijds zitten complexe GSLs en SM aan de exoplasmatische (buiten)kant van het plasmamembraan, anderzijds zitten enkelvoudige GSLs, bijvoorbeeld glucosylceramide (GlcCer), aan de binnenkant van het plasmamembraan. In **hoofdstuk 5** combineren wij twee verschillende technieken om de nano-organisatie van eiwitten aan het plasmamembraan te bestuderen. Om de invloed van sfingolipiden op deze organisatie te meten, hebben wij twee verschillende cellijnen gebruikt, een die GSLs bevat, en een die door een mutatie geen GSLs meer heeft. Onze resultaten tonen aan, dat aan de ene kant GSLs niet noodzakelijk zijn om lipid rafts te vormen, aan de andere kant blijken GSLs belangrijk te zijn om het niveau de mate van interactie tussen verschillende eiwitten in de lipid rafts te beïnvloeden.

Het onderzoek dat in dit proefschrift wordt beschreven heeft nieuwe inzichten opgeleverd in hoe sfingolipiden in verschillende membranen en in het membraan zelf georganiseerd zijn en welke technieken gebruikt kunnen worden, om deze organisatie verder zo goed mogelijk te bestuderen. Zoals bijna altijd in fundamenteel onderzoek zijn er nog vele vragen onbeantwoord en zijn er nog vele vragen bijgekomen, die onderzoekers nog jaren bezig zullen houden.

Acknowledgements

Well, it is done!

After five and a half years doing research in the department Membrane Enzymology, I am looking back on an exciting time, full with frustrations and obstacles, but also filled with a lot of fun and interesting new things I could learn and experience. I want to thank all the people I met during that time, and who helped to finish this booklet, either by helping in a scientific or a motivating way, or just by listening and therefore bearing unstoppable discussions about research and everything connected with it.

Gerrit, thanks a lot for giving me the opportunity to come to Utrecht, to ME. I have been always happy with my decision to come to your department and I have learned so much here. Thanks for being such an enthusiastic and at the same time such a critical researcher. I wanted to thank you for all the support you gave me, especially in the last phase of my PhD time. **Hein**, you left ME already some time before I could finish my PhD. You showed me inspiring ways of approaching scientific problems, thanks for that. Starting a new project in the last phase of my PhD was an exciting step. Thanks, **Joost**, for helping me through this time, for your advices and especially for your feedback. Your motivation for research is very inspiring. **Bruno**, wir haben uns schon bei meinem ersten Bewerbungsgespräch hier getroffen. Damals wolltest du mir nicht so viel drüber erzählen, wie es so ist für längere Zeit im Ausland zu sein! Du wollest mir den Spass nicht verderben es selber rauszufinden! Aber ich denke, dass wir uns mittlerweile in den meisten Punkten wohl finden würden. Schön, dass wir doch noch in einem gemeinsamen Projekt arbeiten konnten, vielen Dank für deine Hilfe, und für die netten Gespräche! Thanks **Hans**, **Arjen** and **Dave**, that you kept trying to find a common language for cell biology and biophysics. Arjen and Dave, I enjoyed the days coming to your department, doing measurements in the cave, being in the dark, listening to music. Thanks for all the discussions and for being helpful and patient all the time. **John** and **Rob,** thanks for giving me the opportunity to come to Brisbane. **Sarah** and **Nick**, I really enjoyed the stay in Australia, thanks for showing me all the procedures and for all the discussion we had. Sarah I am looking forward to see you again at my promotion, thanks for keeping answering all my questions.

Erik, we were on the same project, and it was not easy most of the times. Thanks for sharing knowledge, cells (also if they were dying all the time in the hand of the other) and frustrations. I wish you all the best for your current and all your future projects. **Paul**, thanks for all your input and feedback. **Rob**, thanks for showing me the world of llama antibodies. I enjoyed working together with you in my first year. I also want especially to thank all the people working at the Cell biology department dealing with electron microscopy. I was in constant need for chemicals, tips and tricks. **Hans** and **Chris**, thanks for helping with the electron

microscopes. **Elly**, you invested a lot of time in explaining apparatuses and protocols to me. Thanks a lot for sharing your great knowledge with me.

During my PhD time, I spend of course lots and lots of hours in the labs and in the offices of ME. I want to thank all people, who shared that time with me, for making it colorful through all your input, scientifically, but also on a personal level.

Fikadu and **Joep**, in the last one and a half years we worked together on the worm project. Thanks for discussions and for your support. Fikadu, good luck with finishing up your PhD and finding a PostDoc position. Joep, I also want to thank you for all your efforts to improve the organization of our labs. Thanks also to **Ruud** and you for having lots of nice discussion, beers and for preparing the fun movies.

VMTII, well, sometimes a bit chaotic (I guess that is an understatement), but I enjoyed being in this lab. Thanks to **Seléne**, **Sylvia**, **Jasja**, **Sophie**, **Per**, **Matthijs**, **Ruud**, **Cedric** and of course **David** for sharing equipment, reagents, ideas, successes and failures! Thanks also to my students **Hilde**, **Ruud**, **Jeroen**, **Yadi** and **Laia!** I enjoyed working with you, and I learned a lot about people during these times. Seléne thanks for being also such a nice officemate. I really enjoyed our sometimes endless discussions about “Gott und die Welt” and all the lunches. Somehow it was always lunchtime, or have we been just hungry all the time? Thanks for correcting my Dutch, I guess it was and still is really necessary. Jasja, I am really happy that we stayed in contact after you left the lab. Thanks for being so interested and curious; I am looking forward to our next meeting. Sophie, thanks for bringing some French input into our lab. It was only a short period of time, that we have been in the same lab, but I enjoyed so much having you around. Sylvia, we spent nearly our whole PhD together in VMTII and in the same office. With your positive way, you helped to solve lots of problems. Thanks for finding all the stuff I was constantly unable to find in the lab! Good luck in San Diego! Per, Mister Upper-Level-Research, I am happy to have brought fennel into your life. Thanks for your discussions and for helping moving to Eindhoven!

Susanne, that’s how you can meet again in life, after leaving for Paris, you came back to Utrecht. Thanks for all the talks and discussions and for your friendship. I guess the distance between Eindhoven and Utrecht is not too far, so we will keep seeing each other. **Patricia**, we also shared the biggest parts of our PhDs together at ME. Thanks for all the nice lunches and tea breaks.

Ana, **Catheleyne**, **Hanka** and **RK**, some of you are close to finishing up, some just started. The ”older ones” I wish all the best with the last bits and pieces of your thesis and especially with finding the right positions for you. The ”younger ones“ I wish a lot of strength and creativity. Keep going!

Maarten, you were always open to all kinds of problems. Thanks, for all the discussions and the feedback you gave me. **Guillaume**, I admire your acting qualities. It was great fun to see you in the movies. Guillaume and **Philipp**, it was nice to

have you around, good luck for your further research. **Lily**, I like to think back about our discussions in the East wing! **Pavel, Hanneke, Martijn, Gerry** and **Karel** you were great neighbors and it was nice to have you eventually in our group! **Dick**, thanks for all your technical help and for forcing me to speak Dutch. **Cécile**, thanks for helping with all the small things which are necessary when you pursue a PhD and especially if you move into another country. **Quirine**, **Klazien** and **Nanette** you were part of ME at the beginning of my PhD time. I enjoyed having you around! Nanette, I really enjoyed our trips to Aachen and Maastricht. It is always great fun to see you.

During the PhD time, people outside the lab play an important role.

First, I want to mention the cohabitants of the van Lynden van Sandenburglaan, **Philipp**, **Ben**, **Eunice**, **Wilma**, and **Mutz**. I think we had a great time living in the "Alpen-WG". **Louise**, we only shared a short time in the house, all the best for your research. Sorry Philipp, for all the biochemistry discussions at the dinner table! Thanks for being one of my paranimfs. I guess that is a perfect preparation for your PhD, good luck with it or should I better say: "Sterkte!".

Eric, **Linda**, **Claudia**, **Rachel**, **Victor**, **Ronan**, **Nick**, **Tom**, **Karina** and **Deborah** thanks for nice experiences like the "Wadlopen" and all the nice evenings! **Mitja**, I guess, I know now a good lawyer, in case I should need one. Slovenia is fortunately very close to my home village, so you will not be able to escape from some visits!

Vielen Dank auch an meine früheren Studienkollegen und Freunden aus Graz: **Eva**, **Günter**, **Michael** and **Ernst**. Ihr hattet immer Zeit um mich zu treffen, wenn ich wieder mal in Österreich war. Mir bedeuted das sehr viel, leider war die Zeit immer viel zu knapp.

Anna and **Rebecca**, vielen dank für die vielen „Kaffetscherln" im Beisl. Ich denke die Angestellten wundern sich noch immer, wer diese komischen Ladies sind, die nur 3 bis 4 mal im Jahr im Café auftauchen und dann die Zeit wirklich stundenlang damit verbringen, Kaffee zu schlürfen und zu tratschen. Ich habe diese Momente wirklich genossen!

Babsi, wir kennen uns jetzt seit seit über 16 Jahren, und noch immer verdienen die Telefongesellschaften viel zu viel Geld mit uns. Danke für all diese Gespräche, deine Motivationskünste und für deine Freundschaft!

Ganz liebe Grüsse möchte ich natürlich auch in die Schweiz schicken! **Hildegard**, **Peter** und **Maria**, vielen Dank für eure Unterstützung! Ich komme immer wieder gerne nach Hochdorf, und ich hoffe, dass uns das in der Zukunft auch öfter möglich sein wird!

Sonja, dass wir zwei Schwestern sind, wollte uns eine Zeit lang niemand glauben. Und obwohl unsere Wege ein bisschen anders aussehen, glaube ich, das wir viel gemeinsam haben. Es ist schön, eine Schwester wie dich zu haben!

Natürlich moechte ich mich vor allem bei meinen Eltern bedanken. **Mama** und **Papa**, ihr habt es erst möglich gemacht, dass mir alle Wege offen standen. Ich weiss, dass es nicht einfach für euch war, mich in die Niederlande gehen zu lassen, umso mehr gebührt euch mein Dank. Vielen Dank fuer eure Unterstützung und Liebe! Danke, dass ihr immer für uns da seid!

David, wer hätte gedacht, dass sich alles so entwickelt (herzlichen Dank den Lipiden, die uns beide nach Utrecht geführt haben)! Aber nun sind wir schon seit über 5 Jahren ein Paar und ich hab dich trotzdem lieb ;)! Deine Unterstützung und dein Verständnis haben viel dazu beigetragen haben, damit diese Dissertation überhaupt gelingen konnte. Vielen Dank besonders für deine Geduld und deine Liebe!

Sandra

Curriculum Vitae

Sandra Hötzl was born on April 19, 1978 in Feldbach, Austria. After growing up in Paldau and attending the primary school there, she changed to the Bundesreal-gymnasium in Gleisdorf, were she finished her secondary school education in 1996 with the "Matura" (focusing on biology and chemistry). After that she started her studies of technical chemistry at Graz University of Technology (TU Graz), Austria. In the second part of her studies, she focused on biochemistry, biotechnology and food chemistry. Her master project during these studies, leading to the diploma thesis was titled: "Characterization of organelles of the yeast, *Pichia pastoris*" and was supervised by Dr. Günther Daum at the Biochemistry Department of the TU Graz. In 2003 she graduated as "Diplom Ingenieurin" (DI) and moved then to the Netherlands, where she pursued her PhD project in the department of Membrane Enzymology at Utrecht University under the supervision of Prof. Dr. Gerrit van Meer.